COMPARISON OF PPP AND DOUBLE DIFFERENCING SOLUTIONS

CASE STUDY

CAMPAIGN GPS STATIONS IN TANZANIA

BY:

LEONARD VINCENT BAMUHIGA

A Thesis submitted to the School of Graduate Studies of Addis Ababa University in partial fulfillment of the requirements for the Degree of Masters of Science in Civil Engineering under Geodesy

Addis Ababa, Ethiopia

July, 2013

Addis Ababa University

Addis Ababa Institute of Technology (AAiT)

Department of Civil Engineering

The undersigned hereby certify that they have read and recommended to Addis Ababa Institute of Technology for acceptance of a thesis titled "**Comparison of PPP and Double Differencing Solutions (case study using campaign GPS stations in Tanzania)" by: Leonard Vincent Bamuhiga** in partial fulfillment of the requirements for the degree of Masters of Science.

Supervisor/Advisor:

for
1. Dr. Addisu Hunegnaw — Dr. Tulu Besha — 14/08/13

Signature — Date

Co-Advisor(s):

1. Dr. Tulu Besha Bedada — 14/08/13

Signature — Date

Examiner(s):

1. Elias Lewi — 06/08/13

2. Gefrey Mewa — 14/08/13

3. ______ ______ ______

Signature — Date

DEDICATION

To the people who spent their time and resources in striving to make my life better since my childhood and during primary and secondary education namely, my Parents, (My Mother Asteria Kibate, and my father Vincent Bamuhiga) and, to all my brothers and sisters.

AND

To those who endured hardships during my absence my wife Nyaswa Kalomo and my son Franklin

AKNOWLEDGEMENTS

To the most High, Glorified, Almighty God, I give thanks, for by His Grace I am what I am today. I have not chosen my path but only through His will.

This thesis wouldn’t have come into place without the help of my Advisor Dr. Addisu Hunegnaw. I am sincerely grateful for his unforgettable valuable assistance in developing my research title and throughout the research. I am also grateful for his indomitable efforts to deliver knowledge, without which I wouldn’t have been able to substantiate this research. My heartfelt thanks also go to Dr. Tulu Besha, my co-advisor for his great help which has improved my research and made more significant.

My sincere acknowledgements go the University of Edinburgh[1], University of Addis Ababa –Ethiopia[2] and Ardhi University – Tanzania[3], in particular to the coordinators Dr. Addisu Hunegnaw[1], Dr. Roger Hipkin[1], Dr. Elias Lewi[2], Dr. Prosper Ulotu[3], and Dr. Elifuraha Mtalo[3], for inventing a regional geodesy program, under which this thesis has been conducted. I am also thankful to European Union through Edulink, for financing the program.

In a special way I would like to give my sincere gratitude to Dr. Elias Lewi, for spending his time and resources in striving to make the program incredibly good. I appreciate the way he organised a special course on INSAR in collaboration with Dr. Juliet Biggs of the University of Bristol UK. I greatly thank both of them for adding value on this geodesy program.

I wholeheartedly thank all persons who joined the program as teaching staff Dr. Atatlay Ayele and Tulu Besha, whose dedicated concern will remain in my memories.

My thanks also go to all my classmates, my friends Michael and Mikias, the Tanzanian community (wana-udugu) in Addis Ababa to mention but a few, Ambassador Prof Dr. Joram Biswaro, Ambassador Vincent Kibwana, Mr. Madebe and Mr. Lubuva and all members of Udugu past and current, for making me feel at home all the time.

Lastly but not least I convey my earnest thankfulness to my wife Alice (Nyasa Kalomo) for her encouragement and support, prior to pursuing the course and during my course work and dissertation. I also thank her for being patient during my absence, for I know caring for the family alone wasn’t a simple undertaking.

ABSTRACT

Satellite Positioning systems are world-wide precise positioning systems and very useful for geodetic surveys, crustal deformation studies, station coordinates, absolute and relative station velocities.

Two techniques for GPS data processing to obtain station position coordinates exist. The two methods are Differencing of observations, and Zero differencing techniques, known as Precise Point Positioning.

The main aim of this study was to assess the accuracy of PPP Solution, using the already known accurate Double differencing solution.

The data used in this study are three episodes' campaign GPS stations in Tanzania established in 2006, 2008 and 2010. The data sets are available in RINEX format from the UNAVCO website.

Double differencing was done using GAMIT_GLOBK software, in this case, the campaign data were combined in a solution experiment with reference GPS data for IGS stations in Africa, active from 2006-2010.

The PPP solution was obtained from APPS (online-GIPSY/OASIS). Other available online PPP solution services were also used for comparison purposes. The results from APPS PPP solution were compared with GAMIT/GLOB DGPS solution in order to assess the accuracy of PPP.

From 330, 24hours epochs of observations the results show that the range of the difference between GAMIT/GLOBK and APPS PPP solution is -3.7 to 5.6cm in X component, -3.8 to 5.0cm in Y component and -1cm to 3.4cm in the Z component. The residuals of coordinates (δX, δY and δZ) from the two solutions have mean value of 5.9mm in X component, 1.2mm in Y component and 0.4mm in Z component. Also the standard deviations in δX, δY and δZ are 11mm, 10mm and 4mm respectively.

From the results analysis it has been shown that in most cases, for the data set used, PPP solution is very close to DGPS solution.

Key words: Precise Point Positioning (PPP) Differential GPS (DGPS)

TABLE OF CONTENTS

LIST OF FIGURES

LIST OF TABLES

LIST OF ACRONYMS

GPS	Global Positioning System
GLONASS	Global Navigation Satellite System
GNSS	Global Navigation Satellite Systems
PPP	Precise Point Positioning
GAMIT	GPS Analysis at MIT (Massachusetts Institute of Technology)
GLOBK	Global Kalman Filter
GAPS	GPS Analysis and Positioning Software
UNB	University of New Brunswick
GIPSY-OASIS	GPS-Inferred Positioning System (GIPSY) and Orbit Analysis Simulation Software (OASIS)
APPS	Automated Precision Positioning Service
NRCan	Natural Resources Canada
CSRS	Canadian Spatial Reference System
LSAST	Least Squares Ambiguity Search Technique
LAMBDA	Least-squares AMBiguity Decorrelation Adjustment
FARA	Fast Ambiguity Resolution Approach
OMEGA	Optimal Method for Estimating GPS Ambiguities
FASF	Fast Ambiguity Search Filter
TCAR	Three-Carrier Ambiguity Resolution
QZSS	Quasi-Zenith Satellite System
(φ, λ, h)	Latitude Longitude and ellipsoidal-height respectively
(X, Y, Z)	Cartesian X, Y, Z coordinates
(N, E, U)	Northing, Easting and Up (Local Topocentric coordinates)
ECEF	Earth-Centred Earth Fixed
ECI	Earth Centered Inertial
PRN	Pseudo Random Number
TEC	Total Electronic Content
WAAS	Wide-Area Augmentation System
RINEX	Receive Independent Exchange
FAA	Federal Aviation Administration

SOPAC	Sripps Orbit and Permanent Array Center
UCSD	University of California, San Diego
SIO	Scripps Institution of Oceanography
NASA	National Aeronautics and Space Administration
NSF	National Science Foundation
UNAVCO	University Navstar Consortium (fundend by NSF and NASA)
CDDIS	Crustal Dynamics Data Information System
JPL	Jet Propulsion Laboratory
MIT	Massachusetts Institute of Technology
CORS	Continuously Operating Reference Stations

CHAPTER ONE

1. BACKGROUND

1.1 Introduction

Satellite Positioning systems are world-wide precise navigation and positioning systems formed by a constellation of satellites that emits a radio waves and very useful for geodetic surveys, crustal deformation studies, station coordinates absolute and relative station velocities.

Many Satellite positioning systems exist today a few to mention include; Navigation Satellite Timing and Ranging (NAVSTAR) Global Positioning System (GPS), Global Navigation Satellite System (GLONASS – **GLO**bal'naya **NA**vigatsionnaya **S**putnikovaya **S**istema), Doppler Orbitography Radio Positioning Integrated by Satellite (DORIS), Galileo - formally known as the European Civil Satellite Navigation Program, the Chinese system known as COMPASS Navigation Satellite System, the Japanese system known as Quasi-Zenith Satellite System (QZSS).

Of all these systems, GPS was the first established in the early 1970s. It was established for Military use by the US army and later released for civilian use. Nowadays the Satellite Positioning Systems are integrated and collectively referred to as Global Navigation Satellite System (GNSS). GNSS receivers are capable of tracking more than one Satellite Positioning System like GPS, GLONASS, and COMPASS.

Since the foundation of the GPS during the late 1970s, for precise measurements, relative processing /Differential positioning technique has been and is still dominant in GPS data processing. The technique involves two receivers stationed apart receiving the signals simultaneously, and the collected datasets are processed together so as to get relative position between two observation points. The technique is referred to Differential GPS (DGPS).

In the late 1990s due to the availability of precise GPS orbits/ephemeris and Clock data Products, new method was founded in the form of Precise Point Positioning (PPP) insideGNSS (2006); Nel Samama (2008); Seeber (2003); Kaplan and Hegarty (2006). This new technique is said to have precisions comparable to those achievable from relative processing. In PPP only one dual-frequency receiver is used. Precise ephemerides used in PPP are obtained from a globally distributed network of stations known as International GPS/GNSS Services (IGS) stations. The data are analyzed by estimating receiver parameters whilst satellite orbit and clock parameters are held fixed. This method is independent of base station, simple and incredibly efficient.

Most GPS for precise and geodetic measurements have been done using Differential GPS (DGPS) which is a technique for error mitigation in GPS. The method uses supplementary data from a reference GPS receiver at a known position.

The DGPS principle is that data collected at the user's receiver (rover) and reference receiver are differenced to eliminate most of errors namely; Selective Availability Error (if available), Ionospheric Delays, Tropospheric Delays, Ephemeris Errors, and Satellite Clock Errors.

However, this approach is tedious because it requires that one receiver is stationed at a point of known coordinates as a base station and another receiver station at a new observation point.

It is moreover expensive as it requires purchasing of two or more receivers and two or more observation teams during observation.

In this regard, if Precise Point Positioning can provide the same accuracy with DGPS, then it is more advantageous in terms of cost and time. Moreover, it is globally determined as it is free from errors that would result from base station/s. However due to undifferenced correlated biases, it should be used with great care.

The main difference between DGPS and PPP is the way in which errors are handled and/or mitigated.

In Differential GPS satellite and receiver clock errors and other errors with correlation are eliminated by differencing observation between receivers. Meanwhile in PPP highly precise satellite clock estimates are used to determine absolute receiver coordinates, whereby errors are estimated as part of the least squares solution for the coordinates, or otherwise modeled using linear combination of observations.

Consequently, precise absolute coordinates for a single receiver at an unknown location may be obtained without the need of a second receiver at a known position.

Note that there exists another form of point positioning known as Single Point Positioning (SPP), which does not use precise satellite clock values and uses only Pseudo-Ranges. This differs from PPP as PPP uses both Pseudo ranges and highly precise carrier phase observations and precise satellite clock estimates.

1.2 Problem statement

Differential GNSS technique is expensive. Except in developed countries where sufficient continuous GPS stations like IGS and CORS stations that are freely available and in this case a DGPS only requires having one receiver like the PPP, it requires one to purchase more than one receiver, and in terms of operation it requires at least two teams of operation each of which requires technical personnel. This is too much demanding especially in least developed countries. In this regard a method which meet the same or nearly same or as required for a particular job but simple and cheap in terms of money and personnel is preferably good to implement.

PPP is a very simple technique and relatively cheap. It only requires a single receiver at an unknown location and only one observer or observing team. If tested and found to produce the same result as the differential technique, this method will be a solution for reducing the burden in terms of initial and operational cost to GNSS users.

In this research available data of Campaign GPS stations in Tanzania have been used, figure 1.1 shows a series of campaign stations and the locations within the study area.

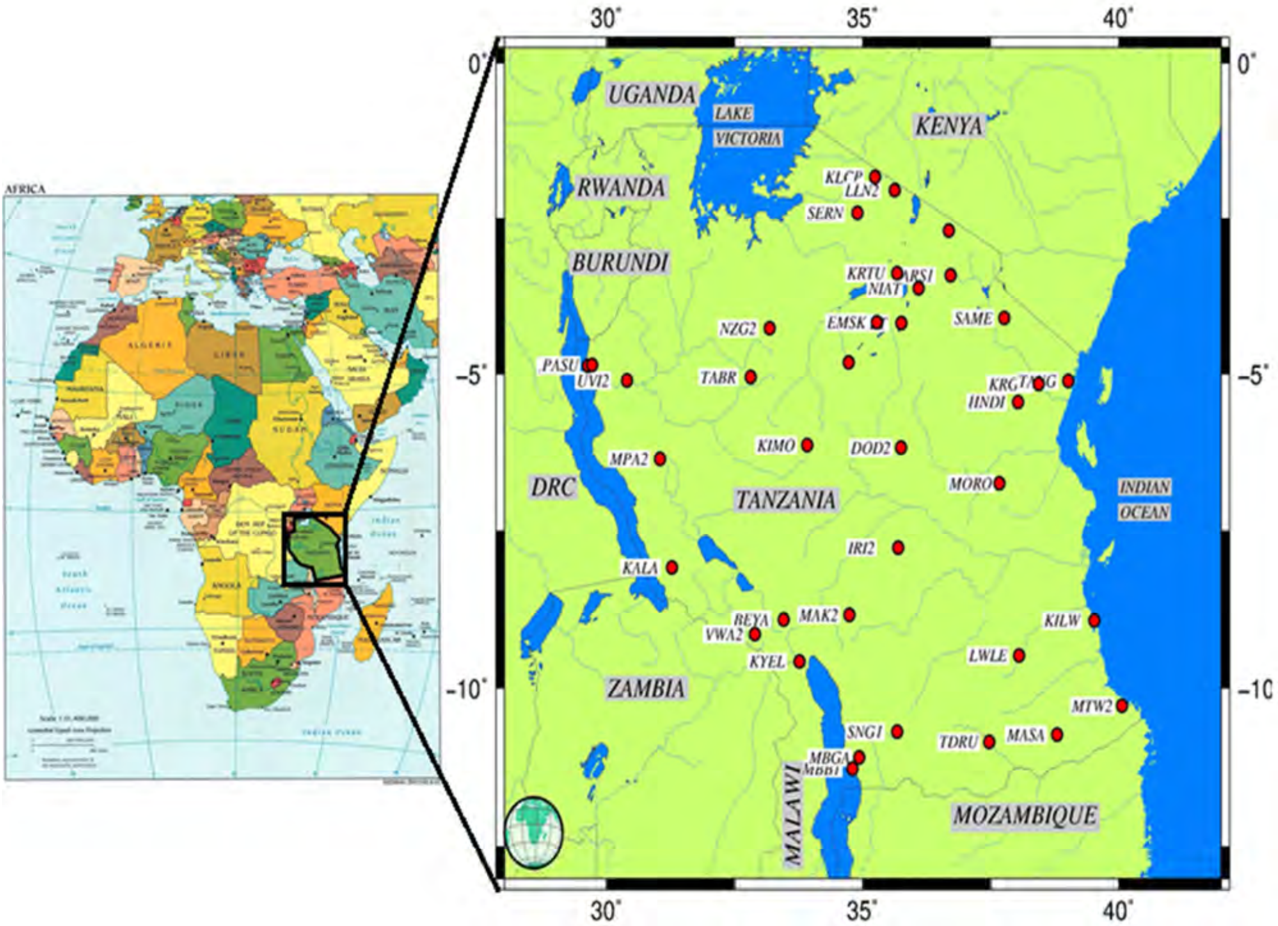

Figure 1. 1: Location map of the study Area. Showing the distribution of GPS campaign sites

1.3 General objective

The general objective is to assess the accuracy obtained using PPP solution by comparing it to Differencing solution from GAMIT/GLOBK.

1.4 Specific objectives

The specific objectives for this study are:

- To obtain coordinates using PPP and Double Differencing solutions.
- To compare the two solutions and asses the quality of PPP

1.5 Thesis outline

Chapter two describes in detail the literature review on the principle of GPS, it describes GPS segment namely; the constellation of GPS satellites in its space segments, and how the system is controlled via the control segment and its applications in the user segment. It further describes errors affecting GPS measurements and Techniques used for mitigation thereof. Chapter three describes the process through which this research has been conducted, starting from techniques involved in data collection and processing. Description of how differencing was done using GAMIT/GLOBK is given and how Precise Point Positioning Solution was obtained, and finally a representation of how comparison of the two methods was made is given.

Chapter four discusses the results and analysis in which double differencing solution from GAMIT/GLOBK is compared with PPP solution from APPS. An overview of the results from online PPP solution is also included and assessment of PPP solution is made.

In chapter five, some conclusions are drawn, and recommendations about the future finds are provided. Finally, there is a list of references used in this research and a list of indices showing the rest of results from GPS data processing.

CHAPTER TWO

2. LITERATURE REVIEW-THEORY OF GPS

2.1 Introduction

The NAVSTAR Global Positioning System (GPS) is a satellite-based navigation system that was developed by the U.S. Department of Defense (DoD) in the early 1970s. Formerly, GPS was developed as a military system to fulfill U.S. military functions. However, it was later made accessible to civilians, and is currently a navigation system in which technology is available for both military and civilian users. GPS provides continuous positioning and timing information, anywhere in the world under any weather conditions.

GPS is comprised of a core constellation of 24 satellites. The constellation of GPS is the arrangement of satellites into six orbital planes which are equally arranged in space surrounding the Earth at an altitude of about 20200km above the earth's surface. Measured from the centre of the earth the semi major axis of GPS orbit is thus about 26,560km (Figure 2.1). With this geometry of constellation, and "if an elevation angle of 10^0 is considered", enables visibility of four to ten GPS satellites everywhere on the globe. Principally, only four satellites are required to give coordinates (X, Y, Z or φ, λ, h) at a given point.

Orbits containing GPS satellites are elliptical but almost circular with $e \cong 0.01$(eccentricity) and inclined at about 55^0 to the equator (tilting of the GPS orbit relative to Earth's equator).

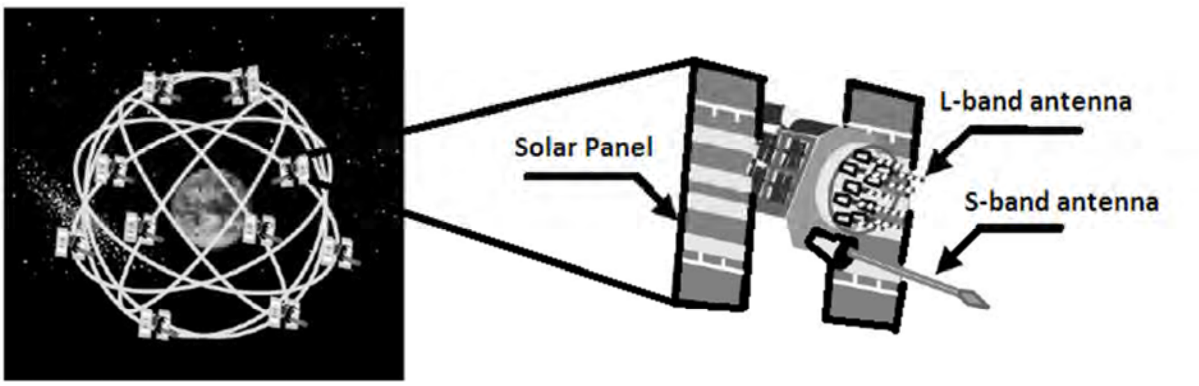

Figure 2.1: GPS Constellation Source: El-Rabbany, (2002)

2.2 GPS segments

GPS consists of three segments including the space segment, the control segment, and the user segment (Figure 2.3).

2.2.1 The space segment

The space segment is a constellation of 24 core satellites and other additional satellites as spares. These segments operate under the principle of electromagnetic wave propagation. The space segment is a passive system in which each satellite transmits a signal, in a sense that it only sends but does not receive any signal. The signal is comprised of two carrier frequencies L1 and L2 which are integer multiples of fundamental frequency of 10.23MHz, two digital codes namely Coarse Acquisition (C/A) code and Precise (P) code , and a navigation message.

The L1 and L2 signals are carried onto which the C/A, and P codes and the navigation message are modulated in binary form and transmitted to the user segment. This transmission is controlled by highly accurate atomic clocks onboard satellite. The distance or ranges between user, receiver and satellite is determined by measuring the time of signal transfer (carrier phase and/or codes) from satellite to receiver. The coordinates of a point is then determined using basically three ranges to satellites whose position information is received via navigation message and assumed known. The fourth satellite is necessary because the satellite position is a function of time.

The space segment is from time to time improved by launching new satellites. Technological advances in satellite positioning are grouped in Blocks. Block I 1978-1985 & Block II 1989-1990 satellites are no longer in service (ftp://tycho.usno.navy.mil/pub/gps/gpsb2.txt).

Figure 2.2 shows operational Blocks their timelines and main innovations introduced by each new satellite block.

Figure 2. 2: GPS satellites blocks features: (De Agostino et al 2008).

In modernized GPS new signals have been invented to increase accuracy in positioning. These signals are L2C, L5, CNAV and L1C. L2C is a second civilian code on Block IIR-M satellites. It is centred on L2 frequency with a chip rate ranging from Civil Moderate (CM=10230chips) to Civil long (CL=767250 chips). L2CM has 10230 chips repeating every 20 milliseconds giving a chipping rate of 511.5kcps. It is modulated by CNAV navigation data. L2CL has 767250 chips and repeats 1.5 seconds giving a chipping rate similar to L2CM. It is without data modulation. L2CM and L2CL are then combined in multiplex so that the chipping rate is the same as the legacy C/A code 1.023Mcps (Leandro et al 2008). L2C is less noise compared to C/A code. It is transmitted by Block IIR-M Block IIF and all modernized subsequent satellites (De Agostino et al 2008).

L5 is a third frequency after L1 and L2 (Block IIF). It is centred at 1176.45MHz with a new civilian (3^{rd} civilian code) with a chip rate ten time greater than C/A and L2C (10230 chips) and stronger than both C/A L2C codes. It will have a significant boost especially in indoor positioning (De Agostino et al 2008).

CNAV (Civil Navigation) is the navigation message (Block IIF) with navigation structure similar to that implemented for L5 code. It is more compact and flexible than the former Navigation message, and more importantly it can broadcast some additional information for instance the code bias from C/A, P1, P2, and L2C codes (De Agostino et al 2008).

L1C is the fourth civil code planned for Block III satellites, which will integrate but not replace C/A code, centred on L1 frequency.

The 1st modernized block IIR-M satellite was launched on Sep 26, 2005. By January 2009 already 1st civilian signals L2C was transmitted by six modernized GPS block IIR-M satellites, (Wübbena et al 2009) and by April 2009 seven modernized GPS block IIR-M transmitting L2C were already in orbit, (Meur et al 2010). The 7th satellite named SV49 with Pseudo random number PRN1 launched on March 24, 2009 also transmits L5 the third frequency, since April 10, 2009. (Meurer et al 2009).

2.1.2 The control segment

The control segment is network of tracking stations distributed worldwide. It consists of a Master Control Station (MCS) and Monitor stations. The master control station, is located at Schriever Air Force Base in Colorado Springs, Colorado, and is responsible for overall management of the remote monitoring and transmission sites. Master Control Station computes position, velocity, right ascension, and declination and other parameters for eventual upload to GPS satellite, via the S-band link.

Monitor Stations: there are six monitor stations located at Schriever Air Force Base in Colorado, Cape Canaveral, Florida, Hawaii, Ascension Island in the Atlantic Ocean, Diego Garcia Atoll in the Indian Ocean, and Kwajalein Island in the South Pacific Ocean. Each of the monitor stations checks the exact altitude, position, speed, and overall health of the orbiting satellites. The control segment uses measurements collected by the monitor stations to predict the behavior of each satellite's orbit and clock. The prediction data is up-linked, or transmitted, to the satellites. These data are finally transmitted back to the users. The control segment also ensures that the GPS satellite orbits and clocks remain within acceptable limits.

2.1.3 The user segment

The user segment consists of all users military and civilian as well having GPS receivers. A GPS receiver is basically a range measurement gadget and a position is determined from satellite position and intersection of receiver-satellite ranges vectors.

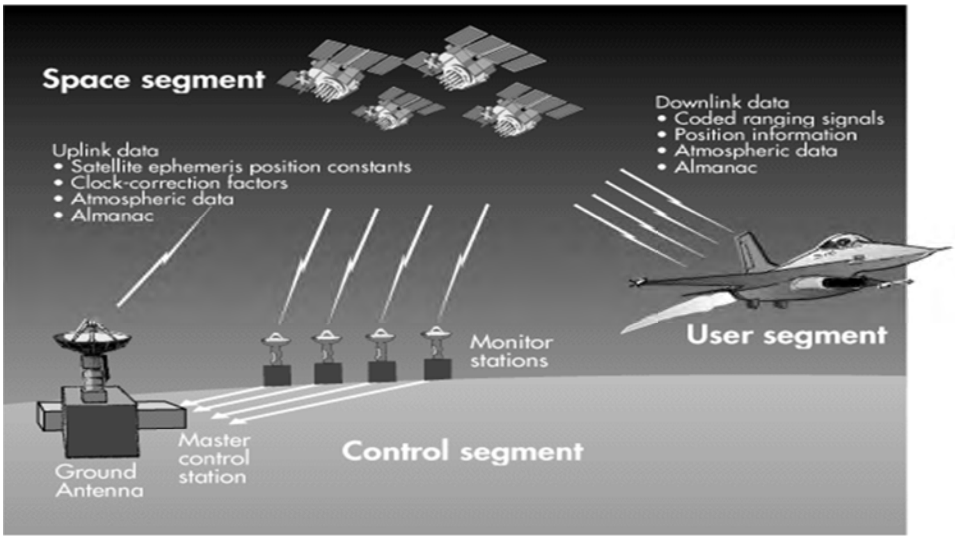

Figure 2. 3: GPS Segments (Source http://www.phy.syr.edu/courses/PHY312.03Spring/GPS/GPS.html)

2.2 Gps Signal (Carrier Phases, Codes and Navigation Messages)

The principle of GPS signal is based on the principle of propagation of electromagnetic wave (Figure 2.4)

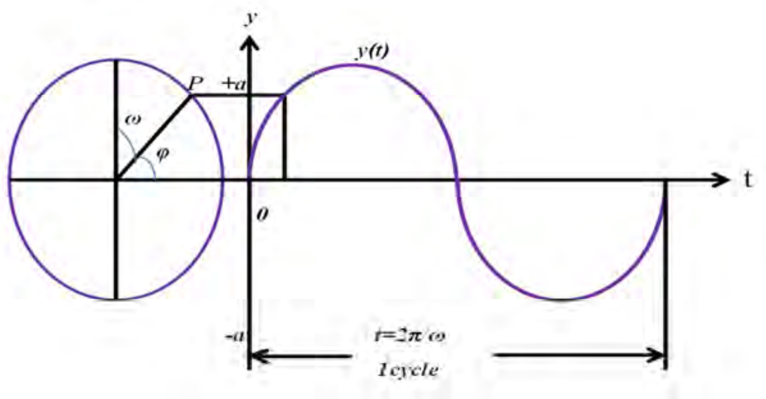

Figure 2. 4: ***Basic EM wave***

$$y(t) = a\sin(2\pi f t + \varphi_o)$$

$$P = \frac{1}{f}, \omega = 2\pi f, \varphi = f\,t$$

The signal transmitted by GPS satellite is a microwave radio signal modulated on two carriers, in L-band namely; L1 and L2. The P code is modulated on both L1 and L2, and the C/A-code is modulated on L1 only 90^0 offset with the P-code.

The frequencies of L1 and L2 are multiples of a fundamental frequency $f_0 = 10.23MHz$. $L_1 = 154xf_0 = 1575.42MHz$ and $L_1 = 120xf_0 = 1227.60MHz$

Other components of the satellite signal include the navigation Message with satellite ephemeris/orbits and the W code (Table 2.1 and Figure 2.5).

Table 2.1: Component of the satellite signal.

Component	frequency	MHz
Fundamental frequency	f_0	10.23
Carrier L1	$f_1=154f_0$	1575.42
Carrier L2	$f_2=120f_0$	1227.60
Carrier L5	$f_5=115f_0$	1176.45
P code	f_0	10.23
C/A code	$\frac{f_0}{10}$	1.023
W-code	$\frac{f_0}{20}$	0.5115
Navigation Message	$\frac{f_0}{204600}$	$50x10^{-6}$

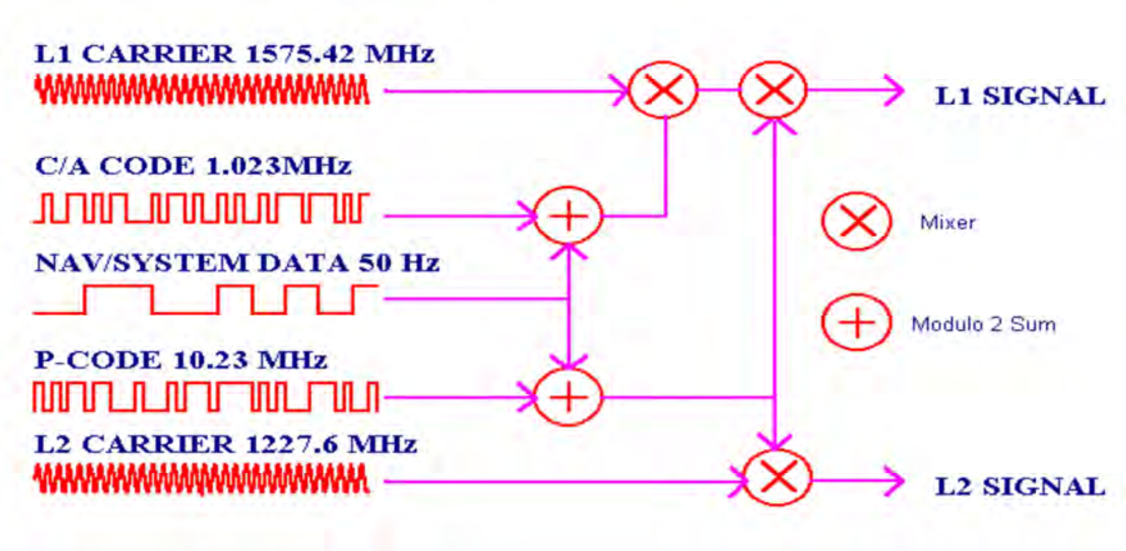

Figure 2. 5: ***Components GPS Signal***

With respect to figure 2.5 the carrier phase model can be written as follows

$$L1(t) = a_1 P(t) W(t) D(t) \sin(2\pi f_1 t + \varphi_0) + a_1 C/A(t) D(t) \cos(2\pi f_1 t + \varphi_0)$$

$$L2(t) = a_1 P(t) W(t) D(t) \sin(f_2 t + \varphi_0)$$

where:

$L_1(t)$ is the range as computed from carrier phase of frequency f_1

$L_2(t)$ is the range as computed from carrier phase of frequency f_2

2.3 Errors affecting GPS measurements

GNSS Measurements are affected by a number of errors, the known errors include, Selective Availability (no longer applicable), Ionospheric Propagation delay, Tropospheric Propagation delays, The Multipath Problem, Ephemeris Data Errors, Onboard/satellite Clock Errors, receiver clock errors, and other unmodeled errors (Figure 2.6).

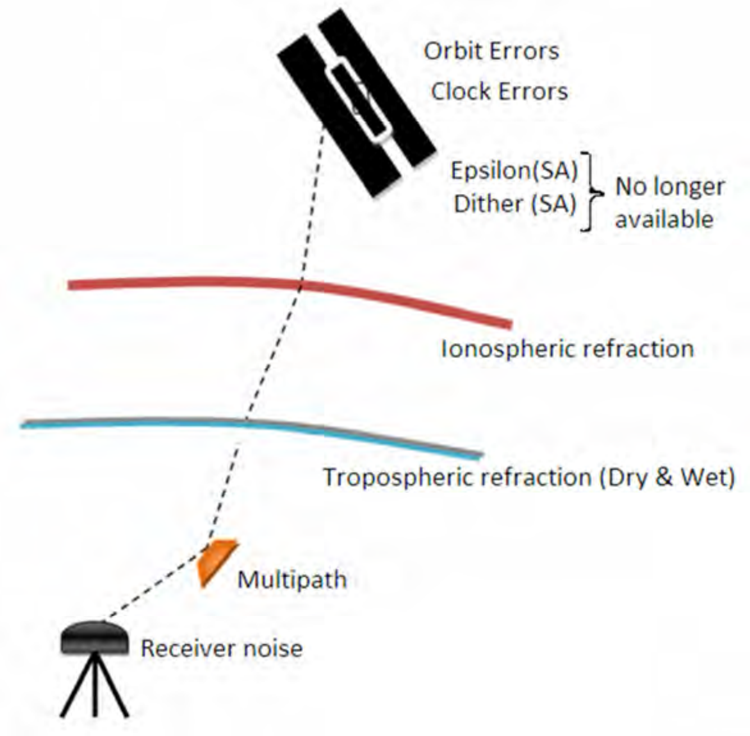

Figure 2. 6: Errors affecting GPS measurements.

2.3.1 Ionosphere

The ionosphere is frequency dependent (i.e. a dispersive medium) which is a major source of range and range-rate error for GPS positioning

It is located in the region between 70 km and 1000 km, formed by the UV ionizing radiation from the sun, thus it contains weekly ionized plasma or gas, which can affect radio wave propagation in various ways (Figure 2.7). Its variability is much larger than the troposphere as it Changes rapidly in absolute value and it is difficult to model.

The delay is dependent on Total Electronic Count (TEC). It is larger from low elevation satellites. It gets its peak in the day time (solar radiation effect) and subsides during the night.

Near the geomagnetic equator /poles the delays are larger and the effects increase during the solar maxima.

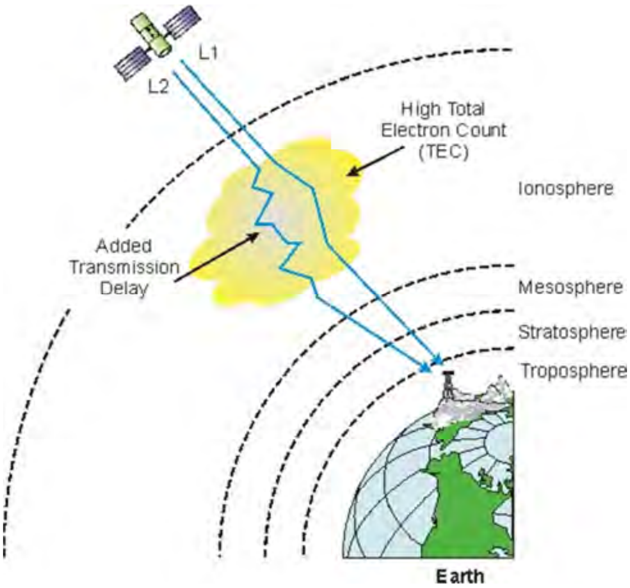

Figure 2. 7: ***shows how ionospheric delay can affect the transmission of GPS radio signals***

Source: http://www.wirelessdictionary.com/Wireless-Dictionary-Ionospheric-Delay-Definition.html

2.3.2 Troposphere

The troposphere is the lower part of the atmosphere up to $70\ km$ altitude; this part of the atmosphere is electrically neutral and thus is a non-dispersive medium with respect to the radio waves up to frequencies of 15GHz. therefore the propagation is frequency independent unlike the ionospheric refraction, consequently it affects both the code and phase measurements the same way. The disadvantage is that an elimination of the tropospheric refraction by dual/triple frequency techniques is not possible. The range delay is divided into dry and wet components, with a total delay exceeding 2.5m in zenith direction and increases approximately proportional to the *cosecant* of the elevation angle. The dry part of the tropospheric delay amounts to 90% of the total delay (Musa, et al, 2005), and is stably predictable based on models, e.g. UNB3m, (Leandro et al, 2006), IGGtrop (Li et al, 2012), the wet delay is 10% of the total delay and is significantly variable, it contains 99% of the water vapour in the lower atmosphere 0 to 10km above Mean sea level. The effect is bigger in tropics up to 40mm and reduces as one comes close to the pole about 1mm. the variability is 3cm per hour during weather front. There is correlation between tropospheric delay and height which makes it more complicated.

Tropospheric refractivity of the transmitted signal is due to variability of the refractive index of the lower troposphere, as a function of pressure temperature and humidity or water vapour.

The ray bends according to Fermat's principle which states that the actual path selected by light makes the value of the integral least(light follows the path of least time) see Figure 2.8 The fundamental principle is that tropospheric effects obey the applicability of geometrical optics. Assuming this to hold true, the tropospheric delay is defined as: (Pany 2003).

$$T = S - G = \int_S nds - \int_G ds$$

where, S is the apparent (or electrical) path and G is the Geometrical Path (straight line), n is the refractive index.

The range measured is given by

$$s = \int_{user}^{sat} nds$$

Fermat's principle

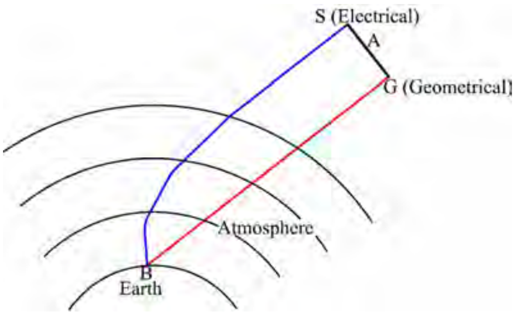

Figure 2. 8: Diagram showing path of GPS signal for a ray from A to B through the atmosphere in geodetic measurements.

2.3.3 Multipath

Multipath refers to the situation when a signal travels more than one path (Figure 2.9). This happens when the signal travels via more than one path by reflection, diffraction, or scattering.

In terrestrial satellite positioning the signals are usually reflected from buildings trees or ground while in airborne surveys, signals are reflected from the host vehicle body.

More on multipath is discussed under 2.6 Mitigation of GPS Errors Using Models and Linear combination of code and phase observations particularly 2.6.4 Multipath Mitigation.

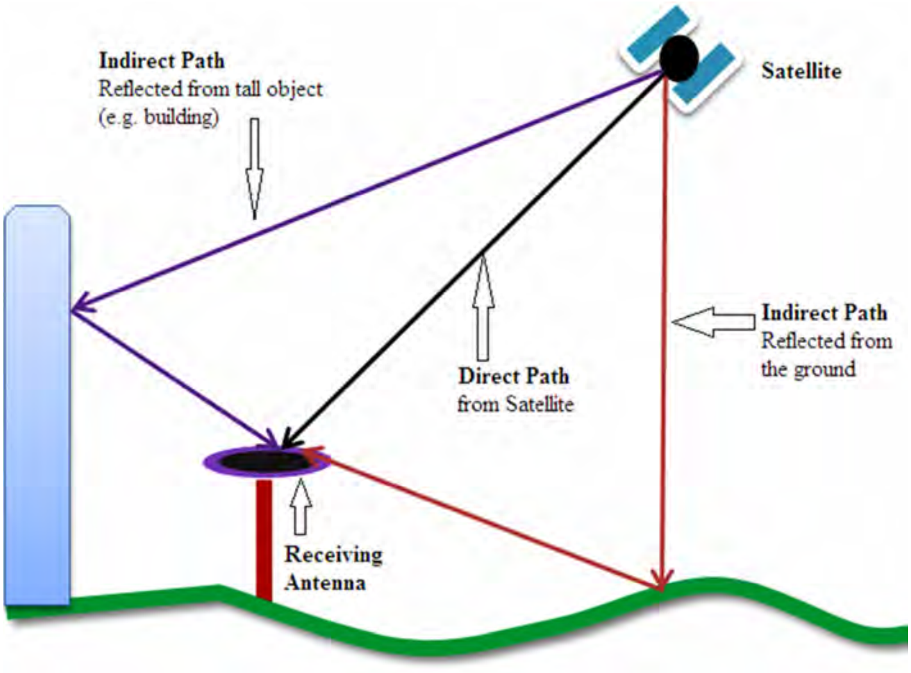

Figure 2. 9: Errors due to Multipath

Referring to Figure 2.9, the satellite signal arrives at the receiver in three different paths, one direct and two indirect ones. Consequently, the received signals have relative offsets and phase differences are proportional to the difference in path lengths.

2.3.4 Satellite clock errors

These are errors in the transmitted clock parameters, and formerly it was including SA.

2.3.5 Receiver noise

These are errors in the receiver's measurement of range caused by receiver clock error, thermal noise.

2.3.6 Satellite orbits /Ephemeris data errors

An "ephemeris error" is a difference between the expected and actual orbital position of a GPS satellite due to failure to model absolutely the forces acting on a satellite. Because GPS receivers use the satellite's location in position calculations, orbital error reduces GPS accuracy. Orbital residual error is significant for long baseline (over 500 km) This can be justified using, as a rule of thumb the expression for studying the effects of orbit errors on baseline determination derived by Vaníček and others (Vaníček et al., 1985):

$$\frac{dB}{B} = \frac{dr}{\rho}$$

Where

dB is the error incurred in estimating a baseline of length B due to an error dr in the assumed position of satellite with approximate range ρ from the receiver.

Broadcast orbit: is determined based on pseudorange with uncertainties ~ 100cm (1m) and the final precise orbit is determined based on phase observables, with uncertainties ~ 2.5cm (0.025m) http://igscb.jpl.nasa.gov/components/prods.html.

Note: that figure 2.10 is much exaggerated for explanation

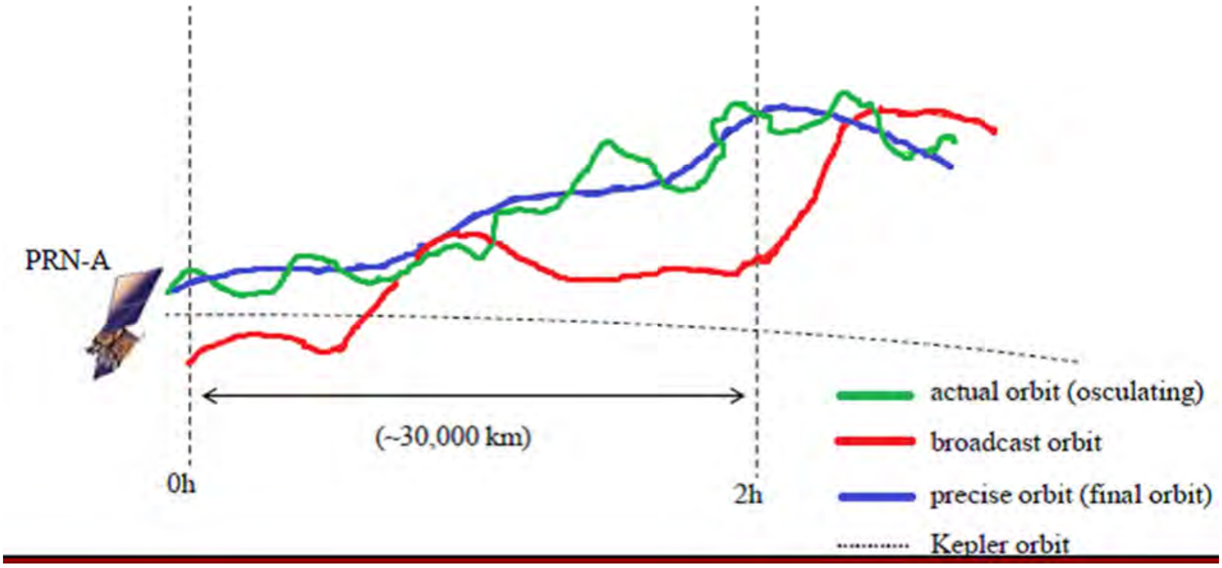

Figure 2. 10: Diagram showing satellite orbits (actual/osculating, broadcast, Precise (final), and Keplerian orbit (Ahn 2012) – UNB.

2.3.7 Miscellaneous GPS errors

2.3.7.1 Geometric errors (GDOP)

GPS ranging errors are magnified due to range vector differences between the receiver and the Satellites. The Geometric Dilution of precision (GDOP) describes the geometric strength of satellite configuration on GPS accuracy (Figure 2.11). At least four satellites in view are required for position computation but satellite geometry can affect the quality of GPS signals and accuracy of receiver position and time.

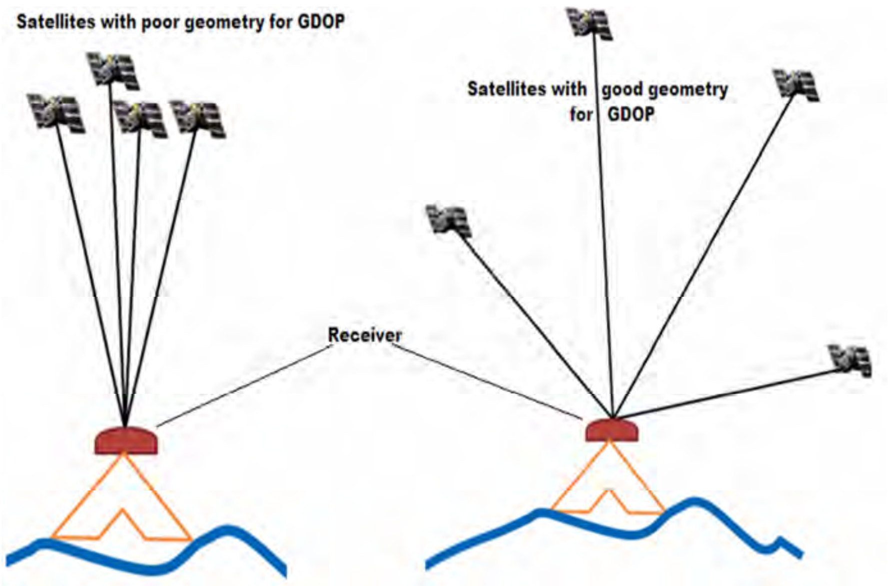

Figure 2. 11: Schematic diagram for GDOP

2.3.7.2 Cycle Slips

Cycle slips are due to Obstruction of Satellite Signals, bad Ionosphere condition, Multi Path, Satellite Elevation, Receiver software failure, and Satellite oscillator malfunctioning.

2.3.7.3 Integer ambiguity (N)

Integer ambiguity (N) refers to the unknown number of whole wavelengths of the carrier signal i.e. the phase of a particular cycle of a carrier wave can be measured very accurately; however it is impossible to discriminate between different carrier cycles since GPS signals are transmitted by the satellites as pure sinusoidal waves, if the modulated messages and PRN codes are ignored. As it is shown in Figure 2.12, the satellite broadcasts a sine wave carrier signal with a certain phase. The signal is received by the GPS antenna with another phase at the time of reception. The receiver generates an identical copy of the signal as the one generated by the satellite and compares the generated phase with the observed one to derive the phase observation. However, the integer number of wavelengths between the satellite and the receiver during the travel time of the signal is not known. This number is called integer ambiguity and is denoted by the letter ***N.***

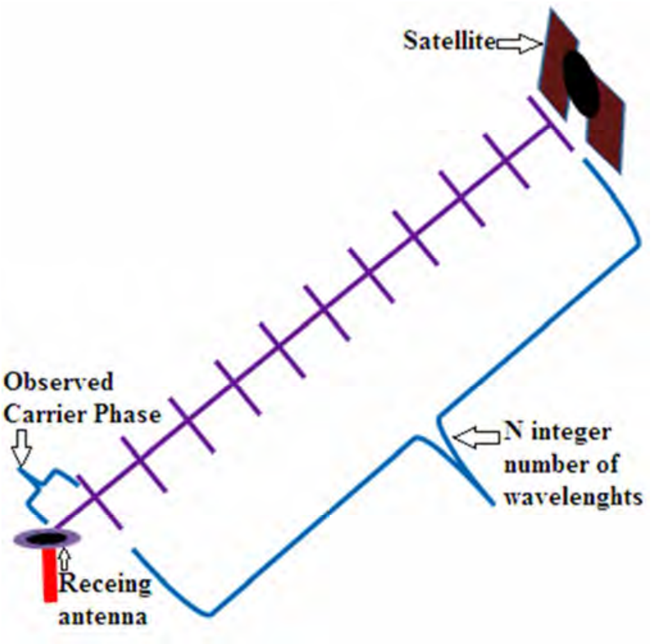

Figure 2. 12: ***physical meaning of Integer Ambiguity***

2.4 GPS standard observation model

GPS receiver position is computed based on satellite positions. The basic principle is measurement of ranges from receiver to satellite by using the principle of propagation of electromagnetic waves. The speed of E.M wave in vacuum is a known constant c=299792458 m/s.

When the signal arrives at the receiving antenna, the time taken from satellite to receiver is measured as $dt = (dt^r - dt^s)$ and the range is derived as $\rho = c.dt$ If we take into account the errors affecting GPS measurements in both codes and carrier phases, we have the following basic equations.

$P_1 = \rho + c(dt^r - dt^s) - I + T + M + b^r_{p_1} - b^s_{p_1} + \varepsilon_{p_1}$

$P_2 = \rho + c(dt^r - dt^s) - q^2 I + T + M + b^r_{p_2} - b^s_{p_2} + \varepsilon_{p_2}$

$\lambda_1(\varphi_1 + N_1) =$

$L_1 = \rho + c(dt^r - dt^s) - I + T + M + b^r_{L_1} - b^s_{L_1} + \varepsilon_{L_1}$

$\lambda_2(\varphi_2 + N_2) =$

$L_2 = \rho + c(dt^r - dt^s) - q^2 I + T + M + b^r_{L_2} - b^s_{L_2} + \varepsilon_{L_2}$

ρ_i is a pseudorange measurement made at frequency i

φ_i is a carrier phase measurement made at frequency i.

L_i is a precise pseudorange measurement made at frequency i

The integer ambiguity N_i is written on the left side to show how it converts the ambiguous phase measurement φ_i into a precise pseudorange L_i.

The factor q represents the ratio of the primary and secondary GPS frequencies; c is the speed of light and λ_i is the frequency-dependent wavelength of the carrier phase measurements. ρ Represents the geometric range between transmitter and receiver antennas, I is the range delay and apparent phase advance on the primary frequency caused by signal propagation through the upper atmosphere (predominantly the Ionosphere), and T is the range delay caused by signal propagation through the lower atmosphere (predominantly the Troposphere), M is the error due to multipath. The remaining, non-geometric, parameters are the oscillator or 'clock' errors for both the transmitter and receiver (dt^s and dt^r), and common-oscillator hardware biases (b_*^*) for each observation. Unmodeled random errors are represented by ε_*.

With the exception of Multipath, most of the above errors are correlated and can be mitigated using differential GPS technique which is hereunder described.

2.5 Mitigation of correlated errors using differential GPS

Differential GNSS or relative positioning employs two GPS receivers simultaneously tracking the same satellites to determine their relative coordinates.

The principle is that, one of the receivers position is known and the other is unknown. The unknown point can be stationary or moving (Kinematic). Relative positioning can be performed with code ranges or phase ranges. The principle is to improve the determined position of a roving station by applying corrections provided by a GPS monitoring station, also called reference station. Different procedures are in use for generating corrections (Seeber, 2003).

(i) Corrections in the *position domain*

The GPS-derived position of the reference station is compared with its a priori known position. Position corrections *{x, y, z}* or, $\{\phi, ,\lambda, ,h\}$ are transmitted and used to correct the rover position.

(ii) Corrections in the *measurement domain*

The observed pseudoranges to all visible satellites are compared with ranges derived from known satellite and station positions. The differences are transmitted to the rover to correct its observed pseudoranges.

(iii) Corrections in the *state space domain*

Observations from several reference stations are used to estimate the state vector of the biases within the working area.

The first option (i) is rather simple, but also not very flexible. It only works if the same satellites are used at the reference and rover stations, and it is only efficient over short distances. It is therefore seldom applied.

Option (ii) is the ordinary DGPS procedure. It is very flexible and works well within a radius of several hundred kilometers about the reference station. Due to decorrelation of the biases with distance (orbit, ionospheric and tropospheric delay) the accuracy decreases roughly by about 1m per 100 km.

Option (iii) is the most flexible procedure, and allows the use of DGPS over larger distances (Wide Area Differential GPS (WADGPS) and for precise applications in surveying and geodesy (networked reference stations). Whereas option (ii) is based on observed pseudorange corrections (scalar corrections), option (iii) is based on correction vectors.

Although DGPS is effective in removing satellite and receiver clock errors, ionospheric and tropospheric errors, ephemeris errors, and selective availability errors, it cannot remove errors due to multipath, receiver inter-channel biases, and thermal noise, since these errors are not common to the roving and reference receivers. (Grewal et al, 2007).

DGPS/DGNSS is categorized based on how the differences are performed or based on the distance and Number/network of reference receivers. Based on how differences are done we have single Double and Triple Differences. Based on the distance between receivers and network of reference receivers we have Local Area Differential GPs (LAGPS), Wide Area Differential GPS (WADGPS), and Global Differential GPS (GDGPS).

Below is a discussion of different differencing techniques, starting with single differences. The so called zero difference will be discussed under Precise Point Positioning (PPP) in 2.7.

2.5.1 Single Differences

In single difference two points and one satellite are involved. Representing the receiver stations by A and B and the satellite by j, the single difference observations (here only phase observables are considered) are constructed as:

$$\mathrm{L}_A^j = \rho_A^j + c\delta t_A - c\delta t^j + T_A^j - I_A^j + M_A^j + E_A^j + \lambda N_A^j + \lambda\delta\varphi_A^j + \delta\varepsilon_A^j \qquad \text{...……….(2.1)}$$

$$\mathrm{L}_B^j = \rho_B^j + c\delta t_B - c\delta t^j + T_B^j - I_B^j + M_B^j + E_B^j + \lambda N_B^j + \lambda\delta\varphi_B^j + \delta\varepsilon_B^j \qquad \text{………..(2.2)}$$

L_A^j , L_B^j = carrier phase measurements for receiver A&B respectively,

ρ_A^j, ρ_B^j = pseudo range from phase measurement for receivers A&B respectively

$\delta t_A, \delta t_B$ = time at which signal was received by receivers A&B respectively

δt^j= time at which signal was transmitted from satellite j

T_A^j, T_B^j =tropospheric delays for receivers A&B respectively

$I_{A,}^j\ I_B^j$ = ionospheric delays for receivers A&B respectively

$M_A^j,\ M_B^j$ = multipath for receivers A&B respectively

$E_A^j,\ E_B^j$ =ephemeris errors (error in transmitted satellite position and velocity)

$N_{A,}^j N_B^j$ = integer Ambiguity for receivers A&B respectively

$\delta\varphi_A^j,\ \delta\varphi_B^j$= Carrier-phase Fractional bias for receivers A&B respectively

$\delta\varepsilon_A^j, \delta\varepsilon_B^j$ Other errors (e.g. poor GDOP, cycle slips & other unmodeled biases)

The single difference between the above two equations are

$$\Delta L_{AB}^J = L_A^J - L_B^J$$

$$= (\rho_A^j + c\delta t_A - c\delta t^j + T_A^j - I_A^j + M_A^j + E_A^j + \lambda N_A^j + \lambda\delta\varphi_A^j + \delta\varepsilon_A^j) - (\rho_B^j + c\delta t_B - c\delta t^j + T_B^j - I_B^j + M_B^j + E_B^j + \lambda N_B^j + \lambda\delta\varphi_B^j + \delta\varepsilon_B^j)$$

$$= (\rho_A^j - \rho_A^j) + (c\delta t_A - c\delta t_B) - (c\delta t^j - c\delta t^j) + (T_A^j - T_B^j) - (I_A^j - I_B^j) + (M_A^j - M_B^j) + (\delta E_A^j - \delta E_B^j) + (N_A^j - N_B^j) + (\lambda\delta\varphi_A^j - \lambda\delta\varphi_B^j) + (\delta\varepsilon_A^j - \delta\varepsilon_B^j)$$

$$= \Delta\rho_{AB}^j + \Delta c\delta t_{AB} + \Delta T_{AB}^j - \Delta I_{AB}^j + \Delta M_{AB}^j + \Delta E_{AB}^j + \Delta\lambda N_B^j + \Delta\lambda\delta\varphi_{AB}^j + \Delta\varepsilon_{AB}^j \quad \text{….(2.3)}$$

The double sub-script is used to denote that the difference is made between two receivers and the triangular sign emphasizes that the difference is between two points on the ground.

Equation (3) is referred to as the single-difference equation.

Single differences are used to cancel common effects shared by signals travelling from a satellite through different paths. (e.g. Satellite clock bias).

The main advantage of the single difference is that, the satellite clock bias is cancelled in the process. Nevertheless, it remains sensitive to both receiver clock errors. Figure 2.13 shows a conceptual view of the single-difference approach.

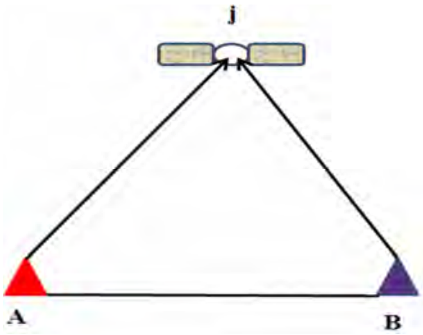

Figure 2. 13: ***Single difference used to reduce satellite clock and orbit errors, and localized atmospheric errors it involves two receivers with one satellite.***

2.5.2 Double Differences

Assuming two stations *A* and *B* and two satellites *j*, *k* (see Figure 2.14), two single differences according to equation (3) can be formed:

$$\Delta L_{AB}^{J} = \Delta\rho_{AB}^{j} + \Delta c\delta t_{AB} + \Delta T_{AB}^{j} - \Delta I_{AB}^{j} + \Delta M_{AB}^{j} + \Delta E_{AB}^{j} + \Delta\lambda N_{AB}^{j} + \Delta\lambda\delta\varphi_{AB}^{j} + \Delta\varepsilon_{AB}^{j} \text{-----(2.4a)}$$

$$\Delta L_{AB}^{K} = \Delta\rho_{AB}^{K} + \Delta c\delta t_{AB} + \Delta T_{AB}^{K} - \Delta I_{AB}^{K} + \Delta M_{AB}^{K} + \Delta E_{AB}^{K} + \Delta\lambda N_{AB}^{K} + \Delta\lambda\delta\varphi_{AB}^{K} + \Delta\varepsilon_{AB}^{K} \text{----(2.4b)}$$

The double difference is formed by subtracting two single differences in equations (2.4a) and (2.4b).

$$\nabla\Delta L_{AB}^{JK} = \left(\Delta\rho_{AB}^{j} + \Delta c\delta t_{AB} + \Delta T_{AB}^{j} - \Delta I_{AB}^{j} + \Delta M_{AB}^{j} + \Delta E_{AB}^{j} + \Delta\lambda N_{B}^{j} + \Delta\lambda\delta\varphi_{AB}^{j} + \Delta\varepsilon_{AB}^{j}\right) -$$
$$(\Delta\rho_{AB}^{K} + \Delta c\delta t_{AB} + \Delta T_{AB}^{K} - \Delta I_{AB}^{K} + \Delta M_{AB}^{K} + \Delta E_{AB}^{K} + \Delta\lambda N_{AB}^{K} + \Delta\lambda\delta\varphi_{AB}^{K} + \Delta\varepsilon_{AB}^{K})$$
$$= \left(\Delta\rho_{AB}^{j} - \Delta\rho_{AB}^{K}\right) + (\Delta c\delta t_{AB} - \Delta c\delta t_{AB}) + (\Delta T_{AB}^{j} - \Delta T_{AB}^{K}) - (\Delta I_{AB}^{j} - \Delta I_{AB}^{K}) + (\Delta M_{AB}^{j} - \Delta M_{AB}^{K})$$
$$+ (\Delta E_{AB}^{j} - \Delta E_{AB}^{K}) + (\Delta\lambda N_{AB}^{j} - \Delta\lambda N_{AB}^{K}) + (\Delta\lambda\delta\varphi_{AB}^{j} - \Delta\lambda\delta\varphi_{AB}^{K}) + \left(\Delta\varepsilon_{AB}^{j} - \Delta\varepsilon_{AB}^{K}\right)$$
$$= \nabla\Delta\rho_{AB}^{JK} + \nabla\Delta T_{AB}^{JK} - \nabla\Delta I_{AB}^{JK} + \nabla\Delta M_{AB}^{JK} + \nabla\Delta E_{AB}^{JK} + \Delta\lambda N_{AB}^{JK} + \nabla\Delta\lambda\delta\varphi_{AB}^{JK} + \nabla\Delta\varepsilon_{AB}^{JK} \ldots\ldots\text{(2.5)}$$

But

$$\nabla\Delta\lambda\delta\varphi_{AB}^{JK} = \Delta\lambda\delta\varphi_{AB}^{j} - \Delta\lambda\delta\varphi_{AB}^{K}$$
$$= \lambda(\varphi_A - \varphi^j) - \lambda(\varphi_B - \varphi^j) - \lambda(\varphi_A - \varphi^k) + \lambda(\varphi_B - \varphi^k) \ldots\ldots\ldots\ldots\ldots\ldots\text{(2.6)}$$

Hence

$$\nabla\Delta L_{AB}^{JK} = \nabla\Delta\rho_{AB}^{JK} + \nabla\Delta T_{AB}^{JK} - \nabla\Delta I_{AB}^{JK} + \nabla\Delta M_{AB}^{JK} + \nabla\Delta E_{AB}^{JK} + \nabla\Delta\lambda N_{AB}^{JK} + \nabla\Delta\varepsilon_{AB}^{JK} \ldots\ldots\ldots\ldots\text{(2.7)}$$

The double super-script is used to denote quantities identified with two satellites and the upside down triangular symbol emphasizes that the difference is made between two points in the sky

The main advantage of double difference is that the receiver clock errors are cancelled to first order, i.e. it cancels large receiver clock errors, even though the residual effect due to “time tag bias” on the range computation does cancel completely, and if receiver separation is too large it must be dealt with.

The double differenced observation has an additional advantage as shown in equation 6 in that the fractional part of the ambiguity term cancels, and hence the ambiguity term is now an integer

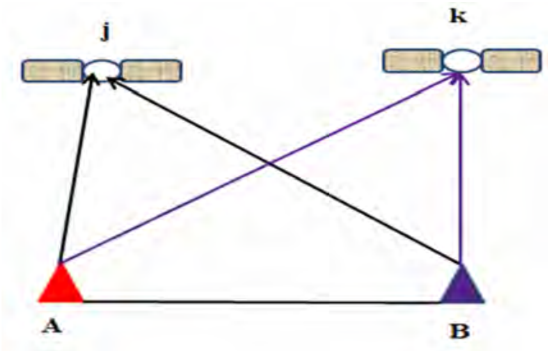

Figure 2. 14: Conceptual representation of double differencing between two satellites

2.5.3 Triple Differences

A triple difference observable is the difference between two double difference observables for consecutive epochs, t_1 and t_2 (Figure 2.15 show satellites J and K at two different epochs both observed by receivers A and B simultaneously).

$\nabla\Delta L_{AB}^{JK}(t_1) = \nabla\Delta\rho_{AB}^{JK}(t_1) + \nabla\Delta T_{AB}^{JK}(t_1) - \nabla\Delta I_{AB}^{JK}(t_1) + \nabla\Delta M_{AB}^{JK}(t_1) + \nabla\Delta E_{AB}^{JK}(t_1) + \nabla\Delta\lambda N_{AB}^{JK} + \nabla\Delta\varepsilon_{AB}^{JK}(t_1)$ ………2.7

$\nabla\Delta L_{AB}^{JK}(t_2) = \nabla\Delta\rho_{AB}^{JK}(t_2) + \nabla\Delta T_{AB}^{JK}(t_2) - \nabla\Delta I_{AB}^{JK}(t_2) + \nabla\Delta M_{AB}^{JK}(t_2) + \nabla\Delta E_{AB}^{JK}(t_2) + \nabla\Delta\lambda N_{AB}^{JK} + \nabla\Delta\varepsilon_{AB}^{JK}(t_2)$ ………(2.8)

Equations 7 and 8 are two double differences. The triple difference is given by their difference

$\delta(t_1, t_2)\nabla\Delta L_{AB}^{JK} = \nabla\Delta L_{AB}^{JK}(t_2) - \nabla\Delta L_{AB}^{JK}(t_1)$

$= \delta(t_1, t_2)\nabla\Delta\rho_{AB}^{JK} + \delta(t_1, t_2)\nabla\Delta T_{AB}^{JK} - \delta(t_1, t_2)\nabla\Delta I_{AB}^{JK} + \delta(t_1, t_2)\nabla\Delta M_{AB}^{JK} + \delta(t_1, t_2)\nabla\Delta E_{AB}^{JK} + \delta(t_1, t_2)\nabla\Delta\varepsilon_{AB}^{JK}$ ……………..(2.9)

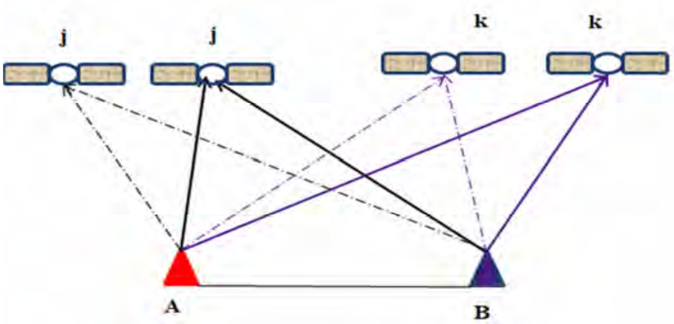

Figure 2. 15: Triple differencing

The main aim of the triple difference is to eliminate the integer ambiguity. Any cycle slips after triple difference will appear as outliers, and can easily be removed by conventional techniques. The weakness of triple difference is that it introduces correlations between observations in time, thus, decreasing the data weights, leading to significant degradation in precision, and therefore not appropriate for precise surveys. Nevertheless, it is very useful in that it helps in the determination of nominal parameters for double difference. It is strong in the detection and hence removal of cycle slips.

2.5.4 Linear model for relative positioning

From double differencing in units (equation 2.7) if we only consider integer ambiguity and ignore other errors, we have

$\nabla\Delta L_{AB}^{JK} = \rho_{AB}^{jK}(t) + \lambda N_{AB}^{jK}$ --- (2.10)

and

$\rho_{AB}^{jK}(t) = \rho_{B}^{K}(t) - \rho_{B}^{j}(t) - \rho_{A}^{K}(t) + \rho_{A}^{j}(t)$ ------------------------- (2.11)

From equation (11) we have four measurement quantities for double differencing. It is necessary to linearize each of the four measurements as follows

$$\rho_{AB}^{jK}(t) = \rho_{B0}^{K}(t) - \frac{X^k(t) - X_{B0}}{\rho_{B0}^{k}(t)}\Delta X_B - \frac{Y^k(t) - Y_{B0}}{\rho_{B0}^{k}(t)}\Delta Y_B - \frac{Z^k(t) - Z_{B0}}{\rho_{B0}^{k}(t)}\Delta Z_B$$

$$-\rho_{B0}^{j}(t) - \frac{X^j(t) - X_{B0}}{\rho_{B0}^{j}(t)}\Delta X_B - \frac{Y^j(t) - Y_{B0}}{\rho_{B0}^{j}(t)}\Delta Y_B - \frac{Z^j(t) - Z_{B0}}{\rho_{B0}^{j}(t)}\Delta Z_B$$

$$-\rho_{A0}^{K}(t) - \frac{X^K(t) - X_{A0}}{\rho_{A0}^{k}(t)}\Delta X_A - \frac{Y^K(t) - Y_{A0}}{\rho_{A0}^{k}(t)}\Delta Y_A - \frac{Z^K(t) - Z_{A0}}{\rho_{A0}^{k}(t)}\Delta Z_A$$

$$+\rho_{A0}^{j}(t) - \frac{X^j(t) - X_{A0}}{\rho_{A0}^{j}(t)}\Delta X_A - \frac{Y^j(t) - Y_{A0}}{\rho_{A0}^{j}(t)}\Delta Y_A - \frac{Z^j(t) - Z_{A0}}{\rho_{A0}^{j}(t)}\Delta Z_A \text{------------------------- (2.12)}$$

Where, the left side of equation (12) can be written with measurement quantities and approximate values.

$L_{AB}^{jK}(t) = \lambda\Phi_{AB}^{jK}(t) - \rho_{B0}^{K}(t) + \rho_{B0}^{j}(t) + \rho_{A0}^{K}(t) - \rho_{A0}^{j}(t)$ ---------------------(2.13)

In relative positioning one point must be known, e.g. station A. If A is known that means

$\Delta X_A = \Delta Y_A = \Delta Z_A = 0$

Thus

$$\rho_{AB}^{jK}(t) = \rho_{B0}^{K}(t) - \frac{X^k(t) - X_{B0}}{\rho_{B0}^{k}(t)}\Delta X_B - \frac{Y^k(t) - Y_{B0}}{\rho_{B0}^{k}(t)}\Delta Y_B - \frac{Z^k(t) - Z_{B0}}{\rho_{B0}^{k}(t)}\Delta Z_B$$

$$-\rho_{B0}^{j}(t) - \frac{X^j(t) - X_{B0}}{\rho_{B0}^{j}(t)}\Delta X_B - \frac{Y^j(t) - Y_{B0}}{\rho_{B0}^{j}(t)}\Delta Y_B - \frac{Z^j(t) - Z_{B0}}{\rho_{B0}^{j}(t)}\Delta Z_B$$

$-\rho_A^K(t) + \rho_A^j(t)$ --- (2.14)

If we consider four satellites (*j, k, l, and m*), we can form double differencing equations for two subsequent epochs of observation t_1, t_2 in vector and matrix form as

AX=L

Where:

$$L = \begin{bmatrix} \lambda\Phi_{AB}^{jK}(t_1) - \rho_{B0}^{K}(t_1) + \rho_{B0}^{j}(t_1) + \rho_{A0}^{K}(t_1) + \rho_{A0}^{j}(t_1) \\ \lambda\Phi_{AB}^{jl}(t_1) - \rho_{B0}^{l}(t_1) + \rho_{B0}^{j}(t_1) + \rho_{A0}^{l}(t_1) + \rho_{A0}^{j}(t_1) \\ \lambda\Phi_{AB}^{jm}(t_1) - \rho_{B0}^{m}(t_1) + \rho_{B0}^{j}(t_1) + \rho_{A0}^{m}(t_1) + \rho_{A0}^{j}(t_1) \\ \lambda\Phi_{AB}^{jK}(t_2) - \rho_{B0}^{K}(t_2) + \rho_{B0}^{j}(t_2) + \rho_{A0}^{K}(t_2) + \rho_{A0}^{j}(t_2) \\ \lambda\Phi_{AB}^{jl}(t_2) - \rho_{B0}^{l}(t_2) + \rho_{B0}^{j}(t_2) + \rho_{A0}^{l}(t_2) + \rho_{A0}^{j}(t_2) \\ \lambda\Phi_{AB}^{jm}(t_2) - \rho_{B0}^{m}(t_2) + \rho_{B0}^{j}(t_2) + \rho_{A0}^{m}(t_2) + \rho_{A0}^{j}(t_2) \end{bmatrix} X = \begin{bmatrix} \Delta X_B \\ \Delta X_B \\ \Delta Z_B \\ N_{AB}^{jk} \\ N_{AB}^{jl} \\ N_{AB}^{jM} \end{bmatrix} \text{---------------- (2.15)}$$

$A =$

$$\begin{bmatrix} -\frac{X^k(t_1)-X_{B0}}{\rho_{B0}^k(t_1)} + \frac{X^j(t_1)-X_{B0}}{\rho_{B0}^j(t_1)} - \frac{Y^k(t_1)-Y_{B0}}{\rho_{B0}^k(t_1)} + \frac{Y^j(t_1)-Y_{B0}}{\rho_{B0}^j(t_1)} - \frac{Z^k(t_1)-Z_{B0}}{\rho_{B0}^k(t_1)} + \frac{Z^j(t_1)-Z_{B0}}{\rho_{B0}^j(t_1)} & \lambda & 0 & 0 \\ -\frac{X^l(t_1)-X_{B0}}{\rho_{B0}^k(t_1)} + \frac{X^j(t_1)-X_{B0}}{\rho_{B0}^j(t_1)} - \frac{Y^l(t_1)-Y_{B0}}{\rho_{B0}^k(t_1)} + \frac{Y^j(t_1)-Y_{B0}}{\rho_{B0}^j(t_1)} - \frac{Z^l(t_1)-Z_{B0}}{\rho_{B0}^k(t_1)} + \frac{Z^j(t_1)-Z_{B0}}{\rho_{B0}^j(t_1)} & 0 & \lambda & 0 \\ -\frac{X^m(t_1)-X_{B0}}{\rho_{B0}^k(t_1)} + \frac{X^j(t_1)-X_{B0}}{\rho_{B0}^j(t_1)} - \frac{Y^m(t_1)-Y_{B0}}{\rho_{B0}^k(t_1)} + \frac{Y^j(t_1)-Y_{B0}}{\rho_{B0}^j(t_1)} - \frac{Z^m(t_1)-Z_{B0}}{\rho_{B0}^k(t_1)} + \frac{Z^j(t_1)-Z_{B0}}{\rho_{B0}^j(t_1)} & 0 & 0 & \lambda \\ -\frac{X^k(t_2)-X_{B0}}{\rho_{B0}^k(t_2)} + \frac{X^j(t_2)-X_{B0}}{\rho_{B0}^j(t_2)} - \frac{Y^k(t_2)-Y_{B0}}{\rho_{B0}^k(t_2)} + \frac{Y^j(t_2)-Y_{B0}}{\rho_{B0}^j(t_2)} - \frac{Z^k(t_2)-Z_{B0}}{\rho_{B0}^k(t_2)} + \frac{Z^j(t_2)-Z_{B0}}{\rho_{B0}^j(t_2)} & \lambda & 0 & 0 \\ -\frac{X^l(t_2)-X_{B0}}{\rho_{B0}^k(t_2)} + \frac{X^j(t_2)-X_{B0}}{\rho_{B0}^j(t_2)} - \frac{Y^l(t_2)-Y_{B0}}{\rho_{B0}^k(t_2)} + \frac{Y^j(t_2)-Y_{B0}}{\rho_{B0}^j(t_2)} - \frac{Z^l(t_2)-Z_{B0}}{\rho_{B0}^k(t_2)} + \frac{Z^j(t_2)-Z_{B0}}{\rho_{B0}^j(t_2)} & 0 & \lambda & 0 \\ -\frac{X^m(t_2)-X_{B0}}{\rho_{B0}^k(t_2)} + \frac{X^j(t_2)-X_{B0}}{\rho_{B0}^j(t_2)} - \frac{Y^m(t_2)-Y_{B0}}{\rho_{B0}^k(t_2)} + \frac{Y^j(t_2)-Y_{B0}}{\rho_{B0}^j(t_2)} - \frac{Z^m(t_2)-Z_{B0}}{\rho_{B0}^k(t_2)} + \frac{Z^j(t_2)-Z_{B0}}{\rho_{B0}^j(t_2)} & 0 & 0 & \lambda \end{bmatrix} \text{(2.16)}$$

For two epochs the system has more unknowns than observation equations. At least one more epoch observation is necessary to solve the system of equations in equation (2.15).

2.5.5 Linear dependence of observations

From a set of observations it is possible to form many double difference equations than the original data. This redundant set of equations is a result of differencing pairs of other double differences. It is therefore necessary to avoid such combinations of data otherwise we would be processing the same data more than once.

To exemplify such redundancies let us consider 3 satellites observed at two receiver positions *A* and *B* (refer to figure 2.16). If we ignore the insignificant combinations, that is: $(\lambda\Phi_{AB}^{jK}(t) = -(\lambda\Phi_{AB}^{jK}(t))$, three double differences can be formed:

$\lambda\Phi_{AB}^{jK}(t) = \left(\lambda\Phi_A^j - \lambda\Phi_B^j\right) - (\lambda\Phi_A^k - \lambda\Phi_B^k)$

$\lambda\Phi_{AB}^{jl}(t) = \left(\lambda\Phi_A^j - \lambda\Phi_B^j\right) - (\lambda\Phi_A^l - \lambda\Phi_B^l)$

$\lambda\Phi_{AB}^{lK}(t) = \left(\lambda\Phi_A^l - \lambda\Phi_B^l\right) - (\lambda\Phi_A^k - \lambda\Phi_B^k)$

Any one of these observations can be formed as linear combinations of the others:

$\lambda\Phi_{AB}^{jK} = \lambda\Phi_{AB}^{jl} + \lambda\Phi_{AB}^{lK}$

$\lambda\Phi_{AB}^{jl} = \lambda\Phi_{AB}^{jk} - \lambda\Phi_{AB}^{lK}$

$\lambda\Phi_{AB}^{lk} = \lambda\Phi_{AB}^{jk} - \lambda\Phi_{AB}^{jl}$

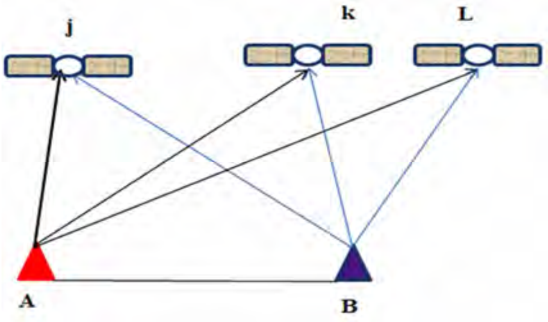

Figure 2. 16: Double difference geometry using three satellites

The data set $\{\lambda\Phi_{AB}^{lK}, \lambda\Phi_{AB}^{jK}, \lambda\Phi_{AB}^{jl}\}$is therefore to be *linearly dependent*. For least squares adjustment, only a linearly independent set must be used. Examples of correct linear independent sets using three satellites with two receiver combinations are:

$\{\, \lambda\Phi_{AB}^{jK}, \lambda\Phi_{AB}^{jl} = N^j = \{\lambda\Phi_{AB}^{ab} | a = j; b \neq j\}$

$\{\, \lambda\Phi_{AB}^{kj}, \lambda\Phi_{AB}^{kl} = N^k = \{\lambda\Phi_{AB}^{ab} | a = k; b \neq k\}$

$\{\, \lambda\Phi_{AB}^{lj}, \lambda\Phi_{AB}^{lj} = N^l = \{\lambda\Phi_{AB}^{ab} | a = l; b \neq l\}$

We can expand the example above to more than 3 satellites. For instance if we consider 5 satellites in view: 1,2,3,4 and 5. We can pick satellite 3 as the reference satellite; therefore our linearly independent set is:

$N^3 = \{\lambda\Phi_{AB}^{ab} | a = 3; b \neq 3\}$

$=\{\lambda\Phi_{AB}^{31}, \lambda\Phi_{AB}^{32}, \lambda\Phi_{AB}^{33}, \lambda\Phi_{AB}^{34}\ , \lambda\Phi_{AB}^{35}\}$

Considering two receivers and a single base line, the number of linearly independent double differenced observations is $s - 1$ where s the number of satellites is being tracked.

If we now consider more than two receivers, and more than two satellites, we must take into account that there will also be linearly dependent set of baselines. Consequently we need to have a reference station common for all sets double differences, to insure linear independence. Considering for instance that we have 4 satellites {1, 2, 3, 4} being tracked by three stations {A, B, C}. If we choose our reference satellite to be 3, and our reference station to be B, then our linearly dependent set is:

$N^3 = \{\lambda\Phi_{cd}^{ab} | a = 3; b \neq 3; c = B, d \neq B\}$

$= \{\lambda\Phi_{AB}^{31}, \lambda\Phi_{AB}^{32}, \lambda\Phi_{AB}^{34}, \lambda\Phi_{BC}^{31}, \lambda\Phi_{BC}^{32}, \lambda\Phi_{BC}^{34}\}$

Note that the number of linearly independent double differenced observations is $(s-1)(r-1)$.where s is the number of satellites being tracked, and r the number of receivers. So, 3 receivers with 4 satellite gives 6 observations. This of course assumes that s satellites are observed by all receivers.

2.5.6 Local-Area Differential GPS

Local-area differential GPS (LAGPS) is a form of DGPS in which the user's GPS receiver also receives real-time pseudorange and, possibly, carrier phase corrections from a local reference receiver generally located within the line of sight. The corrections account for the combined effects of navigation message ephemeris and satellite clock errors and, usually, propagation delay errors at the reference station. With the assumption that these errors are also common to the measurements made by the user's receiver, the application of the corrections will result in more accurate coordinates.

2.5.7 Wide-Area Differential GPS

Wide-area DGPS (WADGPS) is a form of DGPS in which the user's GPS receiver receives corrections determined from a network of reference stations distributed over a wide geographic area. Separate corrections are usually determined for specific error sources such as satellite clock, ionospheric propagation delay, and ephemeris. The corrections are applied in the user's receiver or attached computer in computing the receiver's coordinates. The corrections are typically supplied in real time by way of a geostationary communications satellite or through a network of ground-based transmitters. Corrections may also be provided at a later date for post-processing collected data.

2.5.8 WAAS (not for Geodetic Level)

WAAS (Wide-Area Augmentation System) is a multi-reference-station Differential GPS developed by the Federal Aviation Administration (FAA) that provides vector of corrections to users having WAAS compliant receivers. This vector contains ionospheric, clock and ephemeris corrections that are sent down to the user via geostationary satellites.

The WAAS was initially developed for precise aircraft navigation and is currently in commission serving that purpose and many other high-precision applications.

2.6 Mitigation of GPS Errors Using Models and Linear combination of code and phase observations

2.6.1 Ionospheric mitigation models

2.6.1.1 Single-Frequency Case (Klobuchar Model)

There are a number of different mitigation methods for single frequency GPS users to correct for the ionospheric error. The simplest and most widely used method to correct for the ionospheric error is to utilize the Klobuchar model together with the eight ionospheric coefficients broadcast as part of the navigation message. (Choy et al, 2008).

Klobuchar Model is a simple algorithm for the single-frequency receiver user to correct for approximately 50% of the ionospheric error. It utilizes the eight coefficients from the Navigation message to describe the worldwide behavior of the ionosphere, thus enabling to compute user’s position from ephemeris.

The diurnal variation of TEC is represented by the half cosine form as shown hereunder

$$T_{iono} = Fx\{DC + Acos\left[\frac{2\pi(t - \varphi)}{P}\right]\}$$

where, A = Amplitude, P = period,

DC = offset term, φ = local noon

2.6.1.2 Dual-Frequency Case: (Linear Combination of code and phase observables)

Frequency dependent ionosphere can be eliminated by using a combination, called ionosphere-free linear combination for the first order ionosphere effect. The second order effect is much smaller, a few millimeter or a cm, and cannot be mitigated using dual-frequency.

In Figure 2.17, ionospheric effect mitigation approaches are demonstrated, depending on whether one or two receivers are used and whether the receiver is single or dual frequency.

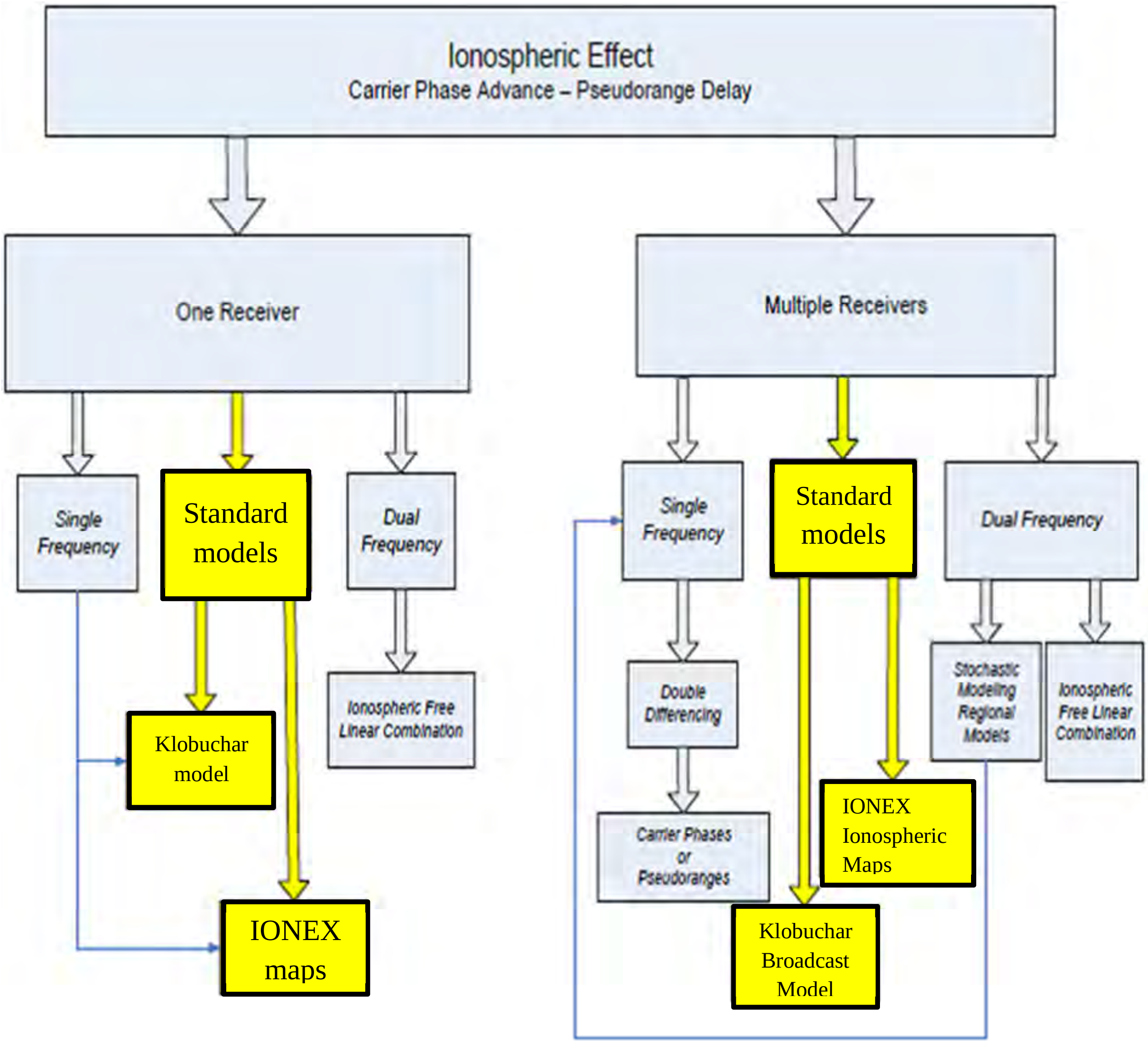

Figure 2. 17: Ionospheric bias Mitigation (Source: http://tekmon.gr/2010/12/gps-ionospheric-bias/)

2.6.2 Types of Linear Combinations of Observations and their applications

Linear combination of carrier phase and code observations, are useful in alleviating GPS errors. The linear combinations can be formed using either zero or double difference measurements.

2.6.2 .1 The Ionosphere-free Linear Combination L_3

The ionosphere-free linear combination described earlier in 2.5.2 above practically eliminates the ionospheric path delay. It has the following form of equations

$L_3 = \frac{1}{f_1^2 - f_2^2}(f_1^2 L_1 - f_2^2 L_2)$ For phase

$P_3 = \frac{1}{f_1^2 - f_2^2}(f_1^2 P_1 - f_2^2 P_2$ For code

Where: L_1, L_2 represent the phase observables (zero or double differences) and P1, P_2 represent the code observables.

2.6.2 .2 The Geometry-free (ionospheric) Linear Combination L4

The linear combination is given as: $L_4 = L_1 - L_2$

The ionospheric (or geometry-free) linear combination is independent of receiver clocks and geometry (orbits, station coordinates). It contains the ionospheric delay and the initial phase ambiguities. It may be used for the estimation of ionosphere models. The same linear combination may be formed using the code observations, too.

2.6.2.3 The Wide-lane Linear Combination WL

The linear combination is given by:

$\boldsymbol{L_{WL}} = \frac{\boldsymbol{1}}{\boldsymbol{f_1 - f_2}} (\boldsymbol{f_1 L_1 - f_2 L_2})$ Or

$$\Phi_{WL} = \Phi_{L1} - \Phi_{L2}$$

This combination is used on the double difference level for phase observations for the purpose of cycle slip fixing and ambiguity resolution.

The formal wavelength λ_{WL} is about 86 cm and is roughly 4 times longer than λ.

2.5.2.4 The Narrow-lane Linear Combination NL

The narrow-lane observable is obtained by adding the two phase equations$(L_1 + L_2)$ expressed in cycles:

$\Phi_{NL} = \Phi_{L1} + \Phi_{L2}$

In more detail:

$$\Phi_{(NL)} = \Phi_{L1} + \Phi_{L2} = \frac{f_{1+}f_2}{c}.\rho - \frac{1}{c}.f_1.d_{ion(L1)} + f_2.d_{ion(L2)} + n_1 + n_2.$$

The effective wavelength of this observable is very small: $\lambda_{NL} = \frac{c}{f_1 + f_2} \approx 0.10m$etres.

The N_{NL} ambiguity is $N_1 + N_2$, and is therefore still an integer.

The wide-lane and narrow-lane combinations are only related to the carrier phase observations and are often used in **ambiguity resolution** applications.

2.6.2.5 The Melbourne-Wübbena Linear Combination

The Melbourne-Wübbena combination is a linear combination of both, carrier phase (L_1 *and* L_2) and P–code (P_1 *and* P_2) observables described by (Wübbena, 1985) and (Melbourne, 1985). This combination eliminates the effect of the **ionosphere**, of the **geometry**, of the **clocks**, and of the **troposphere**.

The combination is given by:

$$\boldsymbol{L_{(MW)}} = \frac{\mathbf{1}}{\boldsymbol{f_1 - f_2}}(\boldsymbol{f_1 L_1 - f_2 L_2}) - \frac{\mathbf{1}}{\boldsymbol{f_1 + f_2}}(f_1 P_1 + f_2 P_2)$$

2.6.3Troposphere Model (Mitigation Model, all zenith direction)

In practice, there are different models available to calculate the effects of the troposphere delay. The tropospheric delays are mitigated using models but with uncertainties due to the assumption each model applies.

Assumption of models include; Homogeneous troposphere: Dry atmosphere; and concentric layers of equal thickness, each equally contributing to the total pressure at the earth's surface.

Other assumptions are that the troposphere is Isothermal: i.e. it is dry, with constant temperature.

Further assumptions take account of a Constant-lapse-rate troposphere: meaning that the temperature varies linearly with height.

Another postulation is to have a Standard troposphere, i.e. a troposphere whose Pressure, Temperature and moisture height profiles, are provided as well as information on latitudinal and seasonal variations of these parameters.

Example of models include; **Hopfield** model (Hopfield 1969), Modified Hopfield, Saastamoinen model, (Saastamoinen 1973).

These models and other models derived from them (e.g. UNB3, UNB3m IGGtrop, are used to estimate the total Zenith Path Delay (ZPD) but the delay is along the propagation path.

Mapping functions are used to transform the Zenith Tropospheric Delay into delays along the satellite path. This transformation of the zenith path delay into the slant tropospheric delay is called tropospheric mapping functions (MF). We have MTT Herring Mapping Functions, (used with Saastamoinen model), Vienna Mapping Function (VMF) Updated Vienna Mapping function (VMF1) Global Mapping Function (GMF) and others. Figure 2.18 depicts the approaches used for tropospheric effects mitigation.

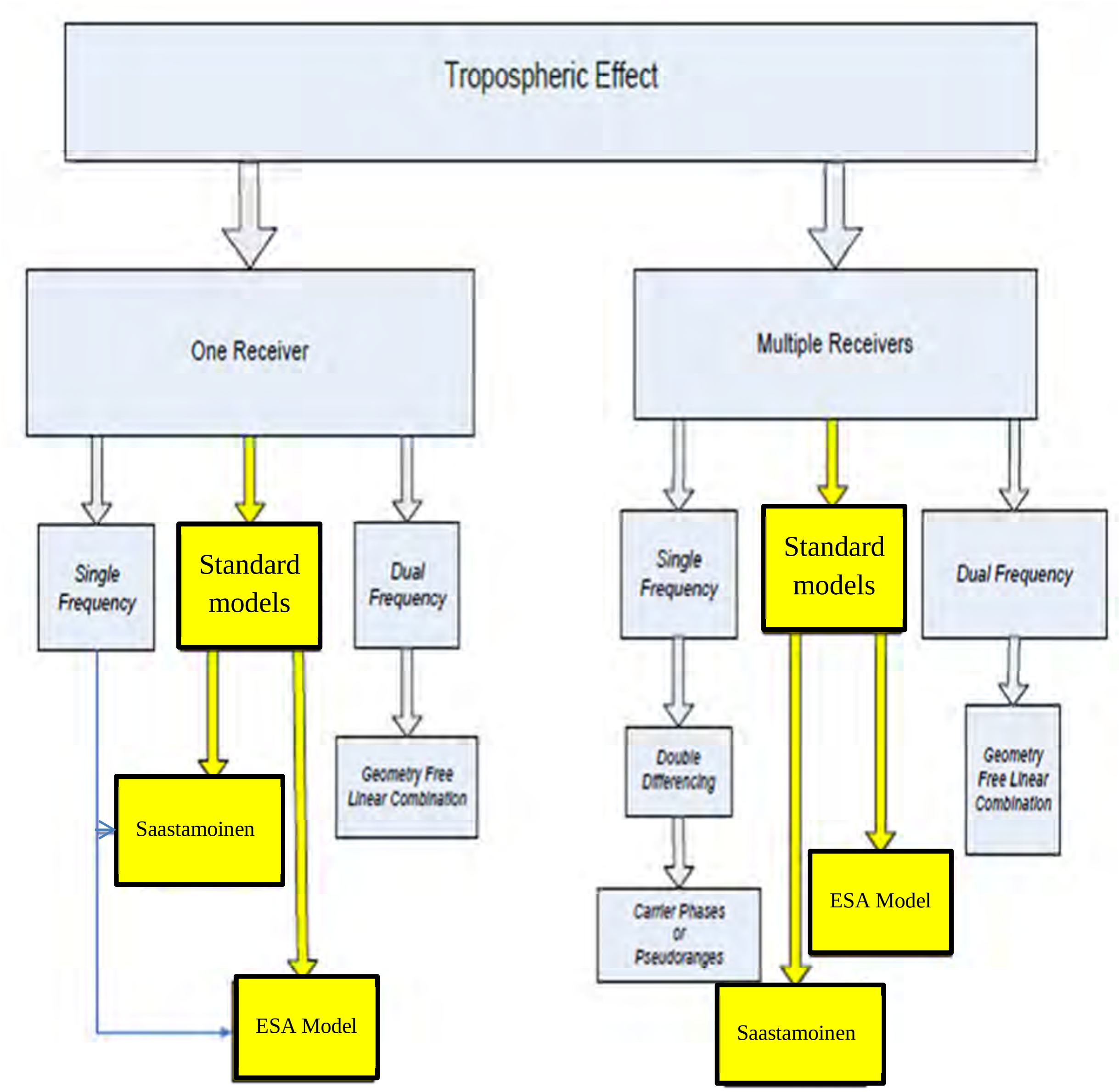

Figure 2. 18: Tropospheric bias Mitigation (Source: http://tekmon.gr/2011/01/gps-tropospheric-bias/)

Recently there has been an new achievement that includes a ray tracer based on Numerical Weather Prediction Model (NWP) e.g. **Rapid Update Cycle 13km** (RUC13) by National Oceanic and Atmospheric Administration (NOAA) in USA, and Global Environmental Multiscale (GEM), from the Canadian Meteorological Centre (MC) of Environment Canada Rapid Update Cycle (RUC20) by NOAA (Ahn et al, 2005) and other various models.

2.6.4 Multipath Mitigation

There is no general model of multipath effect because the geometric situations at observation sites are different. However the effect of the multipath can be estimated using a combination of L1 and L2 code and carrier phase.

Multipath can be mitigated if a good design for observation is made. Observation design to mitigate multipath effects include; selecting the site carefully, to avoid nearby reflectors, using antenna ground plane to avoid reflections from the ground, Deploying absorbing material on the ground, Selecting carefully designed antennas, e.g. choke ring antennas

Observation of sidereal differences is also useful for multipath mitigation that is, by forming sidereal differences between the observables, for example double differences at two consecutive days. It is hence possible to generate multipath free observables. Another method is to use particular signal properties for improving the correlation process. GPS signals are Right-hand polarized. Reflected signals change their polarization, and hence can be detected in the receiver. Reflected signals also arrive later at the antenna and hence can be discriminated.

Another way of multipath mitigation is observing for many hours.

It has also been shown that for ground reflected signals the higher the height of the antenna (figure 2.19), the lower the effects of Multipath (Elosegui et al, 1995). Therefore the use of big antenna heights can significantly reduce the effects of multipath.

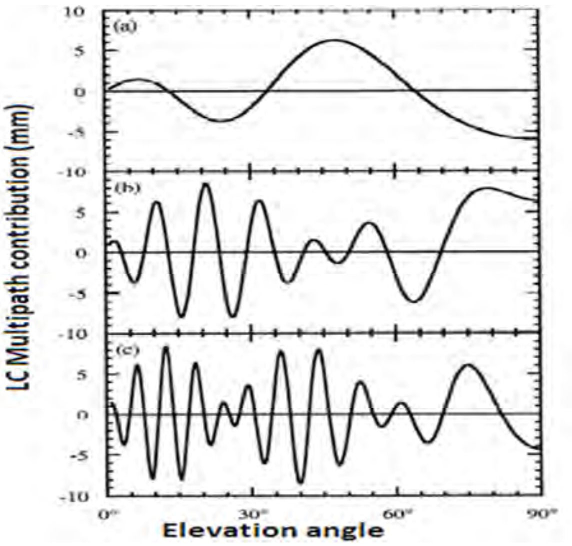

Figure 2. 19: Multipath contributions to observed phase for three different antenna heights (Elosegui et al, 1995) with a function of satellite elevation angle.

Due to the changing satellite geometry, the multipath effect in carrier phases shows a cyclic behaviour. *a* (For antenna height of 0.15m), *b* (For antenna height of 0.6m), and *c* (For antenna height of 1.0 m).

2.6.5 Phase Center Variation (PCV) Mitigation Model

The phase center of a GPS antenna is neither a physical point nor a stable point. For any given GPS antenna, the phase center will change with the changing direction of the signal from a satellite. Ideally, most of this PCV depends on satellite elevation. Azimuthal effects are only introduced by the local environment around each individual antenna site. These phase center variations affect the antenna offsets that are needed to connect GPS measurements to physical monuments. If this variation is ignored, the measured baseline will be between the average phase centers of the two antennas. The corrections of Phase Center Variations are included in IGS products as weighted average of all the individual phase centers for each of the measurements included in the solution, however it has been shown that the antenna phase center variations (PCV) can be absolutely calibrated at field of GPS using a precisely calibrated robot and that this method gives “high accuracy and repeatability” (Böder et al 2001). Thus yielding precise station coordinates independent absolute PCV’s.

2.6.6 Ambiguity Resolution

The OPTIONS for ambiguity resolution include the following:

2.6.6.1 Ambiguity Resolution in Measurement Space

In the measurement space N is geometry independent and insensitive to tropospheric refraction. There is more degrees of freedom and simple verification.

Ambiguity-free solution (“bias” or ambiguity “float” solution)

This refers to adjustment of all ambiguities as free parameters, together with station coordinates i.e. the parameters to be estimated are “rover” coordinates (one end of the baseline) and the ambiguity parameters.

The ambiguity-free solution is generally the first step. After this solution, the values of ambiguity parameters (which theoretically should be integers) may close to integer values (but not exactly integers due to presence of residual biases like atmospheric, orbit, multipath errors and other User Equivalent Range Errors(UERE). If the correct ambiguities are identified they can be held fixed in the subsequent ambiguity-fixed solution. Such solution is very strong as it contains the station coordinate parameters.

In an ambiguity-free solution, no advantage is taken of the integer nature of N as it is indistinguishable from other, non-integer, biases such as orbit uncertainties, multipath and atmospheric refraction (ionosphere and troposphere), and is in fact "contaminated" by them.

Ambiguity-fixed solution (or “bias-fixed” solution)

This refers to resolution of estimated ambiguity parameters to their nearest integer values, and iterating solution. i.e. a solution in which some or all the ambiguity parameters have been resolved to their integer values.

In effect precise unambiguous phase-range data are used. Constraint of an ambiguity value to its correct integer improves the estimation of the remaining geodetic (station coordinate) parameters. The ambiguity fixed solution is attained by increasing length of observation.

Differencing between epochs (or triple differences)

This is done by Differencing data between consecutive epochs to eliminate the phase ambiguity bias. The strongest baseline solution is provided by "carrier-range" (or "phase-range") double-differenced data, formed when ambiguous carrier phase data is "corrected" so as to generate a high precision range-like observable.

Linear combination of observation (for dual frequency receivers)

Various possible linear combinations can be formed like the wide-lane and narrow-lane techniques.

Uses extended smoothed differentially corrected code combination which matches the ionospheric effects of the corrected carrier phase differences.

$$N_d = N_1 - N_2 = \frac{f_1 P_1 + f_2 P_2}{(f_1 + f_2)\lambda_d} - (\varphi_1 - \varphi_2)$$

Use resolved wide-lane measurement to step to narrow lane. This depends upon ionospheric error being small.

$$N_s = N_1 + N_2 = \frac{(\varphi_1 - \varphi_2 + N_d)\lambda_d}{2\lambda_s}$$

$$N_1 = \frac{(\varphi_1 - \varphi_2 + N_d)\lambda_d}{\lambda_s} \times \frac{f_1}{f_1 + f_2} (0.562)$$

$$N_2 = \frac{(\varphi_1 - \varphi_2 + N_d)\lambda_d}{\lambda_s} \times \frac{f_2}{f_1 + f_2} (0.438)$$

2.6.6.2 Ambiguity Resolution in Position Space (or coordinate domain)

In position space N is Geometry dependent and sensitive to tropospheric refraction. There are fewer degrees of freedom and hence tougher verification. In this technique using Ambiguity Function technique initially established by Counselman and Gourevitch (1981). Also described by Remondi (1984) and further improvements by Remondi (1990a) and Mader (1990). The concept is made clear by Hoffmann-Wellenhof et al (2008).

2.6.6.3 Ambiguity Resolution in Ambiguity Space

Also Geometry dependent, sensitive to tropospheric refraction, fewer degrees of freedom and tougher verification

Many variations of techniques to minimize the computational intensity and to minimize the number of epochs of data are required. Several methods have been proposed such as Least Squares Search, Hatch (2006), Fast Ambiguity Search Filter (FASF), by Chen (1993) Chen and Lachapelle (1995), Fast Ambiguity Resolution Approach (FARA) by Frei and Beutler (1990), Dual-space Ambiguity Resolution Approach(DARA) by Yu and Liu (2003) Modified Cholesky decomposition method by Euler and Landau(1992), LAMBDA Decomposition by Teunissen (1994a), and Optimal Method for Estimating GPS Ambiguities (OMEGA) by Kim and Langley (1999). Each of the above has its advantages and disadvantages, according to comparison made by Pais (2011). Among all these approaches, the LAMBDA method developed at the University of Delft is the most commonly used ambiguity resolution method shortly be discussed below.

LAMBDA method.

LAMBDA stands for "Least Squares Ambiguity Decorrelation Adjustment" The LAMBDA method is a procedure to estimate ambiguities based on double difference models by implementation of the least squares principle in maximizing the probability of correct ambiguity resolution (Teunissen, 1994). The basic idea is to transform the original real-valued double difference ambiguities, which are highly correlated, into decorrelated real-valued ambiguities. As such the number of solution candidates is considerably reduced

It consists of two steps: (a) a decorrelation of the double difference ambiguities; and (b) a sequential conditional least-squares based search:

$$\boldsymbol{L} = \boldsymbol{Ax} + \boldsymbol{By} \min_{\hat{\chi}}(\hat{\chi} - \chi)\boldsymbol{Q}_{\hat{\chi}}^{-1}(\hat{\chi} - \chi)$$

The variance covariance matrix of the observation vector **L** is Q_L. the parameter vectors, **x** and **y** represent the unknown integer ambiguities and other unknown parameters such as the baseline and coordinates respectively. **A** and **B** are the design matrices relating the observations to the unknowns.

The minimization is solved by a search over grid points. Each grid point represents an ambiguity vector with all integer values in the ambiguity parameter space. The resulting vector is the least squares estimate of the 'fixed' ambiguities. The result is validated applying a statistical test as the ratio test, (Figure 2.19). If successful the integer values are used in the fixed solution for the derivation of the other sets of parameters, enabling high accuracy since the ambiguous carrier phase observable is transformed to a phase-range observable with cm level resolution. The LAMBDA method is an algorithm that can be employed by GNSS processing software as an autonomous module.

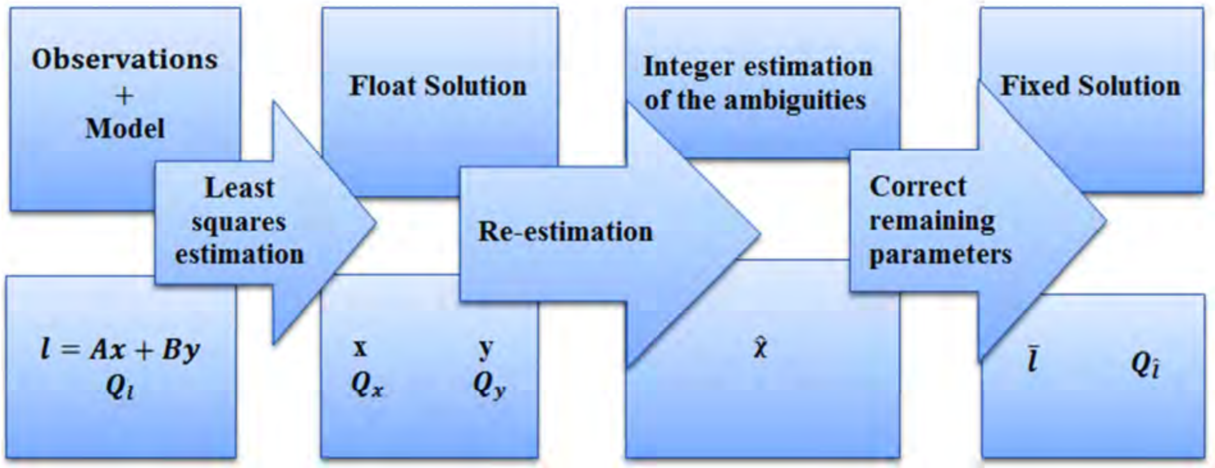

Figure 2. 20: LAMBDA method: Ambiguity Resolution Process (Joosten and Tiberius, 2002)

Ambiguity validation

Once the best set of the fixed ambiguities is identified by the LAMBDA algorithm a discrimination test needs to be applied to determine if there is a detectable difference among the best **X** and the second best $\hat{\chi}_2$ sets of ambiguities. If the test passes then the best set is employed by the fixed solution whereas if it fails the float values are maintained. The test determines if there is enough confidence in the integer solution values. One such test is the ratio test. According to the ratio test, the ratio of the squared norms of the difference of residuals from the float solution is computed and the best fixed **X** solution is accepted, if for **C** being a constant the following condition is satisfied:

$$\frac{\|\boldsymbol{x} - \hat{\boldsymbol{\chi}}_2\|^2_{Qx}}{\|\boldsymbol{x} - \hat{\boldsymbol{\chi}}\|^2_{Qx}} \geq \boldsymbol{c}$$

The critical value **C** is normally selected 2, 2.5 or 3 on an empirical basis.

2.7 Precise Point Positioning (PPP)

2.7.1 Introduction

Precise point positioning is a method that performs precise position determination using a single GPS receiver, or zero difference GPS data processing. It is based on Processing of GPS data using corrections that do not involve differencing from a reference station.

The technique of Precise Point Positioning (PPP) is a viable alternative to differential methods for precise positioning using Global Navigation Satellite Systems (GNSS). PPP is very cost effective since there is no need for data from local or regional reference stations; especially in remote areas the logistic is greatly simplified. The PPP method has a potential for centimeter accuracy for static applications and sub-decimeter accuracy for kinematic applications (Ovstedal et al 2006).

This technique is based on the use of currently available precise GPS orbit and clock data provided by The International GNSS Service (IGS), with various accuracies, (see table 2.2), depending on the delay of availability from real time. So-called “Ultra-rapid” products, available in real time, give around 10 cm of accuracy for the orbits and 5 ns for the clocks. Better accuracies are possible, with increased latency. One advantage of PPP compared to relative techniques is that only a single receiver is required, although there is the need for additional correction methods in order to mitigate some systematic effects that cannot be eliminated through differentiation.

Table 2.2: Accuracy of IGS orbit products

GPS Satellite Ephemerides	**Accuracy (cm)**	**Latency**
Broadcast	≈100	Real time
Ultra Rapid (predicted half)	≈5	Real time
Ultra Rapid (observed half)	≈3	3-9 hrs
Rapid	≈2	17-41 hrs
Final	≈2	12-18 days

Since differencing techniques are not used in PPP algorithms, relative ionospheric delays are not cancelled nor significantly mitigated. Because of this drawback only dual-frequency receivers that are capable of generating 1st order ionosphere-free linear combination are necessary for decimetre-level accuracy positioning. This requirement is similar to DGPS when the inter-receiver distance is large.

2.7.2 The Principle of PPP

The precise Point Positioning (PPP) is based on zero differencing method of determining parameters. Normally, ionosphere-free combination observables formed from undifferenced basic GPS observations, are used in PPP. The ionospheric effects are taken care of by a combination of L_1 and L_2 in ionosphere free combination of undifferenced code pseudoranges and carrier phases as shown in the – equation 2.7.1 and 2.7.2.

$P_{IF} = \frac{f_1^2.P(L1) - f_2^2.P(L2)}{f_1^2 - f_2^2} = \rho - cdT + d_{trop}$ ---------------- (2.7.1) for code pseudorange

$\Phi_{IF} = \frac{f_1^2.\Phi(L1) - f_2^2.\Phi(L2)}{f_1^2 - f_2^2} = \rho - cdT + d_{trop} + \frac{cf_1 N_1' - cf_2 N_2'}{f_1^2 - f_2^2}$ -------- (2.7.2) for carrier phase

Where f_1 and f_2 are the GPS L_1 and L_2 frequencies *P(Li) and Φ(Li)* are the code and phase observations respectively, ρ is the true geometric range, c is the speed of light; *dT* is the receiver clock offset d_{trop} is the tropospheric effect N is the phase ambiguity term in *Φ(Li).*

Equations (2.7a) and (2.7b) show that the unknown parameters to be estimated in PPP include position coordinates, phase ambiguity terms, receiver clock offsets, and the tropospheric effect

The challenges in solving the above equations is that the ambiguity term N is no longer an integer because they are corrupted by the satellite and receiver initial phase biases according the equation 2.7.3.

$N_1' = N_1 + \varphi_i^r(t_0) - \varphi_i^s(t_0)$ ---------------------------- (2.7.3)

Where N_1 is the integer ambiguity term, $\varphi_i^r(t_0), \varphi_i^s(t_0)$ are the receiver and satellite initial phase biases. Research work on the identification and determination of these two biases is currently underway A position model developed at the university of Calgary and based on the following ionosphere – free observation combination has already been proposed which can support integer ambiguity resolution after initial phase biases are eliminated (inside GNSS 2006, www.insidegnss.com).

$P_{IF,L1} = 0.5[P(L1) + \Phi(L1) = \rho - cdT + d_{trop} + 0.5\lambda_1 N_1'$ ---------------------------- (2.7.4)

$P_{IF,L2} = 0.5[P(L2) + \Phi(L2) = \rho - cdT + d_{trop} + 0.5\lambda_2 N_2'$ ---------------------------- (2.7.5)

$\Phi_{IF} = \frac{f_1^2.\Phi(L1) - f_2^2.\Phi(L2)}{f_1^2 - f_2^2} = \rho - cdT + d_{trop} + \frac{cf_1}{f_1^2 - f_2^2} N_1' - \frac{cf_2}{f_1^2 - f_2^2} N_2'$ ------------ (2.7.6)

In order to get a correct position from PPP solution according to equation 2.7.1 and 2.7.6 one needs a very efficient technique for the integer ambiguity N resolution and good tropospheric models. Also, since satellite clock errors are not estimated (or differenced out) nor eliminated by means of any linear combinations, additional information is needed in the PPP approach. Such important information includes correctly determined satellite clock offsets and Precise orbits. The clock parameters are introduced in the processing together with orbit information and Earth orientation parameters. With this information at hand it now possible to solve for the PPP unknowns namely Station coordinates, Receive clock corrections Phase ambiguity, and tropospheric effects. This means that with these precise clock products, the positions of the GPS ground stations are determined by applying zero-difference ambiguity fixing method.

The Major problem in PPP is the difficulty to resolve phase ambiguities. Another problem is that correlation between station errors and clock corrections do not exist, thus a network adjustment is impossible. However, this may be an advantage in that, correlation errors of any misbehaving station cannot be introduced to other stations, but only affect the result of that particular misbehaving station.

Actually the main issue is the convergence time required to achieve ambiguity fixed solution of zero difference to improve efficiency in positioning.

Many researches have been carried out to improve by enabling determination of the PPP unknown parameters Li et al (2010) presented a method, to determine precise zero-differenced atmospheric delays derived from the PPP fixed solution of the reference stations, which are disseminated to, and interpolated at user stations to correct for L1, L2 phase observations or their combinations. With the corrected observations, instantaneous ambiguity resolution can be carried out within the user PPP software, thus achieving the position solutions equivalent to the network real-time kinematic positioning (NRTK). Geng et al (2011) proposed the improved narrow-lane FCBs derived from an ambiguity-fixed GPS network solution, rather than the original (i.e. previously proposed Ge et al. (2008), FCBs derived from an ambiguity-float network solution. Loyer et al (2012) described in detail the practical realization of the two-step, ambiguity-fixing scheme (wide-lane and narrow-lane).

Table 2.3 shows biases and errors that need to be applied or accounted for in typical PPP and differential GNSS

Table 2.3: Biases and errors that need to be applied or accounted for a typical PPP and differential GNSS **(source: Chris RIZOS et al 2012)**

Correction type	**PPP**	**Differential GNSS**
Satellite Specific errors		
Precise satellite clock corrections	✓	x
Satellite antenna phase centre offset	✓	✓
Satellite antenna phase centre variations	✓	✓
Precise satellite orbits	✓	✓ /x
Group delay differential	✓ (L1 only)	x
Relativity term	✓	✓
Satellite antenna phase wind-up error	✓	x

Receiver Specific errors		
Receiver antenna phase centre offset	✓	✓
Receiver antenna phase centre variations	✓	✓
Receiver antenna phase wind up	✓	x
Geophysical models		
Solid earth tide displacements	✓	√ **(or x** for nearby stations)
Ocean loading	✓	√ **(or x** for nearby stations)
Polar tides	✓	√ **(or x** for nearby stations)
Plate tectonic motion	✓	√ **(or x** for nearby stations)
Atmospheric modeling		
Tropospheric delay	✓	✓
Ionospheric delay	✓ (L1 only)	X (for second order and more a DGP does still need corrections)

CHAPTER THREE

3. METHODOLOGY

3.1 Introduction

This chapter describes the techniques involved in data acquisition and processing by using two approaches namely DGPS to generate positions and velocities of the GPS stations using GAMIT/GLOBK software and PPP online services to obtain time series of positions. It gives the details of GAMIT pre-processing, file preparation, daily processing, and the final combined solution to produce GPS positions and velocities using GLOBK. PPP solution is also discussed and its results assessed regarding its accuracy as compared to the DGPS solution.

3.2 Data acquisition

In this project the GPS data used involve existing data from 3 series of campaign GPS stations established in Tanzania by collaboration between Tanzania and USA, With the Technical Support of UNAVCO (www.unavco.org), and funds by NSF (www.nsf.org) for the purpose of quantifying kinematics of the East African rift, and to serve as the first order geodetic network of Tanzania (Field report by Calais (2010) found on facility/unavco.org). The data is available at UNAVCO's data archive on facility.unavco.org/data/gnss/campaign.php Reference stations used are some of continuously observing stations (IGS) saved at IGS data archives like UCSD's SOPAC (website: http://sopac.ucsd.edu data archive: ftp://garner.ucsd.edu) NASA's CDDIS (website: http://cddis.nasa.gov data archive: ftp://cddis.gsfc.nasa.gov), UNAVCO, (website: www.unavco.org, data interface: facility.unavco.org, data archive: ftp://data-out.unavco.org) MIT (website: www.mit.edu IGS products archive ftp://chandler.mit.edu).

3.2.1 Choice of IGS Reference network.

The choice of the IGS reference network was based on the spatial location of the IGS stations from the study area. This was so because for a strong solution a good geometry for the baselines is highly significant. Figure3.1 shows a list of IGS stations used and their spatial distribution.

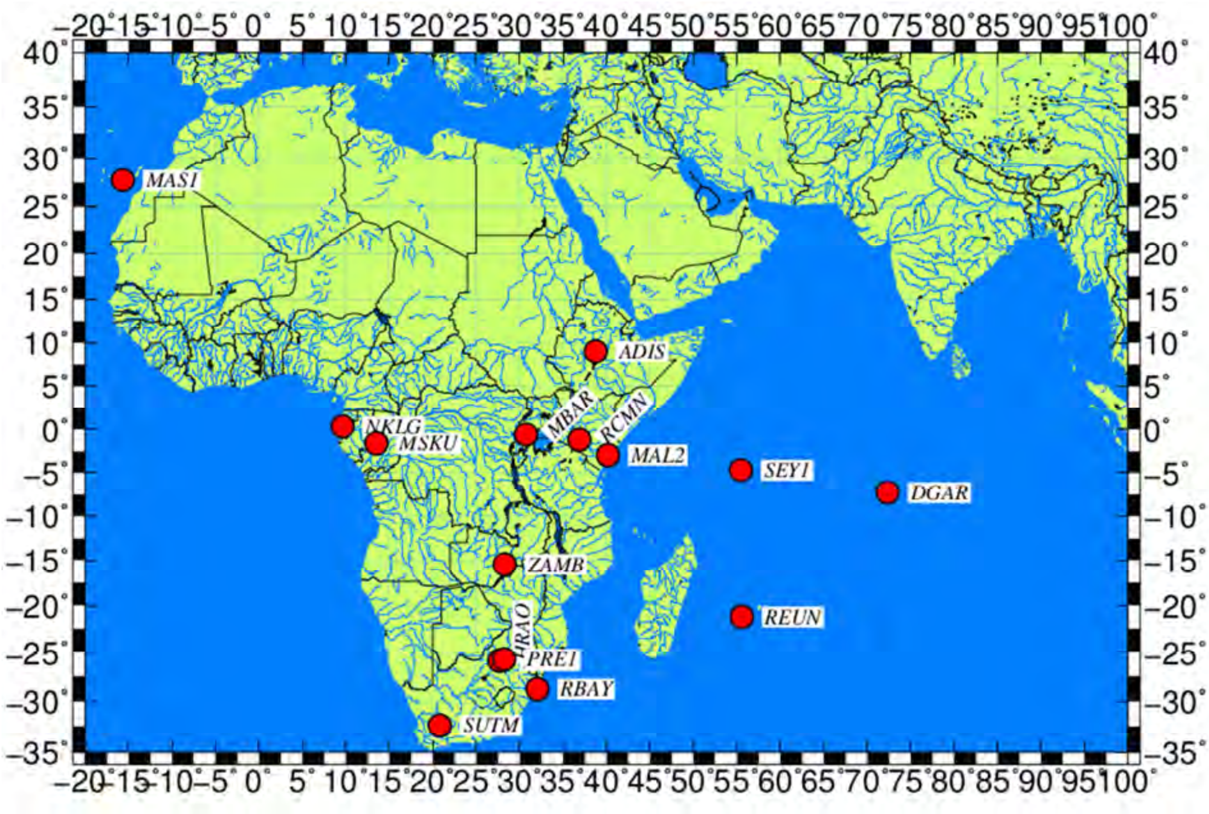

Figure 3. 1: List of IGS stations used as reference for DGPS solution of the Campaign network

3.3 GPS data processing.

3.3.1 Introduction.

Before processing the data it is important to know the structure and how to manipulate. The GPS data for IGS stations were downloaded from the binary archive, in a UNIX compressed Hatanaka ("d.Z file") format, from SOPAC's data archive. (RINEX files more than 60 days old are available in Hatanaka format only). All the observation files were converted first to RINEX format before processing with GAMIT and other software packages. Conversion to RINEX format was done by using c-shell script crx2rnx which comes with GAMIT software package.

Unix "uncompress" command was used to change the downloaded observation files From the UNIX compressed hatanaka format (SITEDOYN.YYd.Z) to hatanaka format with d extension (SITEDOYN.YYd) and thereafter changed to RINEX format (SITEDOYN.YYo) using the script crx2rnx.

In the above general format, SITE refers to 4 Character name of the GPS site, DOY represents Day of the Year, N is a convention for naming and is 0. YY represents year, and o indicates that it is an "observation" file. As an example, a particular observation file in the above formats is given as, NKLG2230.12d.Z (UNIX compressed), (NKLG2230.12d (Hatanaka format), NKLG2230.12o (RINEX format). This refers to observation file at NKLG on the 223rd day of the year 2012. Appendix I shows how GPS data were converted before further processing.

3.3.2 Data Rinexing and Quality Check

In GPS observation, different GPS receivers are used; each of these receivers has its own data format. For this reason all GPS data collected should be translated to a conventionally agreed format known as Receiver Independent Exchange (RINEX) format so that it they can be processed with any GPS processing software. In this research Rinexing was already done using the "Translate, Edit, and Quality Check" (TEQC) software). TEQC is open source software capable of translating, editing, and checking the quality of GPS observables (http://facility.unavco.org/software/teqc/tutorial.html). In this research, data quality check was done using TEQC software. Appendices II and III show a TEQC summary report for KWSI on days 228 and 229 respectively. The former showed good results and the latter yielded bad results in PPP solution.

Data quality check was done especially to the data set which gave inconsistent results. Quality check was done using both pre-processing and post-processing techniques. In pre-processing, TEQC was used for data quality check, and in Post-processing data quality check was done using GAMIT control scripts. Bad results from GAMIT were identified by checking the sites with high rms in autcln.post.sum., and by checking the time series behaviour. If the time series show outliers even when GAMIT results were in normal range, it indicates some problems related to antenna or multipath and water vapor. In this case Sky plots were used to check whether there existed multipath or water vapour effects and residual versus elevation angle plots were used to check the quality of the antenna model. Section 3.3.4 discusses how quality assurance was done using GAMIT.

Appendix III shows TEQC results for station KWSI observed on day 229 of 2006. It is one station that misbehaved in APPS. As seen from the TEQC summary the station had some data gaps and APPS could not give correct position as shown in section 3.7. In GAMIT solution the result was not so bad, but from the sky plot in Figure 3.4 (b) it can be seen that there were no data in the last three time spans.

Some of symbols to be interpreted in TEQC results are as follows (Estey and Wier 2013)

I means one or more ionospheric phase slips in this time bin

M means one or more MP1 and MP2, or MP15 and MP51, slips in this time bin. The MP values are described below.

1 (one) means one or more times in this time bin have multipath MP1 slip only.

c means one or more times in this time bin has L1 and C/A observables only (and hence A/S is not applied)
2 means one or more times in this time bin have multipath MP2 slip only.
* means all GLONASS observables in this time bin are good L1 L2 P1 P2; no A/S was applied.
This * is the usual GLONASS "good" data indication, like o in the time plot lines for GPS.
_, -, 1, 2, and + mean the same as described above.
+ or - mean either a positive or negative millisecond receiver clock reset was detected.
Another symbol is ^ which is lower in the clock symbol hierarchy than either + or -, and indicates at least one missed observation epoch in that time bin.

In TEQC report files, effects of various errors during observations are analyzed for each observed satellite. Files obtained from the quality check are; the derivative of ionospheric delay observables (IOD in m/s), Ionospheric delay observable (ION in m), Multipath on Carrier Phase L1 (MP1), Effect of Multipath on Carrier phase L2 (MP2), Signal- to-Noise ratio on Carrier L1 (S/N-1), Signal- to-Noise ratio on Carrier L2(S/N-2) Satellite azimuthal data (degrees) and Satellite elevation data (degrees). TEQCPLOT (Hedfors, 2005) was used to Read and plot TEQC report files. Figure3.2 shows on the effects of Multipath on L1 for KWSI on days 228 (a) and 229 (b) respectively. The plots were mainly for assessing errors that might have biased the KWSI observation on day 229. On day 228 the plot showed that the data span was 24 hours but on day 229, it was observed that there were data gaps and there were approximately 10 hours of observation. The trend of other effects was almost similar in both cases. Levels of multipath and other factors mention above were within acceptable range as seen on the TEQC summary report in appendices II and III.

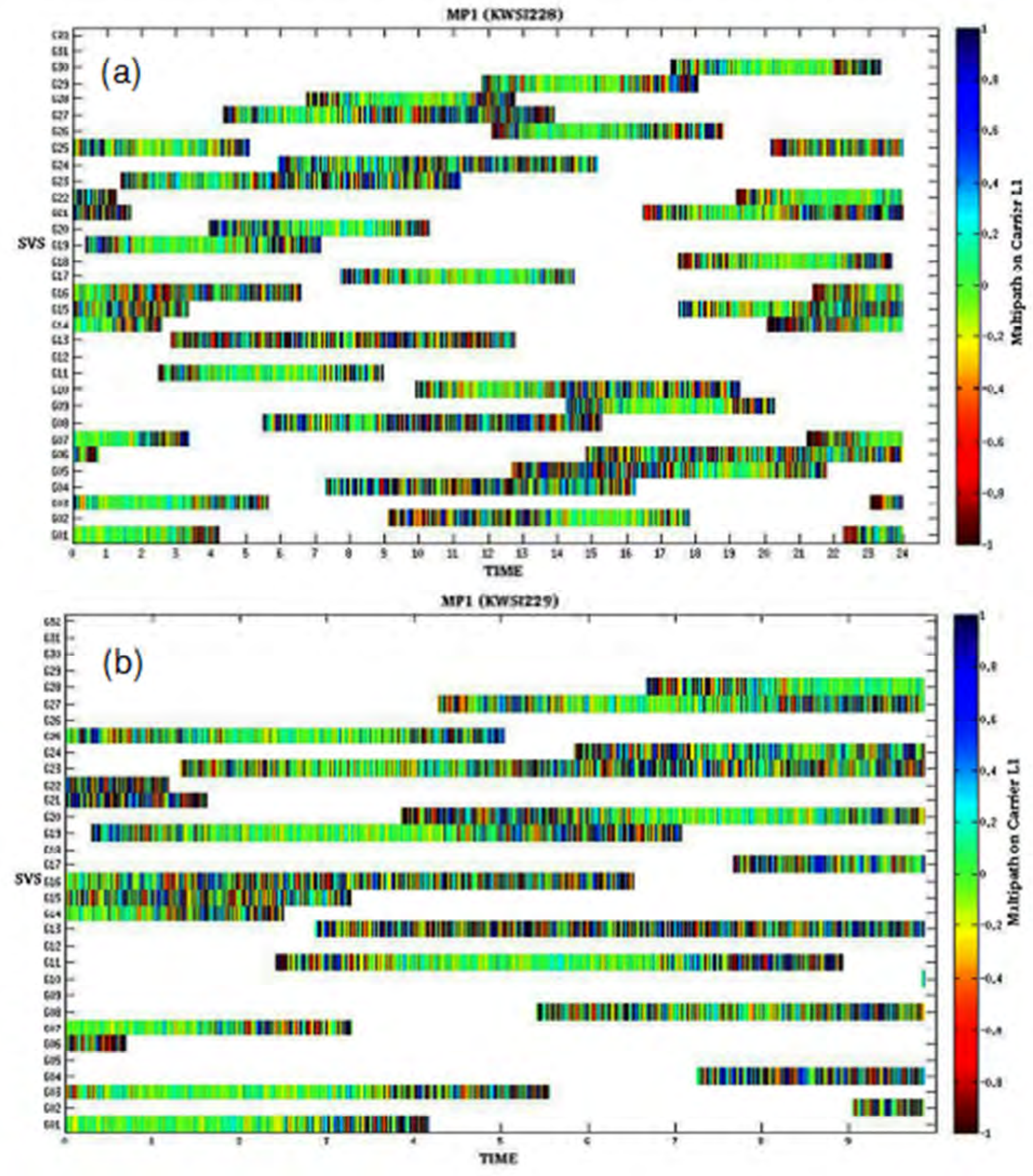

Figure 3. 2: Multipath effect on Carrier L1 from TEQC report file

More about TEQC interpretation is found at http://facility.unavco.org/software/teqc/tutorial.html.

3.3.3 Data Preparation for GAMIT Processing

DGPS data processing was carried out using GAMIT/GLOBK software release 10.4. GAMIT processing helped in daily intervals to solve for station coordinates atmospheric delays (ionospheric and tropospheric) and phase ambiguities using double differenced GPS phase measurements.

Before processing GPS data using GAMIT, it is necessary to understand some of its file naming conventions. This assures a unique definition for each experiment, facilitates data file management, and allows for ease of interactive processing and troubleshooting. First, the information should be organized into sessions, defined as the spans during which all the stations tracks simultaneously the phase of two or more satellites. When a single session is processed in GAMIT, processing the remaining sessions is easy. In this section, description for a single session processing is given. The first step is to create a working directory and copy or link all the necessary files. The main files needed for a single session processing are

1. Files derived from **RINEX** observation

   From RINEX observation, X file (for input in GAMIT) is created using the script MAKEX,

2. Files derived from RINEX navigation (Broadcast ephemeris)

   These are Satellite and station clock values (I-, J-, and K-files). From RINEX navigation; Clock (j-) file is created using the Script MAKEJ

3. Files derived from Products (external ephemerides or Precise orbits) **–G file** &**T-file**

   The script sh_sp3fit generates orbital files for GAMIT processing from the Earth-fixed ephemeris in "SP3" format from an IGS analysis center. Alternatively these files can be created from the broadcast ephemeris on a RINEX navigation file or can be copied directly from SOPAC in a GAMIT-format (**g-file** containing Initial conditions for the satellites' orbits that can only be used in GAMIT GPS data processing) or a **T-file** (GAMIT tabulated ephemeris). Alternatively; A g-file is created either at the time of downloading if the script *sh_get orbit* is used. (*sh_get orbit* downloads into /igs an sp3 file and creates a g-file). Or prepared using the scrip **<*ngstot*>** before GAMIT Processing and this g-file is integrated by the script ARC to get **T-files.**

4. Station coordinates in the form of an **L-file**

   The L-file contains the coordinates of all the stations to be used in the experiment. The L-file can be in spherical format (old GAMIT style), with coordinates only, or in Cartesian format (same as GLOBK apr file) with coordinates and optionally velocities.

   The latter is now preferred since it allows for motion of the station during the session and for better identification of stations displaced by earthquakes. An old-style GAMIT L-file is generated for a particular epoch from a GLOBK apr file using the program *gapr_to_l.*

gapr_to_l <globk.apr> <l-file> <full names> <date>

An updated L-file is written by <*solve*>

5. Receiver and antenna information for each site (file **station.info**);

All of the receiver and antenna information specific to a particular site occupation is recorded in a file station.info, accessed by MAKEXP, MAKEX, MAKEJ and MODEL. The values entered correspond to a single occupation of either one day or a series of days

6. Satellite list and scenario (file **session.info**);

This file contains the start time, sampling interval, number of observations, and satellites to be used in generating the X-file for a particular day

7. Control files for the analysis (**sittbl**. and **sestbl**.);

Sittbl. Contains information on how to treat individual sites, such as apriori constraints on positions

Sestbl. Contains the overall processing parameters such as type of observables model used, and other necessary parameters for the batch run.

8. Links to the following global files: nutations (**nutabl**.); lunar and solar ephemerides (**soltab**. And **luntab**.); geodetic datums (**gdetic.dat**); leap seconds (**leap.sec**); spacecraft, receiver, and antenna characteristics (**svnav.dat** ,**antmod.dat rcvant.dat**); Earth rotation (**pole. ut1**); and ocean tides (**stations.oct** and **grid.oct**)

3.3.4 GAMIT Batch Processing

Batch processing is accomplished by invoking sequentially and with appropriate input files the GAMIT modules that perform the required computations. The command or "batch" files to invoke the modules are created, for each standard type of analysis, by program **fixdrv (Fix table driver)**. The batch run set up by fixdrv would typically go through the following steps:

- generation of an orbital ephemeris with partials (T-file, arc)
- generation of satellite attitude values (Y-file, yawtab)
- generation of atmospheric and loading values (U-file, grdtab)
- generation of residuals and partials (C-files, model)
- automatic edit of residuals (new C-files, autcln)
- solution (M-, Q-files, cfmrg/solve)
- regeneration of residuals and partials with an improved model (C-files, model)
- automatic edit of residuals (new C-files, autcln)
- solution (M-, Q-, and H-files, cfmrg/solve)

The double pass through model, autcln, and solve serves two purposes: 1) the model obtained from the first solution can be used to flatten the residuals, allowing for improved editing and also the display of post-fit (one-way) residuals for evaluation; 2) adjustments station coordinates are reduced to a few centimeters, assuring that non-linearities do not degrade the final estimates. In most cases, the results of processing can be accessed through inspection of the print output (Q-file) of the final solution and the data statistics compiled by autcln (autcln.sum.post). (if the automations script sh_gamit is used; These values are echoed in the sh_gamit_[day]summary file and mailed to you by sh_gamit.)

If there are problems, then one or more steps of the batch job can be run individually, or fixdrv (and occasionally makex) can be run to repeat the complete processing sequence.

GAMIT can be run day by day however this is time consuming process and prone to errors. The more efficient way is to use automation script like sh_gamit created at MIT or GPe a series of scripts developed by Dr. Eric Calais. (Gpe requires internet connection).

In this project, sh_gamit was used to automate the GAMIT processing to produce estimates and associated covariance matrix of station positions (quasi-observations), for input into GLOBK. Figure 3.3 represents a flow chart for GAMIT GPS data processing.

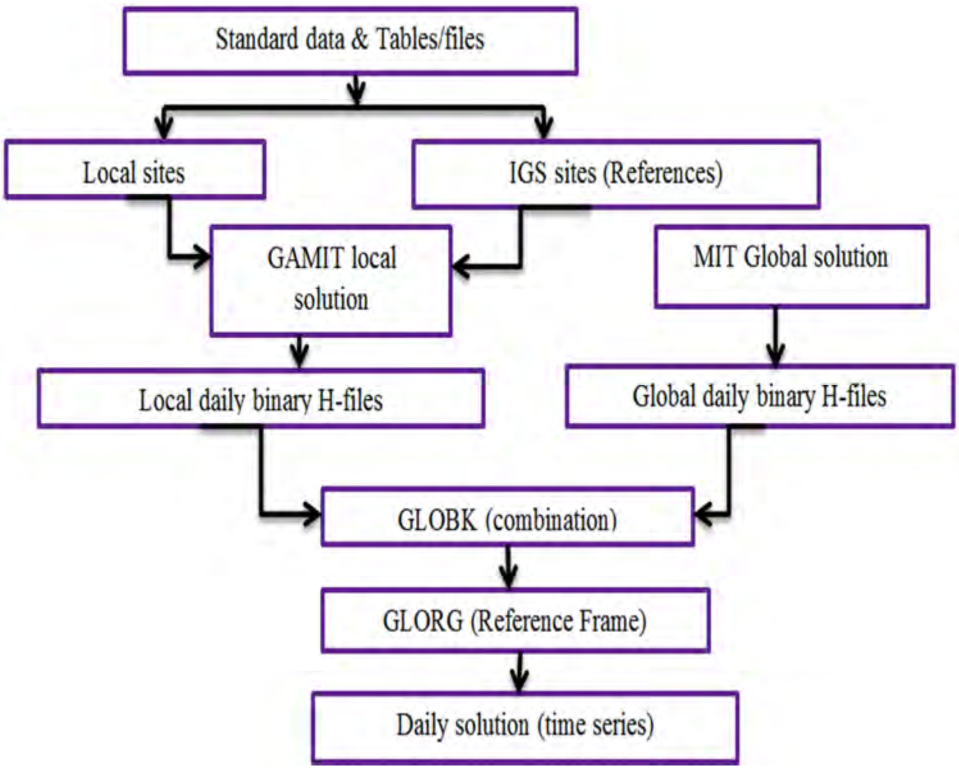

Figure 3. 3: Flow chart for GAMIT/GLOBK DGP Processing

3.3.4 Data Quality Assurance using GAMIT Results

Other method for data Quality check was by using results from the GAMIT processing. Sky plot and phase residual versus elevation plots were was used to check the data for the observations that showed bad root mean squares in the results from the GAMIT processing

3.3.4 .1 Sky plots

Sky Plots are used to assess multipath, water vapor. The red lines symbolize the track of the satellite in the sky; black lines represent phase residuals, the green colour show positive residuals, yellow signifies negative residuals and the blue color indicates that the no data is available during this path. Concentration of residuals at a given place, only at one time, it indicates existence of water vapor, whereas concentration of residuals at a particular place for different times indicate multipath.

Figure 3.4 show sky plot for stations KWSI on day 228 (a) and 229 (b) respectively.

Figure 3.4(b) shows that on day 229 there are data gaps. For half the day (12-24hrs) there were no data collected.

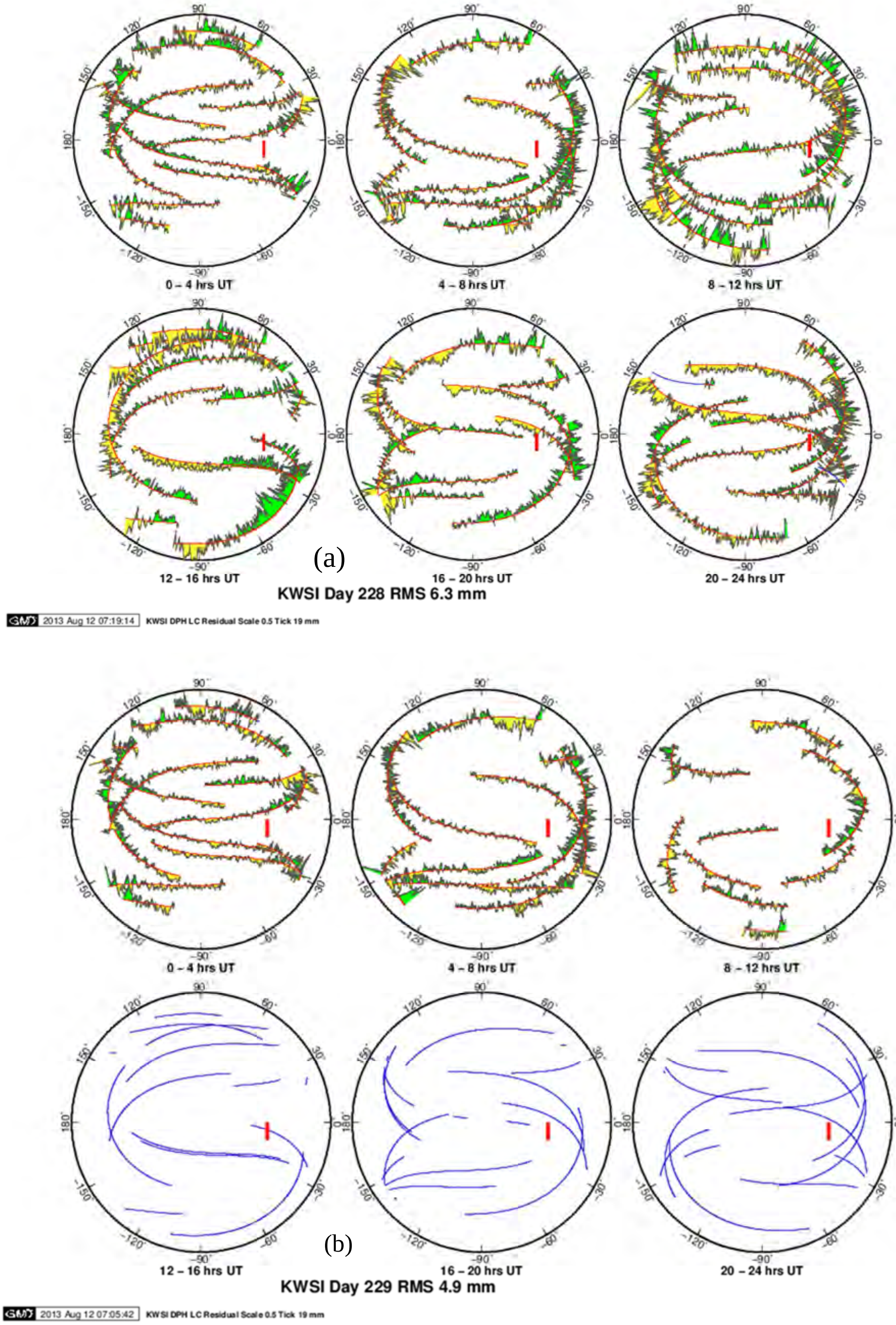

Figure 3. 4: Sky Plot of KWSI on days 228 (a) and 229 (b)

3.3.4 .2 Residual versus Elevation plots

Residual versus Elevation plots are used to assess antenna phase center model. Figure 3.5 show Residual versus elevation plot of stations KWSI on days 228 (a) and 229 (b) respectively. In Both cases the Pattern is good. Bands are high-frequency multipath, red line is a smoothing of individual values, the mid elevation angle noise could be atmospheric errors, Green lines show the elevation-dependent noise model, shown at top of the plots and used to reweight the data in solve.(Herring 2012). The bad pattern is shown in Herring (2012), in which, systematic signature of smoothed values indicates, a poor model of the antenna phase pattern (perhaps a misidentified antenna in station.info)

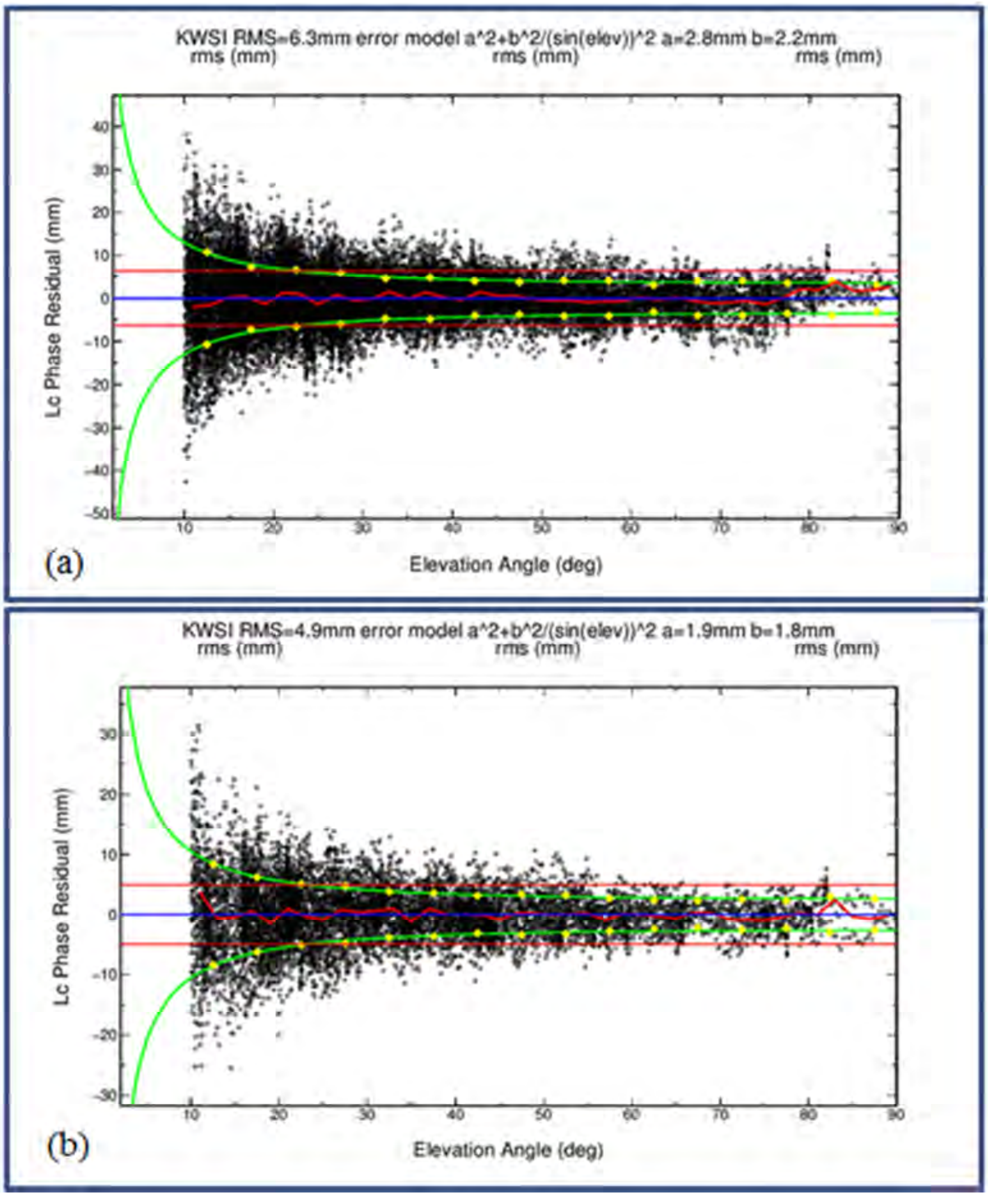

Figure 3. 5: Residual versus Elevation plots for KWSI on days 228 (a) and 229 (b)

3.3.5 Position and Velocity Estimation Using GLOBK

After all necessary checks for quality assurance of the GAMIT solution, GLOBK was used to give estimates for position and velocity.

GLOBK in an ensemble of programs collected in Kalman Filter (kf) directory. GLOBK operates through distinct programs, which can be invoked with a single command or run separately. These programs perform different functions such as conversion of solution files from analysis of primary observations into binary h-files (*htoglb*), combining quasi-observations either from multiple networks and or epochs (*glred* or *globk*), and to impose on this solution a reference frame appropriate to the scientific objective (*glorg*). Note that *globk* and *glred* are the same program, just called in different modes: *glred* to read data from one day at a time for generating time series, *globk* for stacking multiple epochs to obtain a mean position and /or velocity.

GLORG allows coordinates systems to be defined by applying explicitly rotations and translations rather than tightly constraining some stations, it also allows post applications of constraints (e.g. equating velocities at nearby sites). If there are loose constraints on site positions and velocities, apriori coordinates and velocities can be changed. Figure 3.6 shows a flow chart for GLOK solution.

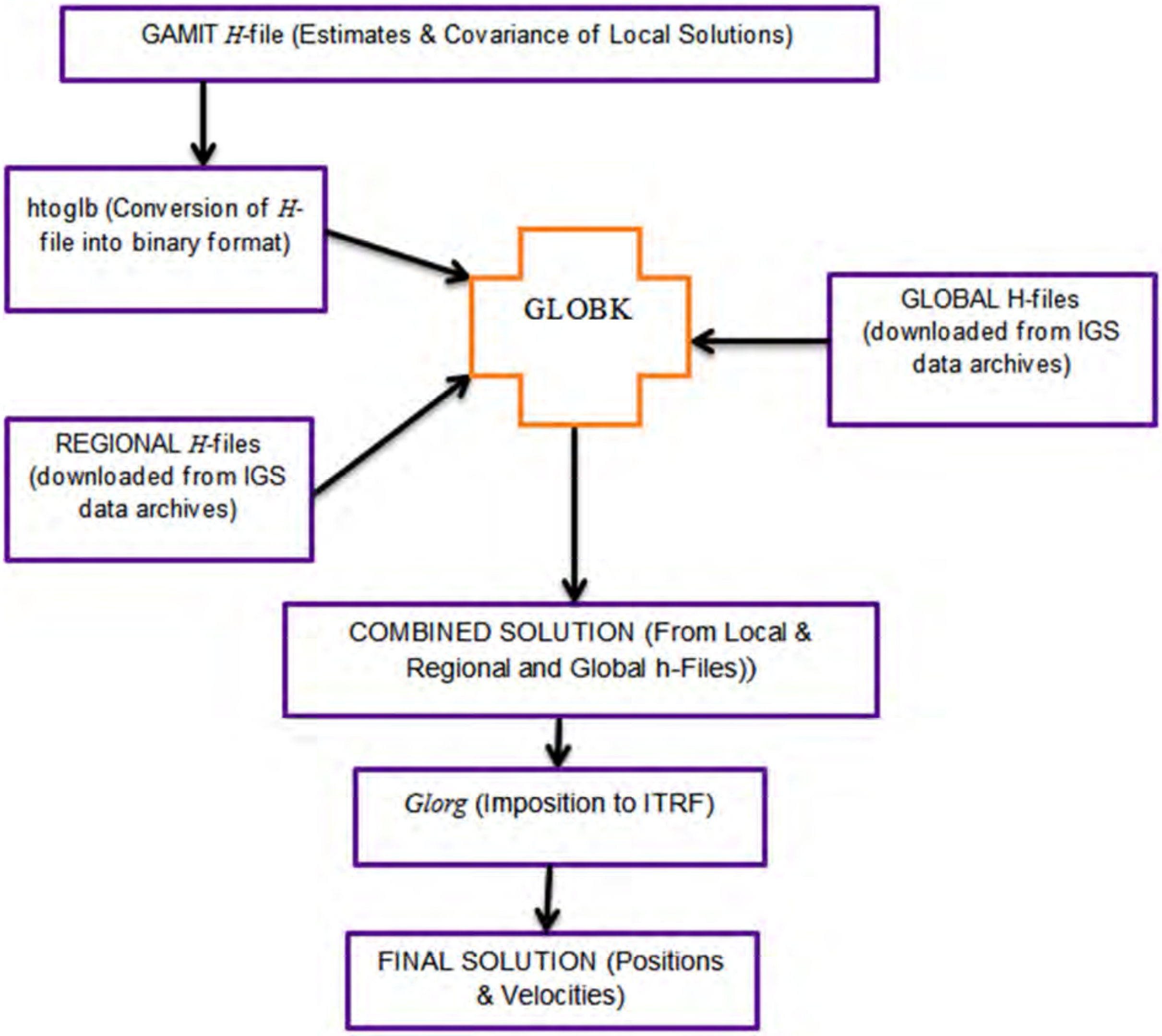

Figure 3. 6: Flow chart of GLOBK data processing

In this research the scripts for automation of GLOBK, such as, sh_glred, glred and globk/glorg, were used. The results from GLOBK run are time series of position estimates and velocities estimated from GAMIT H-files. Sh_glred with necessary specifications was used to automate the production of time series.

The results from GAMIT/GLOB are position time series and Station velocities.

Figure 3.7 shows position-time-series for station ARS1. The time series for other stations are presented on appendix VI

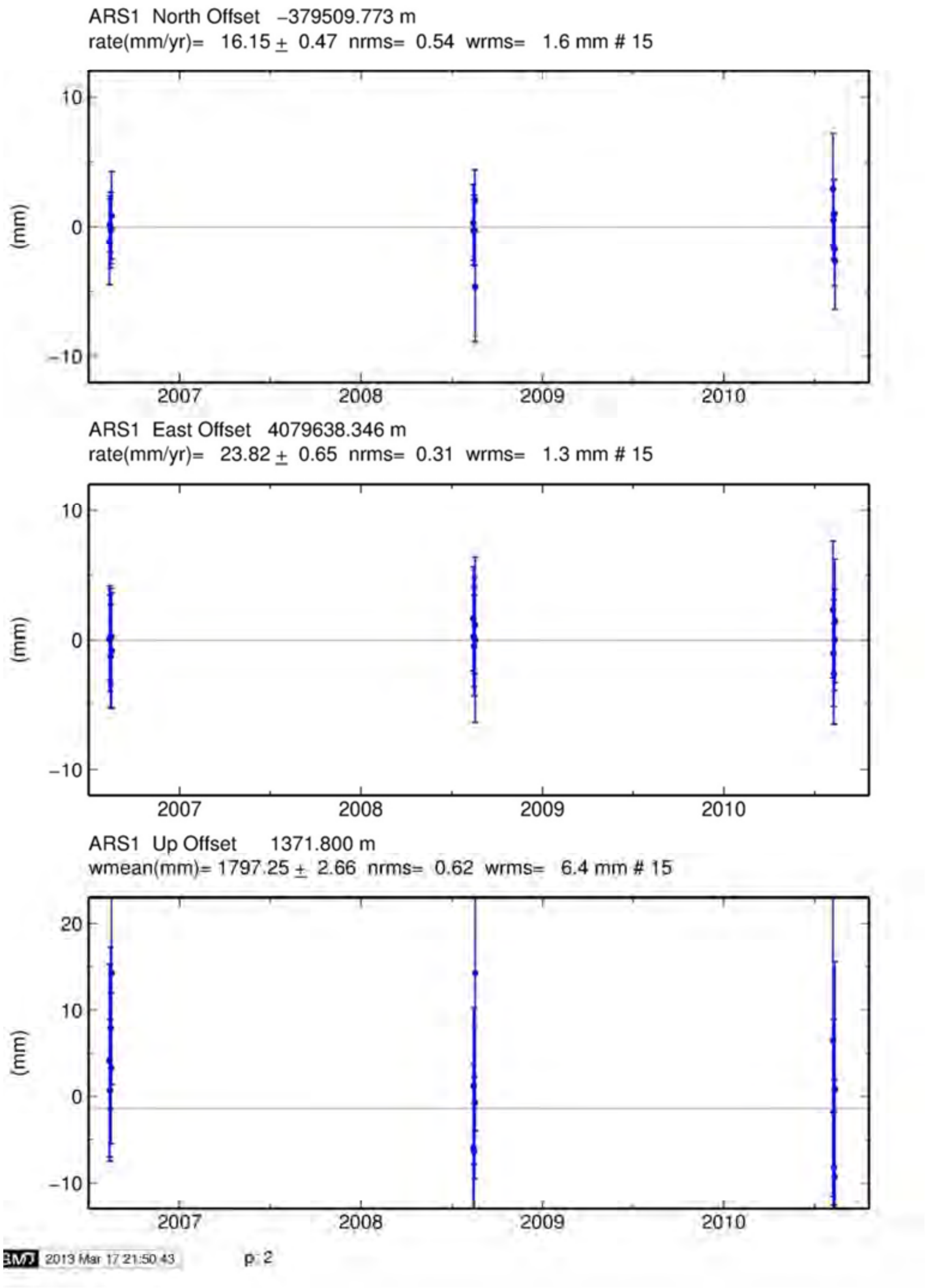

Figure 3. 7: Position Time Series for ARS1

3.4 Precision of the daily solution

A measure of precision of station coordinates of daily repeatability measuring the Position scatter from the mean is determined according to Larson and Agnew (1991) as:

$$wrms = \sqrt{\frac{\frac{N}{N-1}\sum\frac{\{y_i-(a+bt_i)\}^2}{\sigma_i^2}}{N}} \quad \text{.................................. (3.1)}$$

Where:

N is the number of occupation days or number of samples

y_i is the weighted mean of the coordinates of the station

$\sum \sigma_i^2$ is the error of the coordinates for day *i*

$a + b$ are the parameters of the best-fit straight line through the time series, and

The quality of the stabilization for each epoch is used as the first check of the solution using NMRS and WRMS (Herring et al 2010).

The results obtained show that, most of the stations have smaller values of normalized and weighted root mean squares (NMRS and WRMS) respectively (Figures 3.8 and 3.9 show that 95% of all stations are less than 5mm/yr WRMS in North-South and East-west components, 70% of the stations are less than 2 mm/yr (WRMS) in North-South component, and 70% less than 2.2mm/yr (WRMS) in the East-West component. Similarly, With regard to NRMS, over 95% of the stations have repeatability rate less than 1.1mm/yr, 70% less than 0.7mm/yr in all directions. For the Up component however 95% of the stations are less than 1mm/yr NMRS and less than 8.7mm/yr WRMS. The NRMS values for the stabilization must be close to 1mm/yr in all three components, and the WRMS should range between 1-2 mm in horizontal components and 3-10 mm in vertical component (Herring et al 2010).

According to this statistical analysis, these results show good quality of data processing in GAMIT/GLOBK differential solution.

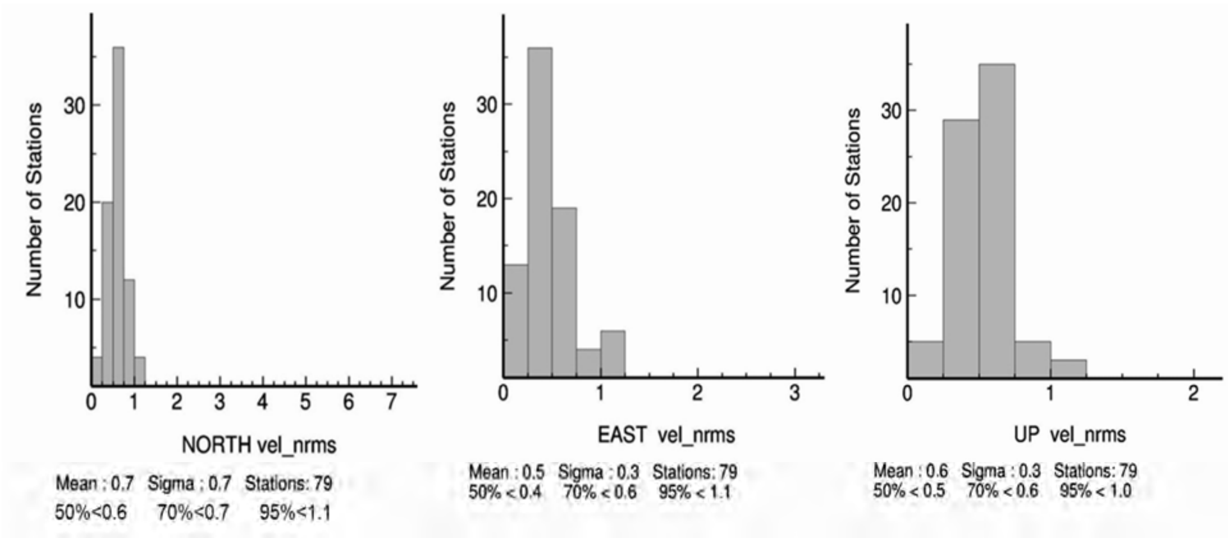

Figure 3. 8: Normalized Root Mean Squares (NRMS) from GLOBK position time series

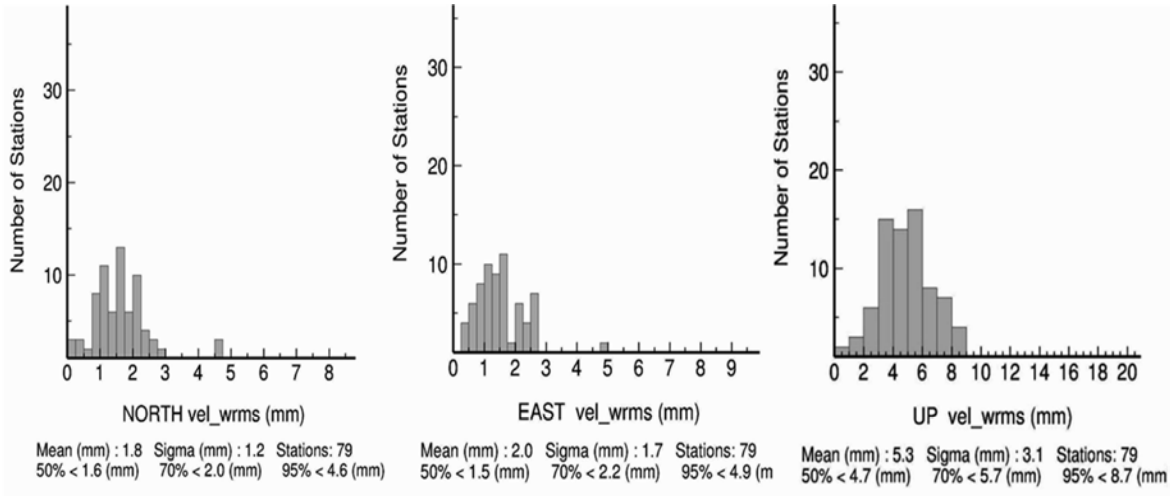

Figure 3. 9: Weighted Root Mean Squares from GLOBK position time series

Regarding WRMS of position repeatabilities (Table3.1 (a) and figure 3.10 (a) in N-E, the uncertainties were 0.1-4.6mm North, and 0.3-8.5mm East. With regard to NMRS the values in N-E were 0.06-1.12(table 3.1(b) and figure 3.10(b). These results depict a very accurate solution

Table 3. 1: Weighted and Normalized Root Mean Squares from GAMIT/GLOBK for local sites

	WRMS(mm)				NRMS(mm)		
STATION	N	E	U		N	E	U
ARS1	1.6	1.3	5.2		0.54	0.31	0.51
LGDO	1.9	4.7	3.2		0.68	1.15	0.33
MTW1	1.8	1	12.1		0.63	0.29	1.18
KWSI	0.1	1	4.4		0.06	0.3	0.61
TABR	0.8	1.6	3.9		0.34	0.44	0.44
KRGW	1.5	2.6	6.4		0.52	0.68	0.67
SAME	1.7	1.1	5.7		0.7	0.3	0.69
SUMB	1.1	1.3	2.4		0.56	0.43	0.36
TANG	1.1	2.4	7.1		0.38	0.64	0.76
NGRS	1.1	2.2	3.3		0.37	0.51	0.29
KILW	1.8	1.3	6.3		0.6	0.33	0.57
MORO	2.1	2.2	5		0.83	0.61	0.54
KLCP	1.8	2.6	6.2		0.64	0.65	0.71
KIBY	1.4	1.5	7.9		0.57	0.45	1.01
SERN	1.9	3.9	5.3		0.7	1	0.62
ITIG	2.1	0.7	4		0.84	0.19	0.48
KIMO	1.4	1.7	4		0.57	0.46	0.46
KYEL	2.3	1.3	4.4		0.98	0.39	0.5
KOND	1.7	1.7	3.8		0.66	0.47	0.45
BABT	2.1	2.6	18.2		0.76	0.68	1.9
EMSK	2.1	3.4	13.9		0.82	0.92	1.53
SGDA	4.6	8.5	4		2.12	2.52	0.52
MAKA	1.1	0.9	4.2		0.47	0.27	0.46
MAS2	1.3	1.6	4.9		0.54	0.51	0.59
BEYA	1.8	1	4.1		0.9	0.32	0.53
VWA2	1.7	0.9	3.3		0.69	0.23	0.3
GEL4	1.6	0.3	1.4		0.6	0.08	0.15
KRT2	2.1	1.5	3.6		0.81	0.4	0.44
NIAT	2.2	1.1	3.2		0.78	0.28	0.33
TDRU	1.6	1.2	3.2		0.39	0.23	0.17
MBB1	0.9	2.7	2.4		0.37	0.75	0.24
MPA2	1.3	2	5.8		0.35	0.37	0.33
HNDI	2	2.3	4.6		0.59	0.51	0.34
MBGA	1.1	1.4	4.2		0.56	0.48	0.6

IRI2	2	1.6	3.7		0.79	0.45	0.43
DOD2	1.5	1.3	5.1		0.64	0.39	0.66
NZG2	1.3	2.4	5.5		0.52	0.63	0.67

(a) (b)

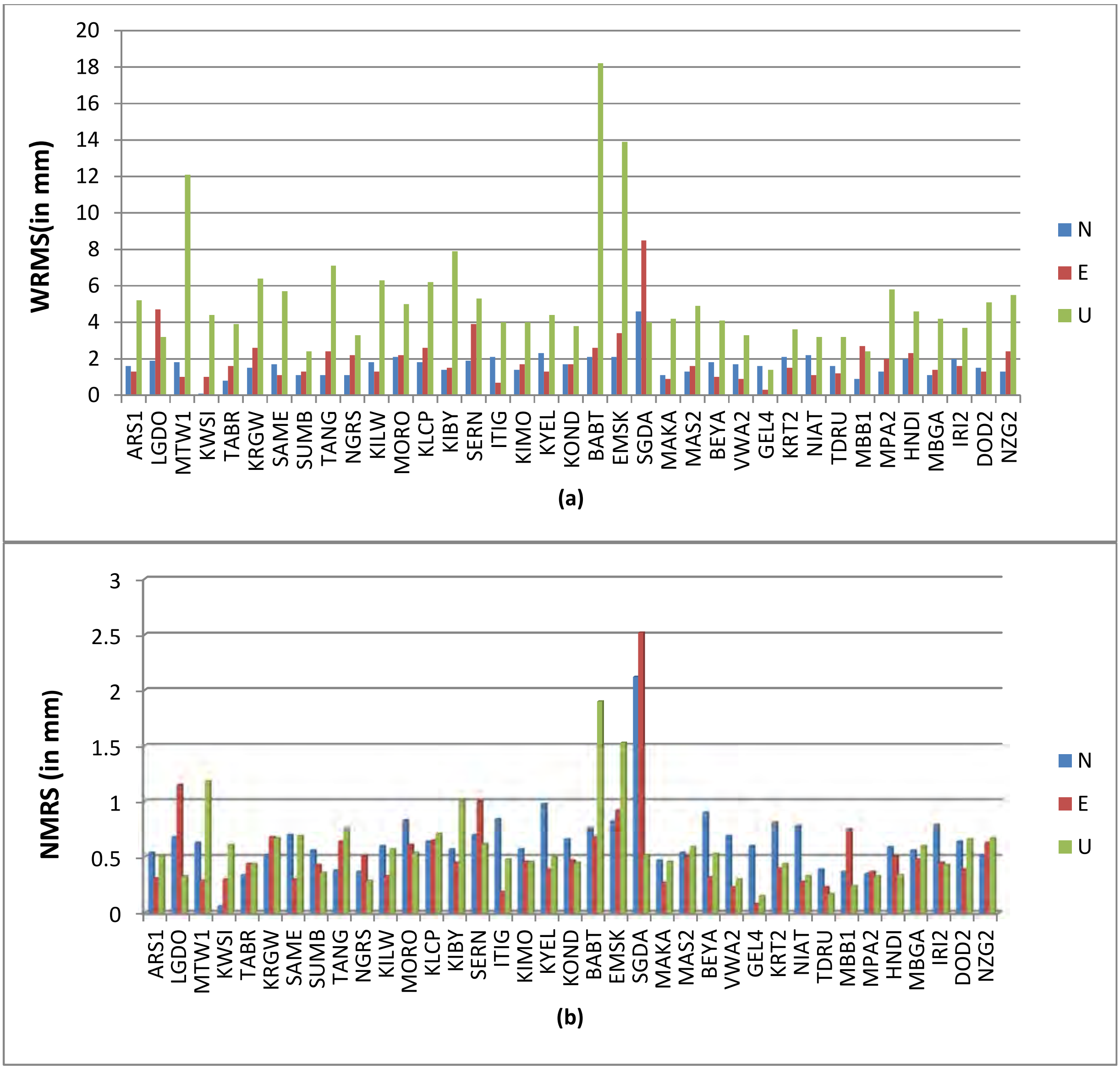

Figure 3. 10: WRMS (a) and NMRS (b) for campaign GPS sites

The obtained Position coordinates for each site from GAMIT/GLOBK solution, was used as a reference for assessing the corresponding solution from APPS PPP solution. The analysis of the results obtained from the comparison is given in chapter four.

3.6 Precise Point Position Estimation Using Online services.

Many software packages for GPS precise Point Position exist. One such software is GIPSY-OASIS developed at the National Aeronautics and Space Administration (NASA) Jet Propulsion Laboratory (JPL) in Pasadena, California. To run the GIPSY-OASIS software, an active license is required. Procedures required to obtained the license are available at https://gipsy-oasis.jpl.nasa.gov/

However there are online services for PPP solutions. The online GIPSY-OASIS service is called **APPS** (Automated Precision Positioning Service), which replaced Auto-GIPSY. It does a basic analysis of GPS data in a RINEX format. To use APPS GIPSY is not required; all the processing occurs on a computer at JPL.

There are other free online PPP services, as listed hereunder. When submitting RINEX observation files on each website, the data will be processed by those services and then the PPP solution is obtained and sent back.

GAPS: by University of New Brunswick (UNB) available as an online post-processing engine via their webpage. Static as well as kinematic processing is possible. They accept an observation file in the RINEX formats with GPS data. IGS orbits and clocks necessary for processing the observations are automatically retrieved from one of the IGS global data centers.

magicGNSS by GMV : processing static and kinematic GPS and GLONASS real-time data in RINEX format. Only dual-frequency PPP is supported. Real-time GPS and GLONASS orbits and clocks needed by PPP are generated internally (magicODTS). Rapid and final GPS orbits and clocks from IGS are also used, if available.**CSRS-PPP by Natural Resources Canada (NRCan)** provides post-processed position estimates from GPS observation files submitted by the user in RINEX format. Precise position estimates are referred to the Canadian Spatial Reference System (CSRS) standard North American Datum of 1983 (NAD83) as well as the International Terrestrial Reference Frame (ITRF).Currently, users need only specify the mode of processing -- static or kinematic -- and the reference frame for position output -- NAD83(CSRS) or ITRF.

The PPP GPS solution technique is also available in Bernese software, which has both PPP and Differential (relative) modes (Dach et al 2007).

In this research all the above online services were used. After assessing the comparison of the online results, APPS was chosen as the basis to compare with GAMIT/GLOBK results.

APPS was chosen because in many of the comparisons via PPP Software Centre of the University of New Brunswick (UNB) it showed stable consistent results between epochs of each observation. (http://gge.unb.ca/Resources/PPP). The comparison of PPP solutions is done online; just a submission of RINEX file with all naming conventions obeyed to *ppp@unb.ca* gives the results of the four PPP software packages available online. For example, by submitting observation file in RINEX format for a reference station DGAR for day 225 of 2006, via e-mail to ppp@unb.ca the results for PPP solutions from four software packages were obtained. The resulting coordinates are as shown in table 3.2, and a comparison between the available PPP online solutions are represented in figure 3.8 to figure 3.12. The comparison was made among NRCan/CSRS, GAPS, APPS and MagicGNSS by GMV (ww.gmv.com). The results obtained from this comparison show that APPS give a stable solution compared to other software packages. However, section 3.7 shows that station KSW for day 227 of 2006 misbehaved in APPS, yielding inconsistent results compared to results from GAMIT/GLOBK and other online PPP software packages. The following shows a report generated based on the results of Table 3.2 by the PPP software comparisons from UNB's PPP Software Centre, for the submitted RINEX file. Figures 3.11 to 3.15 show the comparison in time series of parameter estimations of latitude, longitude, height, tropospheric Zenith delays and receiver clock offsets respectively.

PRECISE POINT POSITIONING SOFTWARE CENTRE

THE PRECISE POINT POSITIONING SOFTWARE CENTRE:
http://gge.unb.ca/Resources/PPP/

RINEX OBSERVATION FILE PROCESSED: dgar2250.06o.gz

REPORT CREATED ON: Sun Jul 07 14:41:10 2013 (UTC Time)

PROCESSING MODE: Static

PPP RESULTS ARE PROVIDED BY:
CSRS-PPP: http://www.geod.nrcan.gc.ca/online_data_e.php
GAPS: http://gaps.gge.unb.ca
APPS: http://apps.gdgps.net/
magicGNSS: http://magicgnss.gmv.com/ppp

ERROR MESSAGES: none

COMMENTS:
- Refer to http://gge.unb.ca/Resources/PPP/OnlinePPPs.html for more details regarding the processing characteristics of each software.
- For acknowledging the PPP Software Centre, please use the following reference:
Banville, S., R.B. Langley and M.C. Santos (2009). "The Precise Point Positioning Software Centre: An Insight Into Online PPP Services", Poster presented at the IAG 2009 Meeting, Buenos Aires, Argentina, August 31.

Table 3. 2: Sample of Final Coordinate Estimates from 4 online PPP solutions compared

Software	X	Y	Z	h
NRCan	1916269.338	6029977.473	-801719.848	-64.947
GAPS	1916269.338	6029977.460	-801719.873	-64.955
APPS	1916269.329	6029977.449	-801719.844	-64.973
magicGNSS	1916269.344	6029977.489	-801719.866	-64.927

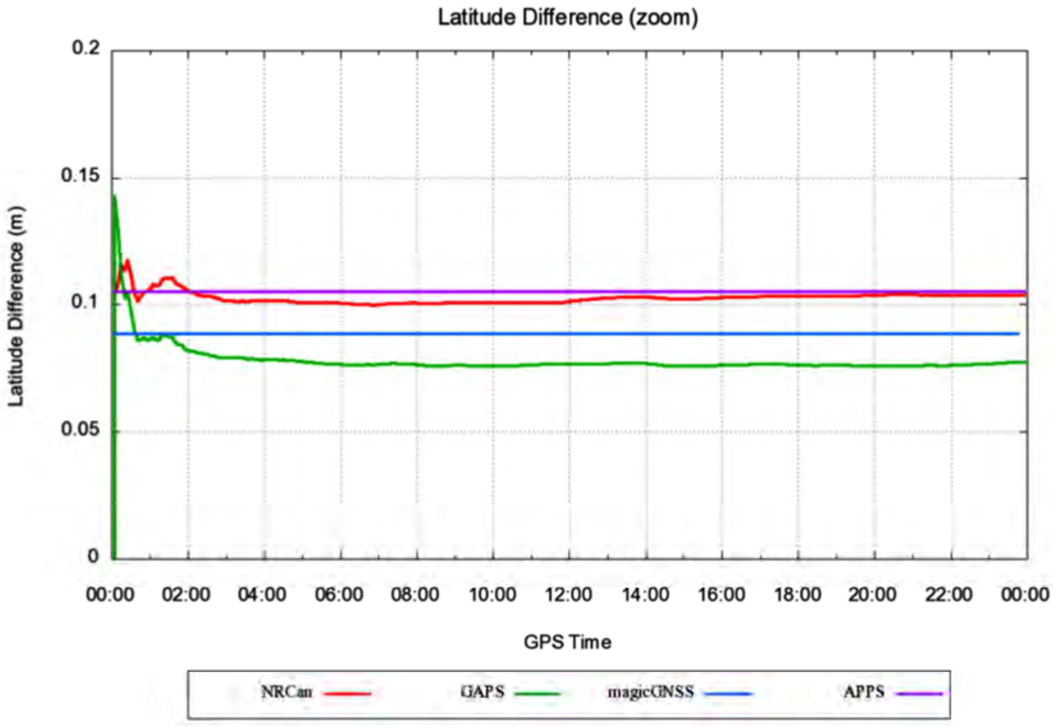

Figure 3. 11: Comparison of PPP solutions using Latitude difference vs. GPS time

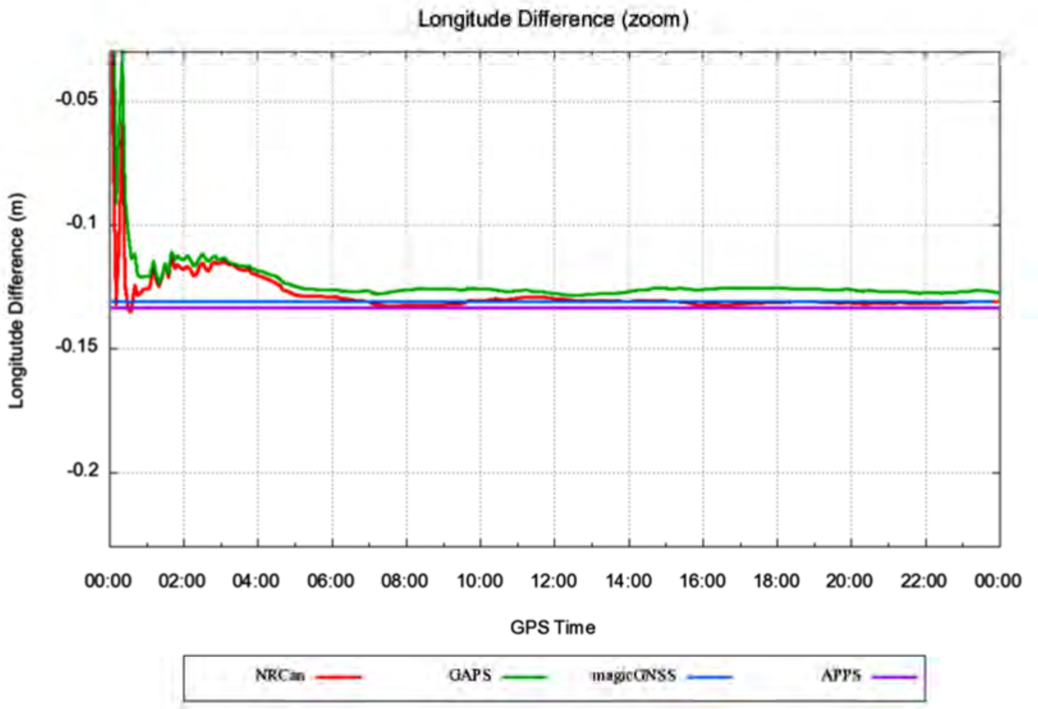

Figure 3. 12: Comparison of PPP solutions using Longitude difference vs GPS time

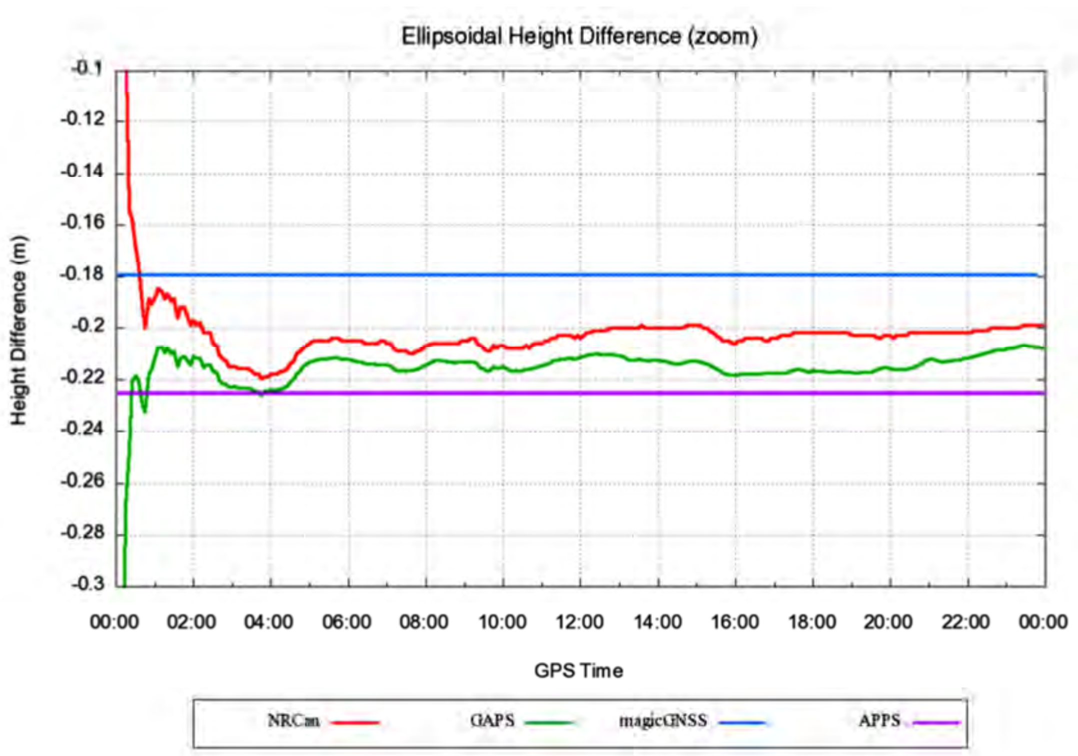

Figure 3. 13: Comparison of PPP solutions using Height difference vs. GPS time

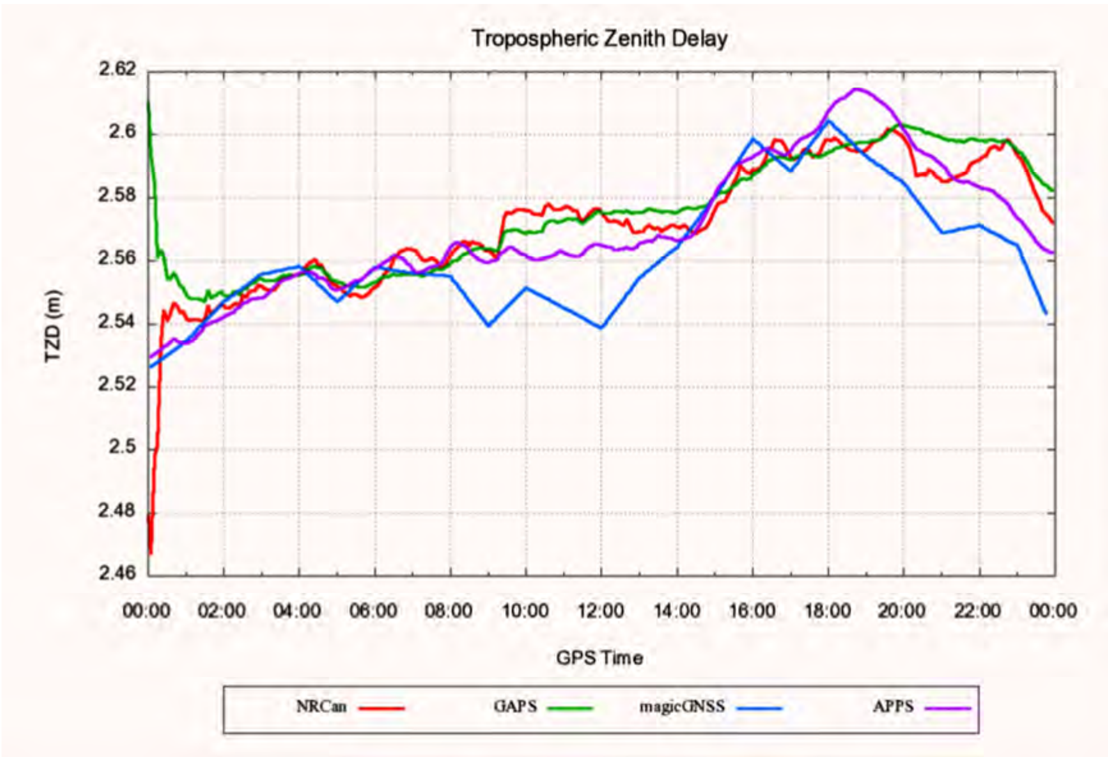

Figure 3. 14: Comparison of PPP solutions using Tropospheric Zenith Delay (ZTD) vs. GPS time

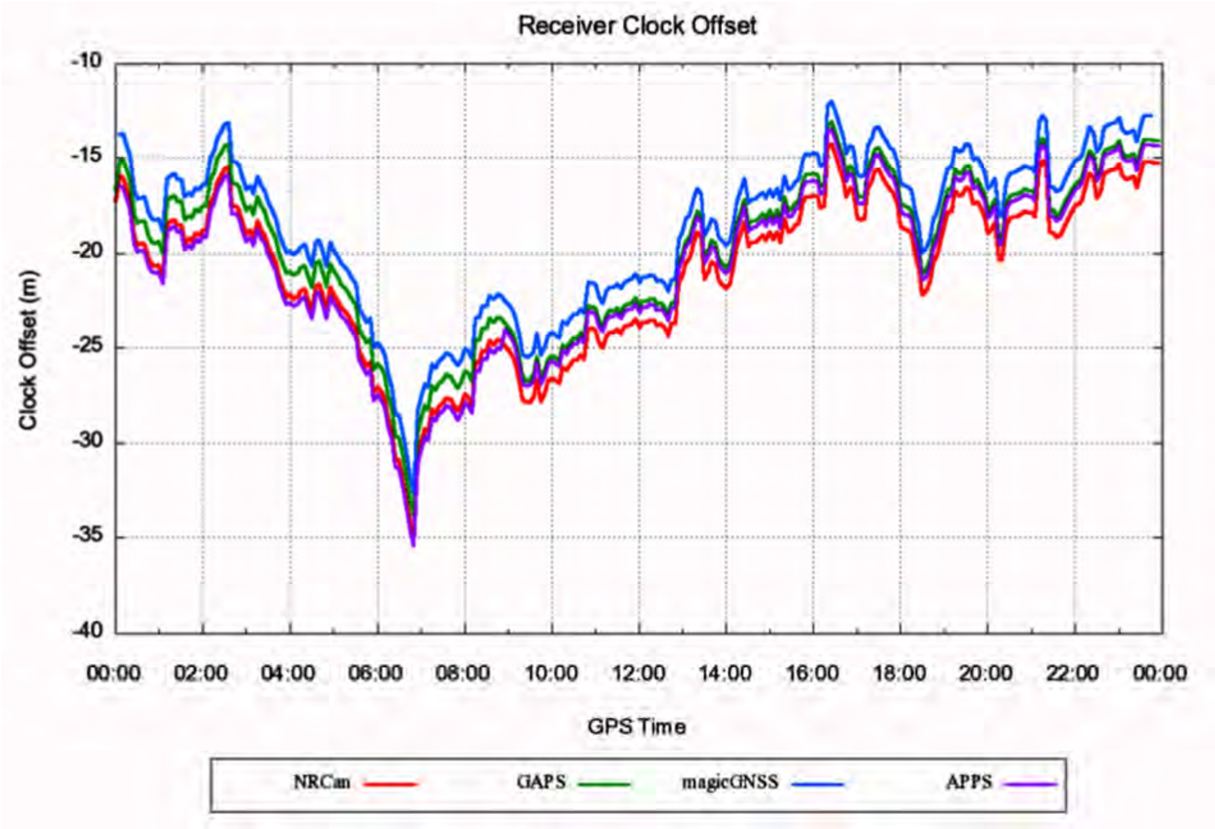

Figure 3. 15: Comparison of PPP solutions using Receiver Clock Offsets vs. GPS time

3.6.1: Data structure and Coordinate Extraction from output files

To get XYZ from the processed station, it can be easy if one studies the data structure contained in each resulting file. In APPS solution, X Y Z are saved in a file of certain nomenclature year-month-date.stationId.sum eg. 2006-08-13.ARS1.sum. the data format support unix regular expressions to extract desired information.

Similarly the coordinates in org file from GAMIT/GLOBK are arranged in a format that supports unix regular expression to extract required information. A description of how X, Y, Z coordinates were extracted is given in appendix VII describes how coordinates X, Y, Z from GAMIT/GLOBK were extracted.

3.6.2 Computation of residuals

Each list of coordinates from PPP solution was compared to its corresponding list of coordinates obtained from GAMIT/GLOBK's differential solution. The difference in Time series was the basis for assessment of PPP's solution accuracy.

The differences between two datasets namely GAMIT/GLOBK solution and GIPSY/OASIS - (APPS) were computed using R program (open source programming language and software environment for statistical computing data analysis and graphics downloaded from http://www.r-project.org/. It is user friendly and very efficient in array computations. The mean and standard deviation of the differences were also computed using R function. Appendix VIII shows a sample code of R-Program used in computation of residuals, and their corresponding Mean and Standard deviations.

3.7 Blunders detected

In 2006, the difference between two solutions for station KWSI on 226th day was extremely large. By investigating the preceding results of the same station it was found that the data on that particular date greatly misbehaved in APPS with the values of position coordinates obtained were

5173766.9415 3713805.5576 -372990.8979 instead of

~ 5138279.682 3761453.901 -383792.314 for X Y and Z respectively

The source of such big blunder could not be identified. After pointing out this blunder, the online solution was repeated for the four available files of KWSI but this time using also other online PPP services. This was done in order to check whether this data would misbehave in all PPP online services.

The results of DGPS using GAMIT/GLOBK were stable and consistent within 0 to $\pm$5mm. In PPP solution two software packages namely, NRCan and GAPS were Consistent. Considering differences between measurement as a measure of goodness, NRCan gave the best (0 to $\pm$6mm) followed by GAPS (0 to 2cm) But APPS and MagicGNSS gave inconsistent results. MagicGNSS gave worse 16.4km in X, 16.4km in Y and 3.9km in Z components and APPS gave the worst result approximately; 35.5km in X, 47.6km in Y and 10.8km in Z. The coordinates X, Y and Z values for the 4 series measurements at KWSI from DGPS solution and from PPP solutions are shown in tables 3.3 to 3.7. The graphs showing the Magnitude in differences between measurements are also presented in figure 3.16(a, b and c) for consistent results and figure 3.17(a and b) for inconsistent results.

The reason to why such inconsistences occur only in PPP solutions of APPS and MagicGNSS is not well known to the researcher, but may be due data gaps identified in sections 3.3.2 and 3.3.4. Bu the main reason may be undifferenced clock biases and phase ambiguity resolutions which are main factors affecting PPP GPS measurements. In Appendices IV and V, summary of results of the well behaved data set KWSI2280.06o and the misbehaved station KWSI2290.06o from APPS are given. Appendix V shows that there were biased receiver clock estimations.

Table 3. 3: GAMIT/GLOBK Results for 4 series of measurement at KWSI campaign GPS station (units in m)

STATION_DOY	X	Y	Z	SigX	SigY	sigZ
KWSI2260.06o	5138279.674	3761453.889	-383792.3134	0.0068	0.0054	0.0023
KWSI2270.06o	5138279.679	3761453.892	-383792.314	0.006	0.0047	0.0028
KWSI2280.06o	5138279.673	3761453.889	-383792.3134	0.0056	0.0045	0.0025
KWSI2290.06o	5138279.678	3761453.89	-383792.3138	0.0067	0.0052	0.0028

Table 3. 4: PPP Results from KWSI2260.06o (units in m)

Software	X	Y	Z	h
NRCan	5138279.666	3761453.883	-383792.318	1419.589
GAPS	5138279.635	3761453.855	-383792.345	1419.549
APPS	5138279.667	3761453.885	-383792.311	1419.591
magicGNSS	5138279.680	3761453.888	-383792.341	1419.604

Table 3. 5: PPP Results from KWSI2270.06o (units in m)

Software	X	Y	Z	h
NRCan	5138279.665	3761453.880	-383792.318	1419.587
GAPS	5138279.655	3761453.863	-383792.338	1419.569
APPS	5138279.670	3761453.890	-383792.311	1419.595
magicGNSS	5138279.676	3761453.893	-383792.341	1419.604

Table 3. 6: PPP Results from KWSI2280.06o (units in m)

Software	X	Y	Z	h
NRCan	5138279.669	3761453.881	-383792.319	1419.590
GAPS	5138279.660	3761453.876	-383792.340	1419.581
APPS	5138279.677	3761453.906	-383792.314	1419.611
magicGNSS	5138279.674	3761453.896	-383792.342	1419.605

Table 3. 7: PPP Results from KWSI2290.06o (units in m)

Software	X	Y	Z	h
NRCan	5138279.665	3761453.877	-383792.316	1419.585
GAPS	5138279.660	3761453.870	-383792.332	1419.576
APPS	5173768.620	3713805.707	-372991.344	1541.243
magicGNSS	5154663.552	3745069.386	-379846.008	4758.558

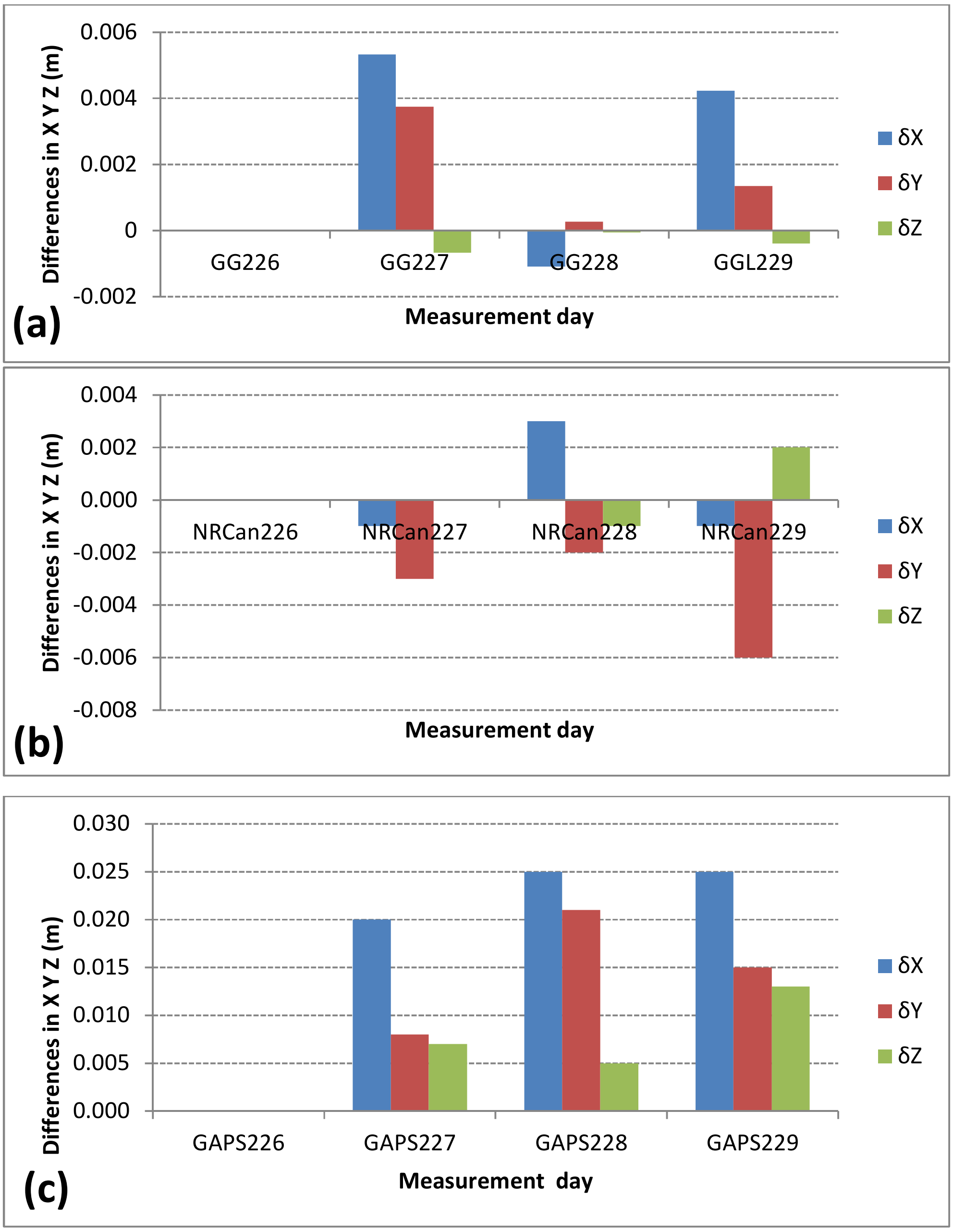

Figure 3. 16: Graph showing how GAMIT/GLOBK (a), NRCan (b), GAPS(c) yielded consistent results from all 4 days despite biases in the 4th day measurement of the 2006 series in KWSI campaign GPS station

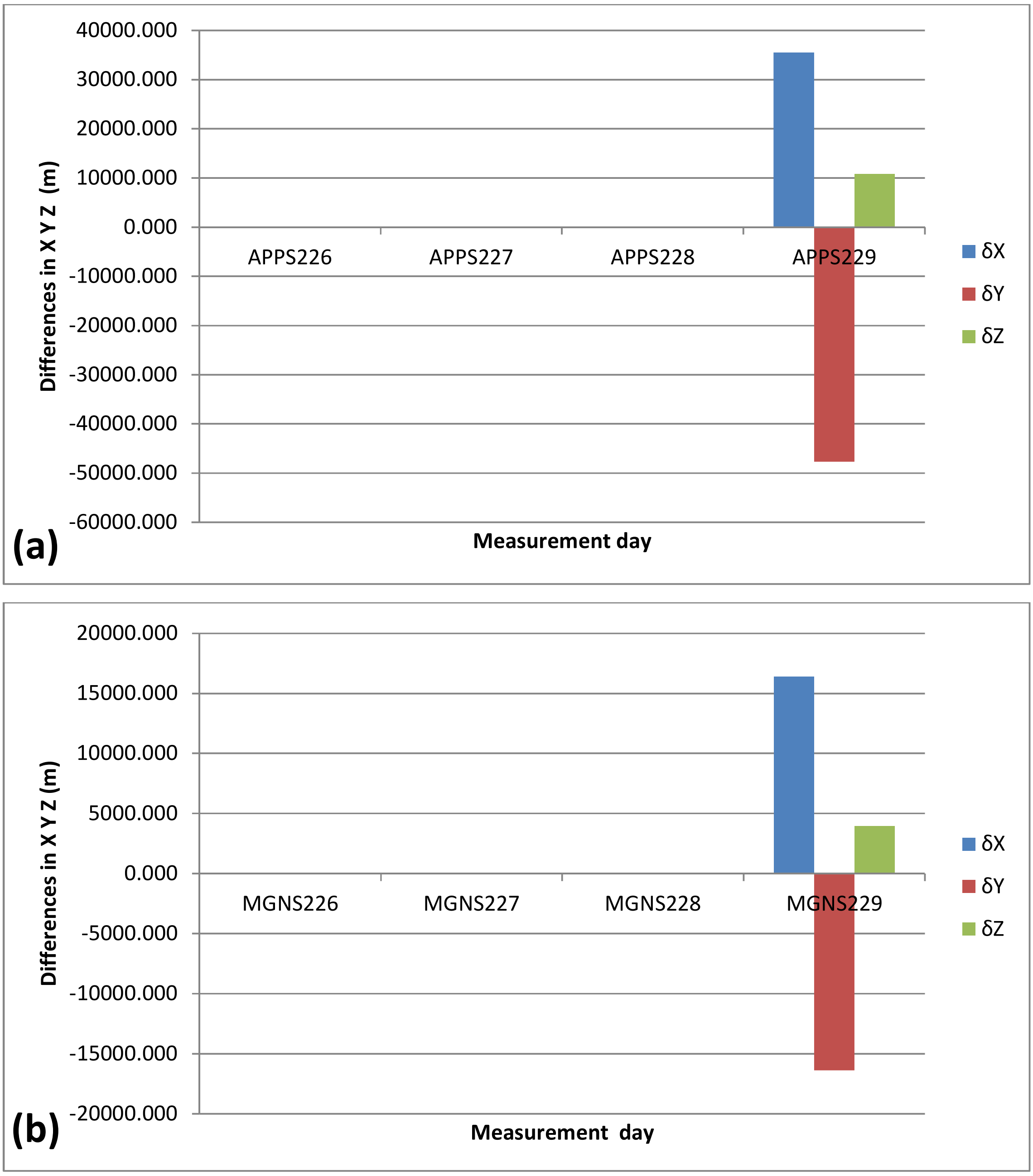

Figure 3. 17: Graph showing how APPS (a) and MagicGNSS (b) yielded inconsistent results at 4th day measurement of the 2006 series in KWSI campaign GPS station

Due to this inconsistence the observation on the 229th day of 2006 for KWSI was excluded from APPS results and it's corresponding though good GAMI/GLOBK solution was also excluded so that it should not bias the comparison results.

CHAPTER FOUR

4. OVERALL RESULTS COMPARISON AND ANALYSIS

4.1 Introduction

This chapter discusses the combined results and analyses the output of GPS Differential data processing using GAMIT/GLOBK and PPP solution using online services. Results from DGPS are compared with PPP solution and assessment of PPP solution is made regarding its accuracy in Geodetic GPS positioning. The average position for the sites with their respective sigmas from GAMIT/GLOBK are presented both in tabular form (table 4.1) and a bar chart showing sigma variations (figure 4.1) is presented. In Addition, the station velocities of sites for which comparison is made (table 4.1 and figure 4.2) are also presented for showing consistence of GAMIT/GLOBK solution.

4.2 Combined Solution from GAMIT/GLOBK

4.2.1 Average Position Estimates from GAMIT-GLOBK

The output of processing the GPS data is positions and velocities. The accuracy attained for each position in X, Y and Z components is shown in table 4.1 and in figure 4.1. The accuracy in the X component ranges from1.5 to 21mm. The accuracy of the Y component is between 1.7mm to 17mm while the accuracy of the Z component ranges from 0.5mm to 7.5mm.This range shows that, the position for all stations, were determined within allowable accuracy for a normal geodetic measurement.

Table 4. 1: Average Position Estimates from GAMIT-GLOBK

STATION	X	Y	Z	σ_X	σ_Y	σ_Z
MTW1	4803736.775	4039763.58	-1130484.71	0.00362	0.00319	0.00157
KILW	4860790.194	4010018.45	-983048.513	0.00454	0.00396	0.00177
TANG	4935956.633	3999612.71	-564352.842	0.00328	0.00293	0.00132
MAS2	4884806.584	3927015.92	-1180534.36	0.00768	0.00631	0.00293
KRGW	4976274.865	3949092	-569292.851	0.00349	0.00313	0.00136
HNDI	5001689.672	3912740.26	-600989.535	0.01886	0.01659	0.00506
SAME	5029956.694	3896912.21	-452207.43	0.00261	0.00231	0.00107
MORO	5014378.873	3871378.57	-744021.873	0.00248	0.00223	0.00108
TDRU	4972476.261	3811459.7	-1193269.92	0.01974	0.01587	0.00747
ARS1	5105080.291	3807010.37	-376832.822	0.00335	0.0029	0.00119

LGDO	5110559.16	3806980.91	-297693.186	0.00363	0.00274	0.00115
KIBY	5102872.553	3784458.33	-583703.017	0.00257	0.0023	0.00104
KWSI	5138279.676	3761453.89	-383792.312	0.00257	0.00226	0.001
NIAT	5144898.443	3750149.41	-399718.721	0.00498	0.00432	0.00159
GEL4	5154734.605	3745969.55	-290705.742	0.01113	0.00917	0.0031
NGRS	5163194.368	3734499.03	-289428.5	0.00432	0.00371	0.00133
KOND	5155315.158	3718174.4	-542673.114	0.00312	0.00271	0.00114
BABT	5163437.223	3717750.67	-461733.872	0.00368	0.00303	0.00127
DOD2	5147538.796	3705474.45	-681044.934	0.00358	0.00306	0.00129
IRI2	5134104.613	3688327.5	-856890.236	0.00943	0.00729	0.00294
KRT2	5173789.688	3713821.82	-372993.205	0.00449	0.00372	0.00147
EMSK	5194795.928	3674971.55	-460118.612	0.00359	0.00297	0.00123
KLCP	5208165.457	3679619.61	-202913.768	0.00317	0.00268	0.00109
MBGA	5133179.54	3585103.87	-1219588.17	0.00774	0.00619	0.00283
SERN	5227925.078	3646553.27	-266310.654	0.00364	0.003	0.00121
MBB1	5137403.428	3570627.72	-1238815.2	0.00932	0.00758	0.00355
MAKA	5180739.897	3592346.87	-973905.417	0.00393	0.00305	0.0014
SGDA	5225073.858	3621317.55	-531758.941	0.00286	0.00238	0.00103
ITIG	5232125.664	3594688.1	-630365.342	0.00302	0.00247	0.00107
KIMO	5264331.64	3539137.54	-677106.734	0.0035	0.00274	0.00117
KYEL	5229270.782	3496099.21	-1054842.94	0.00274	0.00221	0.00104
BEYA	5258838.151	3475046.97	-982047.332	0.01279	0.00923	0.00404
NZG2	5324448.514	3481978.32	-470360.767	0.00458	0.00368	0.00146
VWA2	5289322.415	3421043.48	-1007373.23	0.01135	0.00809	0.00326
TABR	5340925.784	3443571.05	-557118.184	0.00318	0.00245	0.00103
SUMB	5374975.545	3321519.01	-884441.365	0.00204	0.00171	0.00074
MPA2	5432552.992	3269449.98	-700761.083	0.02131	0.01591	0.00475
MBAR	5482951.251	3260442.67	-66519.7767	0.00149	0.00172	0.00052
UVIN	5480740.838	3214994.97	-563140.796	0.00361	0.00265	0.00109

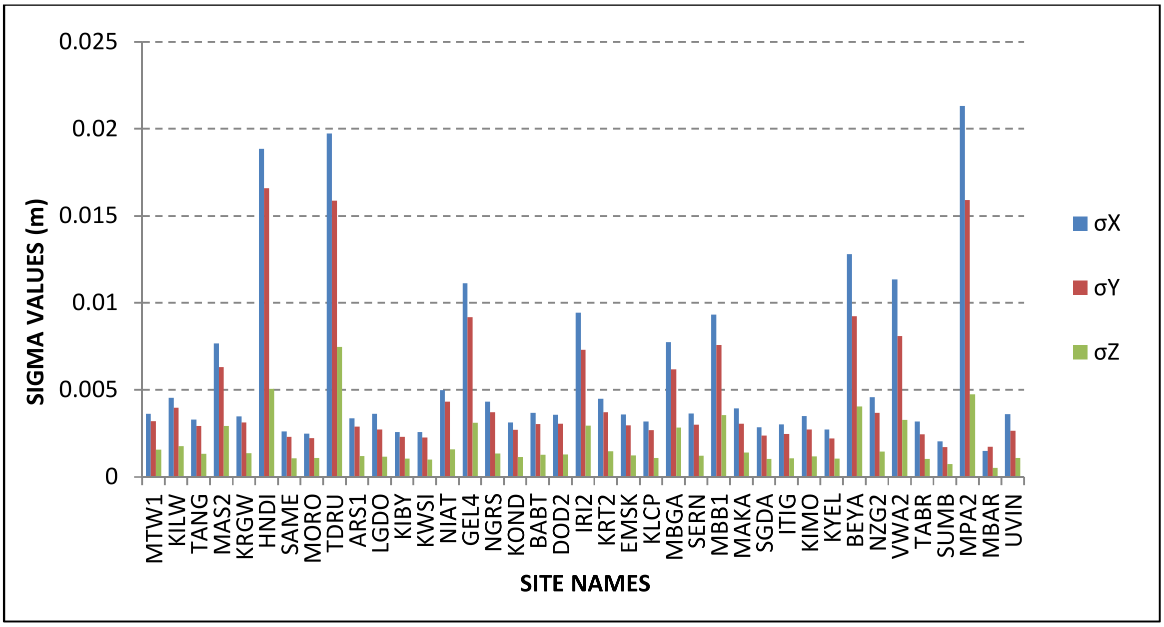

Figure 4.1: Sigma values in Position determination

4.2.2 Velocity Estimates from GAMIT-GLOBK

Velocity of GPS sites is very useful in the study of earth's crustal movement and deformation. They can be used to study and monitoring of deformation (El-Rabbany 2002 , Prasad and Ruggieri 2005) caused by earthquakes, water loading and other natural seismic events, in measurement of Geodynamic phenomena like Earth rotation, polar, motion, and plate tectonics (Seeber 2003). The obtained Site velocities and their respective geographic position and accuracies are presented in table 4.2.

Table 4. 2: Velocity Estimates and their corresponding sigma values in (mm/yr) from GAMIT-GLOBK LONG and LAT are geographical longitude and latitude in decimal degrees

LONG	LAT	Vel_N	Vel_E	$\sigma_{Vel.N}$	$\sigma_{vel.E}$	Corr_NE	STATION
38.76630	9.035140	24.41	19.62	0.47	0.37	-0.001	ADIS
36.71299	-3.409190	23.89	16.59	0.42	0.35	0.139	ARS1
35.75444	-4.178540	24.21	16.57	0.46	0.4	0.015	BABT
33.45678	-8.914170	21.73	17.78	0.59	0.46	0.043	BEYA
72.37024	-7.269680	47.4	33.05	0.19	0.13	0.144	DGAR
35.74836	-6.169770	24.05	16.91	0.6	0.49	0.04	DOD2
35.27686	-4.163540	24.71	16.83	0.45	0.39	0.014	EMSK
-15.63430	27.764780	16.69	18.35	0.21	0.14	-0.345	GMAS

27.70725	-25.886960	17.54	18.91	0.09	0.08	0.079	HARB
38.03549	-5.442550	25.99	17.92	1.46	1.16	0.074	HNDI
27.68698	-25.890100	21.68	16.9	0.09	0.08	0.093	HRAO
35.69337	-7.770730	24.48	18.2	0.73	0.58	0.044	IRI2
39.52170	-8.925760	21.16	14.82	0.52	0.41	0.02	KILW
33.91240	-6.133530	23.53	16.8	0.38	0.3	0.013	KIMO
35.24158	-1.834820	22.71	18.16	0.38	0.32	0.017	KLCP
38.43495	-5.155050	23.02	16.7	0.39	0.33	0.022	KRGW
35.67134	-3.374310	25.62	18.37	0.66	0.58	0.022	KRT2
33.76524	-9.582510	21.28	15.64	0.39	0.32	0.039	KYEL
36.68333	-2.692570	26.15	16.44	0.44	0.35	0.034	LGDO
34.73761	-8.839940	121.56	27.05	0.45	0.36	0.002	MAKA
40.19414	-2.996050	27.25	15.91	0.26	0.22	0.071	MAL2
-15.63330	27.763740	16.69	18.35	0.21	0.14	-0.345	MAS1
38.79666	-10.737200	22.17	15.82	0.65	0.49	0.05	MAS2
30.73788	-0.601470	23.24	16.83	0.14	0.12	-0.044	MBAR
34.80030	-11.273710	14.55	20.94	0.99	0.74	0.005	MBB1
34.93113	-11.094790	21.27	17.51	0.67	0.52	0.05	MBGA
37.67013	-6.743270	22.55	17.31	0.72	0.59	0.048	MORO
31.04061	-6.348970	22.22	19.65	1.64	1.16	0.133	MPA2
13.55200	-1.631600	-51.15	90.84	20.15	16.07	-0.078	MSKU
40.06259	-10.277500	23.53	16.01	1	0.8	0.036	MTW1
36.08855	-3.616670	23.21	17.55	0.77	0.66	0.048	NIAT
9.67213	0.353910	23.19	19.33	0.2	0.18	-0.082	NKLG
33.18310	-4.256790	24.24	16.68	0.74	0.6	0.007	NZEG
33.18310	-4.256790	24.24	16.68	0.74	0.6	0.007	NZG2
28.22404	-25.746340	18.1	18.69	0.07	0.06	0.096	PRE1
32.07839	-28.795550	15.93	17.75	0.11	0.1	0.036	RBAY
36.89348	-1.220830	25.58	16.86	0.27	0.23	0.03	RCMN
55.57172	-21.208230	16.63	12.58	0.14	0.11	0.016	REUN
37.76640	-4.092450	34.61	30.21	0.3	0.25	-0.005	SAME
34.89633	-2.408550	22.72	17.93	0.39	0.33	0.024	SERN
55.47941	-4.673720	23.91	10.98	0.21	0.18	0.076	SEY1
34.72449	-4.813460	33.04	25.06	0.32	0.26	0.027	SGDA
20.81046	-32.380210	17.02	18.88	0.07	0.07	0.278	SUTH
20.81091	-32.381430	17.02	18.88	0.07	0.07	0.278	SUTM
32.81197	-5.043820	23.35	19.49	0.39	0.32	0.025	TABR
39.01790	-5.110440	20.39	14.74	0.41	0.34	0.022	TANG

37.47058	-10.854350	22.87	16.2	1.56	1.29	-0.042	TDRU
32.89410	-9.145980	22.56	17.8	0.97	0.72	0.084	VWA2

Generic Mapping Tools (GMT) map making software (Wessel and Smith 2013) was used to map the velocities of points in the research area. The neighbouring reference IGS sites (Figure 4.2) are also shown.

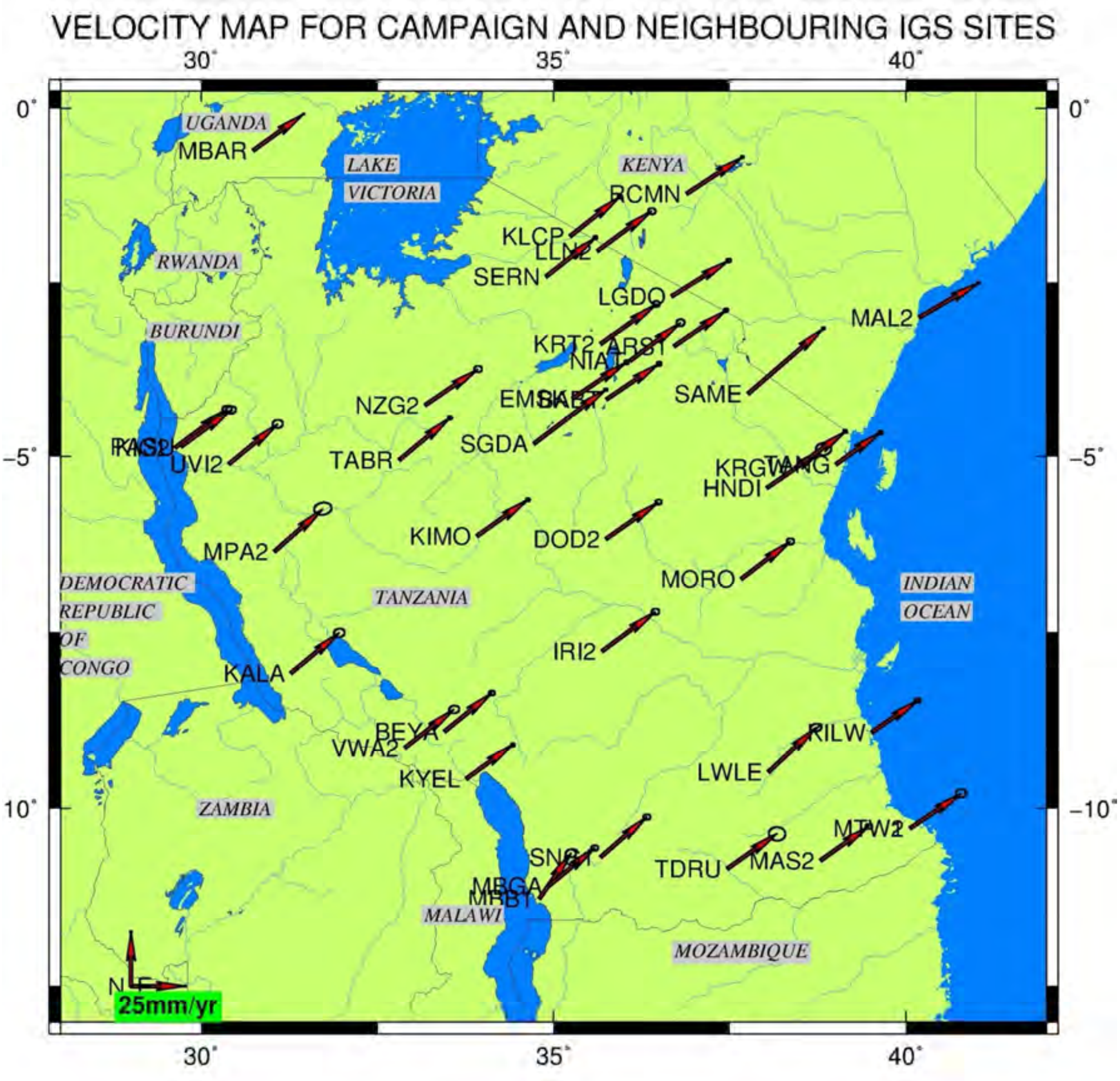

Figure 4. 2: Velocity map of Campaign GPS sites including neighbouring IGS sites used

4.2.3 Precise Point position estimates from APPS

The output from APPS, the online service of GIPSY/OASIS software for PPP solution are the ITRF realized X Y Z coordinates and geographical coordinates Longitude Latitude and height above the ellipsoid (h) with their respective sigmas.

All stations for which position was computed in GAMIT/GLOBK were also computed by means of Precise Point Positioning method.

The emphasis of PPP positioning here is not to show the values of station coordinates but rather the deviations from the deemed known position from GAMIT/GLOBK solution.

The results of comparison are given for episodic observation based on the year of observations that is 2006, 2008 and 2010. Lastly the results are combined for all the episodes.

4.2.4 Results from 2006 campaign data set

From the 2006 data set, the residuals between the GAMIT/GLOBK derived GPS sites position coordinates and equivalent GPS sites position coordinates calculated using PPP method have mismatches of -4cm to +4cm in X component, -4 to +5cm in Y component and -0.8 to +3.4cm in Z component. The residuals (δX, δY and δZ) have a mean value of 2mm with standard deviations 11mm in X and Y components and 5mm in the Z component (table 4.3).

A graphic representation of the 2006 data analysis is show on figure 4.3.

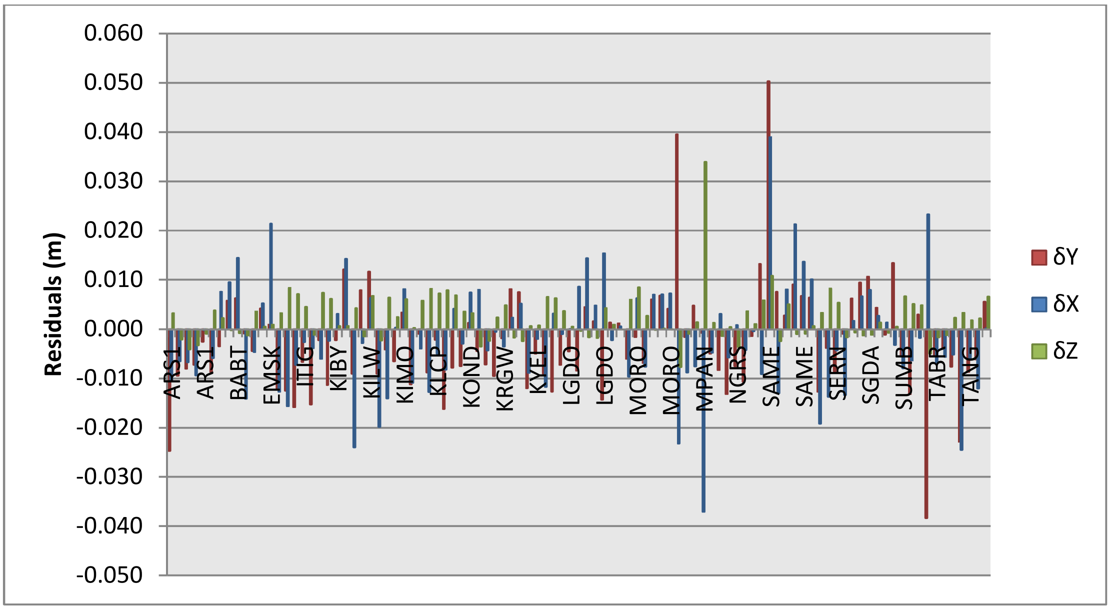

Figure 4. 3: Graph showing difference between GAMIT/GLOBK DGPS and APPS PPP solution for 2006 data set

Table 4. 3: mean and standard deviations of the differences between GAMIIT/GLOBK DGPS and APPS PPP solution for 2006 data

GAMIT/GLOBK - APPS	δX	δY	δZ
Mean (m)	-0.002	-0.002	0.002
STDV (m)	0.011	0.011	0.005

4.2.5 Results from 2008 campaign data set

The comparison between the GPS sites position coordinated derived from GAMIT/GLOBK and APPS from the 2008 campaign data set has difference of -1.3 to 2.6cm in X component, -3.3 to 2.6cm in Y component and -0.7cm to 1 cm in Z component. The residuals (δX, δY and δZ) between the two solutions have a mean of 8mm in X components -1mm in Y component and 1mm in Z component. The standard deviations are 9mm in X and Y components and 4mm in the Z component as shown on table 4.4 and graphically represented on figure 4.4.

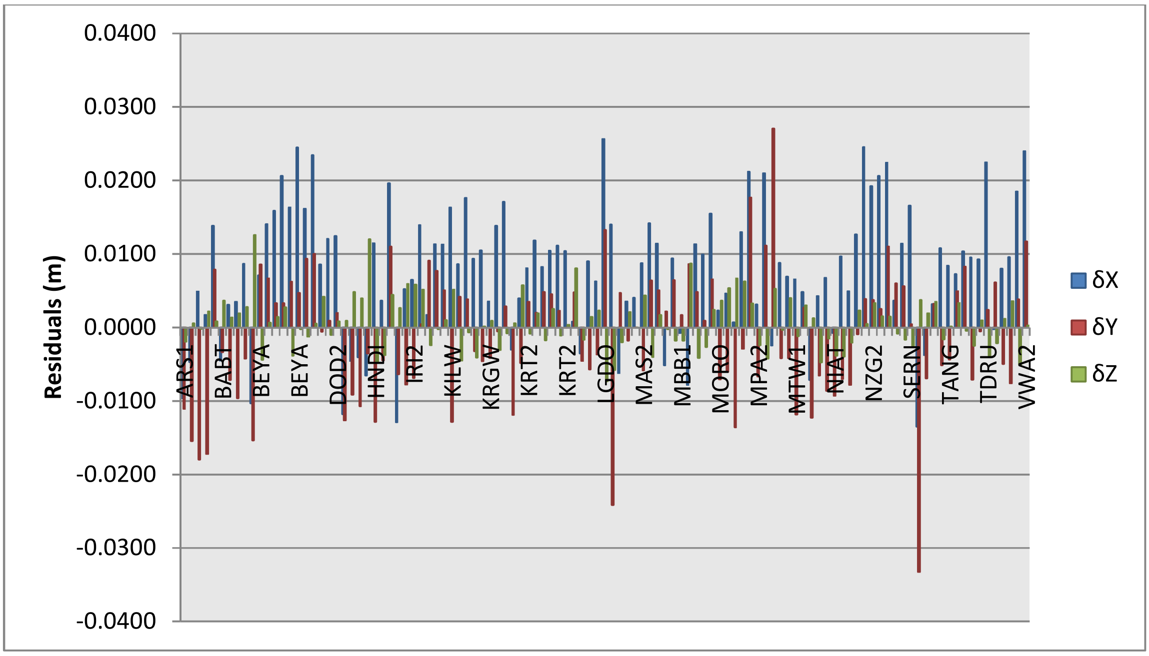

Figure 4. 4: Graph showing difference between GAMIT/GLOBK DGPS and APPS PPP solution for 2008 data

Table 4. 4: Mean and Standard deviations of the differences between GAMIIT/GLOBK DGPS and APPS PPP solution for 2008 data

GAMIT/GLOBK - APPS	δX	δY	δZ
Mean (m)	0.008	-0.001	0.001
STDV (m)	0.009	0.009	0.004

4.2.5 Results from 2010 campaign data set

From 2010 solution, the results show that the range of the differences in δX, δY and δZ obtained by subtracting the APPS PPP solution from the GAMIT/GLOBK DGPS solutions are -2 to 5.6cm in X component, -3 to 3.1cm in Y component and -0.3cm to 0.8cm in Z component. The residuals (δX, δY and δZ) have mean values of 10mm, 6mm and -1.4mm in X, Y and Z components respectively. Also, the residuals (δX, δY and δZ) have standard deviations of 10mm and 8mm and 3mm in X, Y and Z components respectively. A pictorial representation of the difference between the GAMIT/GLOBK and APPS PPP derived position estimates from the 2010 campaign data set is given in figure 4.5 and a summary result is tabulated in table 4.5.

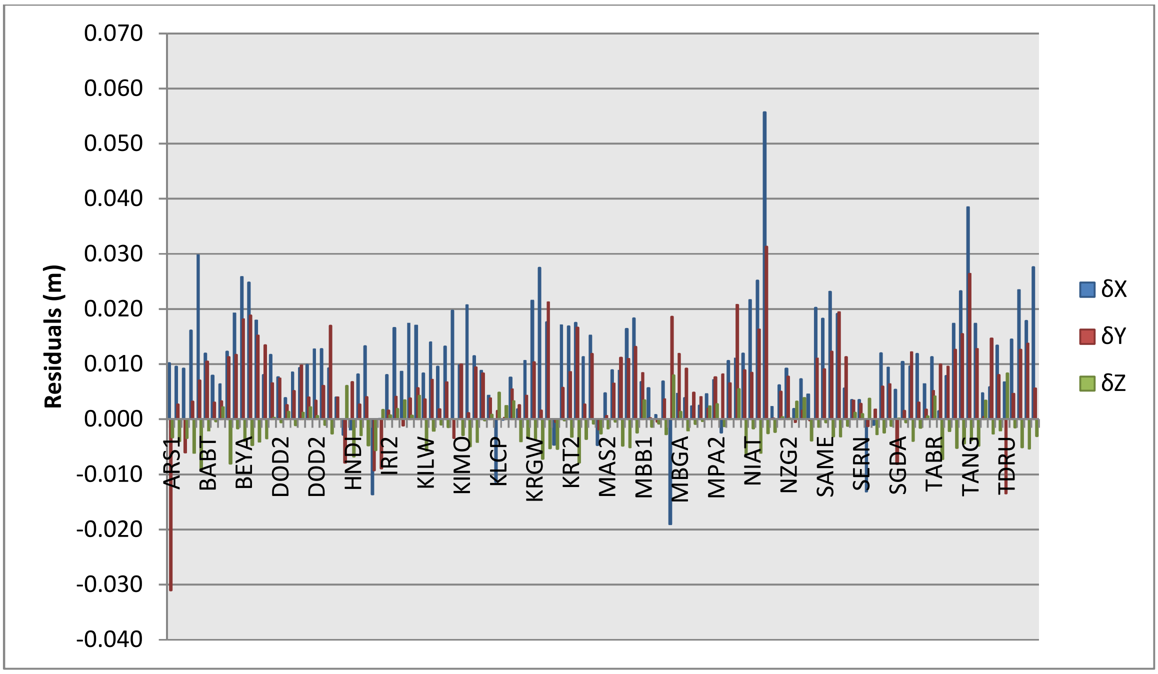

Figure 4. 5: Graph showing difference between GAMIT/GLOBK DGPS and APPS PPP solution for 2010 data

Table 4. 5: Mean and Standard deviations of the differences between GAMIIT/GLOBK DGPS and APPS PPP solution for 2010 data

GAMIT/GLOBK - APPS	δX	δY	δZ
Mean (m)	0.010488	0.006221	-0.00142
STDV (m)	0.009771	0.007743	0.003334

4.2.6 Overall Comparison between results obtained using GAMIT/GLOBK DGPS and PPP solutions for all episodes

From 330, 24hours epochs of observations (Table 4.7), the results show that the range of the difference between GAMIT/GLOBK and APPS PPP solution is -3.7 to 5.6cm in X component, -3.8 to 5.0cm in Y component and -1cm to 3.4cm in the Z component. As represented in table 4.6, the difference between GAMIT/GLOBK DGPS and APPS PPP coordinates (δX, δY and δZ) have mean value of 5.9mm in X component, 1.2mm in Y component and 0.4mm in Z component. Also the standard deviations in δX, δY and δZ are 11mm, 10mm and 4mm respectively. Figure 4.6(a, b and c) shows a pictorial representation of the residuals δX, δY and δZ obtained by subtracting the APPS PPP coordinates from DGPS GAMIT/GLOBK coordinates. Table 4.7 gives a list of computed differences for each station at every 24hours epoch of observation. The year for each observation is shown in the first column but the days of the year are not shown, however most observations were made between 220 to 242 days of the year for all three episodes. Figure 4.7 is a residual plot showing the overall scatter of coordinate differences. It shows that most of the residuals lie between -2 to 2cm.

Table 4. 6: Mean and Standard deviations of the differences between GAMIT/GLOBK DGPS and APPS PPP solution for the three episodic campaign GPS observations (2006, 2008 and 2010)

GAMIT/GLOBK - APPS	δX	δY	δZ
Mean	0.0059	0.0012	0.0004
STDV	0.0111	0.0099	0.0042
MINIMUM VALUE	-0.037	-0.038	-0.009
MAXIMUM VALUE	0.056	0.050	0.034

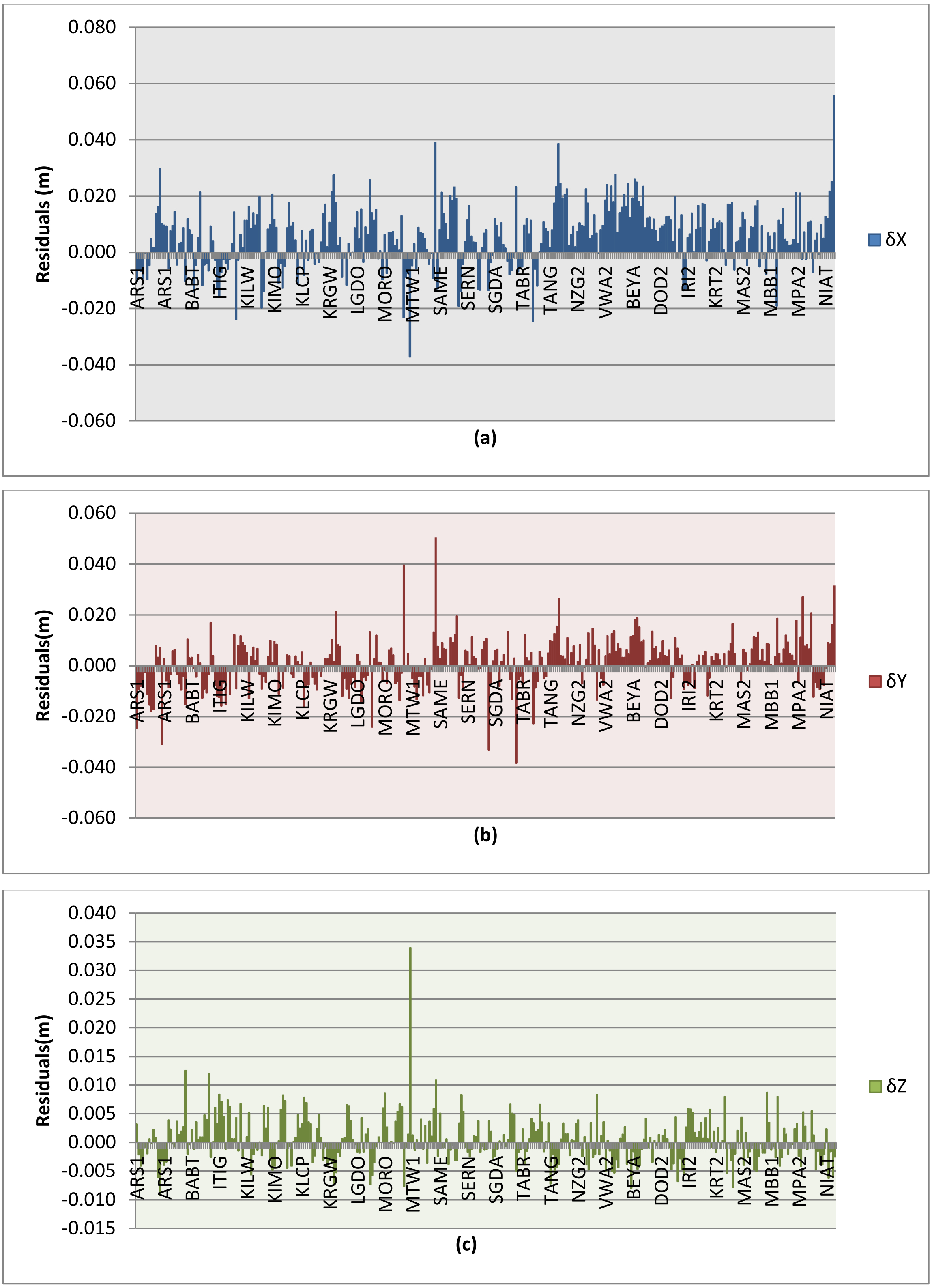

Figure 4. 6: Overall Comparison results between GAMIT/GLOBK DGPS and PPP solutions for all episodes the residuals δX, δY and δZ are shown in (a), (b) and (c) respectively.

Table 4. 7: Computed differences between DGPS GAMIT/GLOBK and PPP APPS solution (Units in m)

YEAR	STATION	δX	δY	δZ
2006	ARS1	-0.010	-0.025	0.003
2006	ARS1	-0.007	-0.009	-0.002
2006	ARS1	-0.007	-0.008	-0.004
2006	ARS1	-0.009	-0.007	-0.003
2006	ARS1	0.000	-0.003	-0.001
2008	ARS1	-0.0096	-0.0111	-0.0019
2008	ARS1	-0.0047	-0.0154	0.0006
2008	ARS1	0.0049	-0.0180	-0.0002
2008	ARS1	0.0017	-0.0172	0.0022
2008	ARS1	0.0138	0.0078	0.0008
2010	ARS1	0.016	0.003	-0.006
2010	ARS1	0.030	0.007	-0.009
2010	ARS1	0.010	-0.031	-0.003
2010	ARS1	0.010	0.003	-0.004
2010	ARS1	0.009	-0.006	-0.003
2006	BABT	-0.006	-0.009	0.004
2006	BABT	0.008	-0.003	0.002
2006	BABT	0.010	0.006	0.000
2006	BABT	0.014	0.006	-0.001
2008	BABT	-0.0045	-0.0034	0.0037
2008	BABT	0.0031	-0.0071	0.0013
2008	BABT	0.0035	-0.0096	0.0019
2008	BABT	0.0087	-0.0042	0.0028
2008	BABT	-0.0103	-0.0154	0.0125
2010	BABT	0.012	0.010	-0.002
2010	BABT	0.008	0.003	0.000
2010	BABT	0.006	0.003	0.002
2006	EMSK	-0.014	-0.001	-0.001
2006	EMSK	-0.005	-0.004	0.004
2006	EMSK	0.005	0.004	0.000
2006	EMSK	0.021	0.001	0.001
2008	EMSK	-0.0118	-0.0127	0.0009
2008	EMSK	-0.0045	-0.0091	0.0048
2008	EMSK	-0.0040	-0.0107	0.0039
2008	EMSK	-0.0066	-0.0035	0.0120
2010	EMSK	0.009	0.017	-0.003
2006	KILW	-0.003	0.008	-0.001
2006	KILW	0.006	0.012	0.007
2008	KILW	0.0017	0.0091	-0.0024
2008	KILW	0.0113	0.0077	-0.0003
2008	KILW	0.0113	0.0051	0.0010
2008	KILW	0.0163	-0.0128	0.0052
2010	KILW	0.008	0.004	-0.006
2010	KILW	0.014	0.007	-0.002
2010	KILW	0.010	0.002	-0.001
2010	KILW	0.013	0.007	-0.001
2010	KILW	0.020	-0.003	0.000
2006	KIMO	-0.020	-0.009	-0.002
2006	KIMO	-0.014	-0.004	0.006
2006	KIMO	0.000	-0.007	0.002
2006	KIMO	0.008	0.003	0.006
2010	KIMO	0.010	0.010	-0.003
2010	KIMO	0.021	0.001	-0.005
2010	KIMO	0.012	0.009	-0.004
2010	KIMO	0.009	0.008	0.000
2006	KLCP	-0.011	-0.011	0.000
2006	KLCP	-0.004	-0.001	0.006
2006	KLCP	-0.013	-0.009	0.008
2006	KLCP	-0.005	-0.002	0.007
2008	KLCP	0.0086	0.0042	-0.0045
2008	KLCP	0.0176	0.0038	-0.0007
2008	KLCP	0.0093	-0.0032	-0.0041
2008	KLCP	0.0105	-0.0046	0.0001
2010	KLCP	0.004	0.004	0.001
2010	KLCP	-0.011	0.002	0.005
2010	KLCP	0.000	0.000	0.002
2010	KLCP	0.008	0.005	0.003
2006	KOND	-0.008	-0.016	0.008
2006	KOND	0.004	-0.008	0.007
2006	KOND	-0.003	-0.007	0.004
2006	KOND	0.007	0.001	0.003
2006	KRGW	0.008	-0.004	-0.004

YEAR	STATION	δX	δY	δZ
2010	EMSK	0.004	0.004	0.000
2010	EMSK	-0.003	-0.008	0.006
2006	ITIG	-0.013	-0.012	0.003
2006	ITIG	-0.016	-0.013	0.008
2006	ITIG	-0.007	-0.016	0.007
2006	ITIG	-0.003	-0.007	0.005
2006	KIBY	-0.004	-0.015	-0.001
2006	KIBY	-0.006	-0.002	0.007
2006	KIBY	-0.002	-0.011	0.006
2006	KIBY	0.003	-0.002	0.001
2006	KIBY	0.014	0.012	0.001
2006	KILW	-0.024	-0.009	0.004
2006	KWSI	0.005	0.007	-0.002
2006	KWSI	-0.009	-0.012	0.001
2006	KYEL	-0.002	-0.005	0.001
2006	KYEL	-0.012	-0.009	0.007
2006	KYEL	0.003	-0.013	0.006
2006	KYEL	-0.001	-0.007	0.004
2006	LGDO	0.000	-0.005	0.000
2006	LGDO	0.009	-0.008	0.000
2006	LGDO	0.014	0.004	-0.002
2006	LGDO	0.005	0.002	-0.002
2006	LGDO	0.015	-0.014	0.004
2008	LGDO	-0.004	-0.005	-0.002
2008	LGDO	0.009	-0.006	0.001
2008	LGDO	0.006	-0.004	0.002
2008	LGDO	0.026	0.013	-0.007
2008	LGDO	0.014	-0.024	-0.006
2010	LGDO	0.011	0.003	-0.004
2010	LGDO	0.015	0.012	-0.001
2006	MORO	-0.002	0.001	0.001
2006	MORO	0.001	0.001	0.000
2006	MORO	-0.010	-0.006	0.006
2006	MORO	0.006	-0.002	0.009
2006	MORO	-0.008	-0.007	0.003
2006	MORO	0.007	0.006	0.000

YEAR	STATION	δX	δY	δZ
2006	KRGW	-0.004	-0.007	-0.002
2006	KRGW	-0.001	-0.010	0.002
2006	KRGW	-0.004	-0.002	0.005
2008	KRGW	0.0035	-0.0041	0.0009
2008	KRGW	0.0138	-0.0006	-0.0031
2008	KRGW	0.0171	0.0028	-0.0008
2010	KRGW	0.002	0.003	-0.004
2010	KRGW	0.011	0.004	-0.003
2010	KRGW	0.022	0.010	-0.004
2010	KRGW	0.027	0.002	-0.007
2010	KRGW	0.018	0.021	-0.005
2006	KWSI	0.002	0.008	-0.002
2006	SAME	0.021	0.009	-0.001
2006	SAME	0.014	0.007	-0.001
2006	SAME	0.010	0.006	0.001
2010	SAME	0.005	0.000	-0.004
2010	SAME	0.020	0.011	-0.001
2010	SAME	0.018	0.009	-0.001
2010	SAME	0.023	0.012	-0.003
2010	SAME	0.019	0.019	-0.003
2006	SERN	-0.019	-0.013	0.003
2006	SERN	-0.014	-0.004	0.008
2006	SERN	-0.004	-0.009	0.005
2008	SERN	0.004	0.006	-0.001
2008	SERN	0.011	0.006	-0.002
2008	SERN	0.017	0.000	-0.003
2010	SERN	0.006	0.011	-0.001
2010	SERN	0.004	0.003	0.001
2010	SERN	0.004	0.003	0.001
2010	SERN	-0.013	-0.001	0.004
2006	SGDA	-0.013	-0.001	-0.002
2006	SGDA	0.002	0.006	-0.001
2006	SGDA	0.007	0.009	-0.001
2006	SGDA	0.008	0.011	-0.001
2008	SGDA	-0.013	-0.033	0.004
2008	SGDA	-0.004	-0.007	0.002

YEAR	STATION	δX	δY	δZ
2006	MORO	0.007	0.007	0.000
2006	MORO	0.007	0.004	0.000
2008	MORO	0.002	-0.007	0.004
2008	MORO	0.005	-0.006	0.005
2008	MORO	0.001	-0.014	0.007
2008	MORO	0.013	-0.003	0.006
2006	MPAN	-0.023	0.040	-0.008
2006	MPAN	-0.009	-0.002	-0.001
2006	MPAN	-0.008	0.005	0.001
2006	MPAN	-0.037	-0.001	0.034
2006	MTW1	-0.005	-0.005	0.001
2006	MTW1	0.003	-0.008	-0.001
2006	MTW1	-0.006	-0.013	0.000
2008	MTW1	0.009	-0.004	0.000
2008	MTW1	0.007	-0.004	0.004
2008	MTW1	0.007	-0.012	-0.001
2008	MTW1	0.005	0.003	0.003
2006	NGRS	0.001	-0.008	-0.004
2006	NGRS	-0.004	-0.011	0.004
2006	NGRS	0.000	-0.001	0.001
2006	NGRS	-0.009	0.013	0.006
2006	SAME	0.039	0.050	0.011
2006	SAME	-0.013	0.008	-0.002
2006	SAME	0.008	0.003	0.005
2008	TANG	0.011	-0.0051	-0.002
2008	TANG	0.008	-0.0043	0.000
2008	TANG	0.007	0.0049	0.003
2010	TANG	0.002	0.010	-0.007
2010	TANG	0.008	0.010	-0.002
2010	TANG	0.017	0.013	-0.005
2010	TANG	0.023	0.016	-0.004
2010	TANG	0.039	0.026	-0.004
2008	NZG2	0.025	0.0039	0.001
2008	NZG2	0.019	0.0037	0.003
2008	NZG2	0.021	0.0025	0.002
2008	NZG2	0.022	0.0110	0.002

YEAR	STATION	δX	δY	δZ
2010	SGDA	-0.001	0.002	-0.003
2010	SGDA	0.012	0.006	-0.002
2010	SGDA	0.009	0.006	-0.001
2010	SGDA	0.005	-0.008	0.000
2010	SGDA	0.010	0.002	-0.001
2006	SUMB	0.003	0.004	0.001
2006	SUMB	0.001	-0.001	-0.001
2006	SUMB	-0.003	0.013	0.000
2006	SUMB	-0.008	-0.005	0.007
2006	SUMB	-0.006	-0.013	0.005
2006	SUMB	-0.002	0.003	0.005
2006	TABR	0.023	-0.038	-0.005
2006	TABR	-0.007	-0.005	-0.002
2006	TABR	-0.006	-0.004	-0.001
2006	TABR	-0.005	-0.008	0.002
2010	TABR	0.010	0.012	-0.004
2010	TABR	0.012	0.003	-0.001
2010	TABR	0.006	0.002	0.001
2010	TABR	0.011	0.005	0.004
2006	TANG	-0.025	-0.023	0.003
2006	TANG	-0.006	-0.009	0.002
2006	TANG	-0.012	-0.006	0.002
2006	TANG	0.000	0.006	0.007
2008	TANG	0.003	0.003	0.004
2008	DOD2	0.016	0.009	-0.001
2008	DOD2	0.024	0.010	0.001
2008	DOD2	0.009	-0.001	0.004
2008	DOD2	0.012	0.001	-0.001
2008	DOD2	0.012	0.002	0.001
2010	DOD2	0.008	0.013	-0.003
2010	DOD2	0.012	0.007	0.000
2010	DOD2	0.008	0.007	-0.001
2010	DOD2	0.004	0.003	0.001
2010	DOD2	0.008	0.005	-0.001
2010	DOD2	0.009	0.010	0.001
2010	DOD2	0.010	0.004	0.002

YEAR	STATION	δX	δY	δZ
2010	NZG2	0.002	0.000	-0.002
2010	NZG2	0.006	0.005	0.000
2010	NZG2	0.009	0.008	0.000
2010	NZG2	0.002	0.000	0.003
2010	NZG2	0.007	0.002	0.004
2008	TDRU	0.0104	0.0083	-0.000
2008	TDRU	0.0095	-0.007	-0.003
2008	TDRU	0.0093	-0.001	0.001
2008	TDRU	0.0225	0.0024	-0.004
2010	TDRU	0.017	0.013	-0.005
2010	TDRU	0.005	0.000	0.003
2010	TDRU	0.006	0.015	-0.003
2010	TDRU	0.013	0.008	-0.002
2010	TDRU	0.007	-0.013	0.008
2008	VWA2	-0.0002	0.0061	-0.002
2008	VWA2	0.0080	-0.005	0.001
2008	VWA2	0.0095	-0.008	0.004
2008	VWA2	0.0185	0.0038	-0.005
2008	VWA2	0.0240	0.0117	0.0003
2010	VWA2	0.014	0.005	-0.001
2010	VWA2	0.023	0.013	-0.005
2010	VWA2	0.018	0.014	-0.005
2010	VWA2	0.028	0.006	-0.003
2008	BEYA	0.0071	0.0086	-0.004
2008	BEYA	0.0140	0.0067	0.001
2008	BEYA	0.0159	0.0033	0.0014
2008	BEYA	0.0206	0.0033	0.003
2008	BEYA	0.0163	0.0062	-0.004
2008	BEYA	0.0245	0.0047	-0.000

YEAR	STATION	δX	δY	δZ
2010	DOD2	0.013	0.003	0.001
2010	DOD2	0.013	0.006	-0.001
2008	HNDI	0.0114	-0.0128	-0.0047
2008	HNDI	0.0037	-0.0045	-0.0037
2008	HNDI	0.0196	0.0110	0.0044
2010	HNDI	-0.002	0.007	-0.007
2010	HNDI	0.008	0.003	-0.003
2010	HNDI	0.013	0.004	-0.005
2010	HNDI	-0.014	-0.009	-0.006
2008	IRI2	-0.013	-0.0064	0.0027
2008	IRI2	0.0052	-0.0078	0.0059
2008	IRI2	0.0065	-0.0069	0.0058
2008	IRI2	0.0139	0.0005	0.0051
2010	IRI2	0.000	-0.009	0.002
2010	IRI2	0.008	0.002	0.001
2010	IRI2	0.017	0.004	0.002
2010	IRI2	0.009	-0.001	0.003
2010	IRI2	0.017	0.004	0.001
2010	IRI2	0.017	0.006	0.004
2008	KRT2	-0.003	-0.0119	0.0006
2008	KRT2	0.0039	-0.0049	0.0057
2008	KRT2	0.0081	0.0035	-0.0008
2008	KRT2	0.0118	0.0020	0.0019
2008	KRT2	0.0082	0.0048	-0.0018
2008	KRT2	0.0104	0.0045	0.0025
2008	KRT2	0.0111	0.0023	-0.0011
2008	KRT2	0.0104	-0.0001	0.0003
2008	KRT2	0.0008	0.0048	0.0080
2010	KRT2	-0.005	0.000	-0.005

YEAR	STATION	δX	δY	δZ
2010	BEYA	0.012	0.011	-0.008
2010	BEYA	0.019	0.012	-0.002
2010	BEYA	0.026	0.018	-0.004
2010	BEYA	0.025	0.019	-0.005
2010	BEYA	0.018	0.015	-0.004
2008	MAS2	0.004	0.000	0.000
2008	MAS2	0.009	-0.006	0.004
2008	MAS2	0.014	0.006	-0.004
2008	MAS2	0.011	0.005	0.002
2010	MAS2	-0.005	-0.002	-0.003
2010	MAS2	0.005	0.001	-0.002
2010	MAS2	0.009	0.006	0.000
2010	MAS2	0.009	0.011	-0.005
2010	MAS2	0.016	0.011	-0.005
2010	MAS2	0.018	0.013	-0.002
2008	MBB1	-0.005	0.002	0.000
2008	MBB1	0.009	0.006	-0.002
2008	MBB1	-0.001	0.002	-0.002
2008	MBB1	-0.008	0.009	0.009
2010	MBB1	0.007	0.008	0.003
2010	MBB1	0.006	0.000	-0.001
2010	MBB1	0.001	0.000	-0.001
2010	MBB1	0.007	0.004	-0.003
2010	MBB1	-0.019	0.019	0.008
2008	MBGA	0.011	0.005	-0.004
2008	MBGA	0.010	0.001	-0.003
2008	MBGA	0.015	0.007	0.002
2010	MBGA	0.005	0.012	0.001

YEAR	STATION	δX	δY	δZ
2010	KRT2	0.017	0.006	0.000
2010	KRT2	0.017	0.009	-0.003
2010	KRT2	0.018	0.017	-0.008
2008	MAS2	-0.006	0.0047	-0.0020
2008	MAS2	0.0035	-0.0018	0.0021
2010.	MBGA	0.004	0.009	-0.002
2010	MBGA	0.002	0.005	-0.001
2010	MBGA	0.002	0.004	0.000
2010	MBGA	0.005	0.002	0.002
2008	MPA2	0.021	0.018	0.003
2008	MPA2	0.003	-0.007	-0.002
2008	MPA2	0.021	0.011	-0.004
2008	MPA2	-0.002	0.027	0.005
2010	MPA2	0.007	0.008	0.003
2010	MPA2	-0.002	0.008	-0.001
2010	MPA2	0.011	0.007	0.000
2010	MPA2	0.011	0.021	0.006
2008	NIAT	-0.007	-0.012	0.001
2008	NIAT	0.004	-0.007	-0.005
2008	NIAT	0.007	-0.009	-0.002
2008	NIAT	-0.001	-0.009	-0.004
2008	NIAT	0.010	-0.007	-0.004
2008	NIAT	0.005	-0.008	-0.002
2008	NIAT	0.013	-0.001	0.002
2010	NIAT	0.012	0.009	-0.006
2010	NIAT	0.022	0.008	-0.002
2010	NIAT	0.025	0.016	-0.006
2010	NIAT	0.056	0.031	-0.003

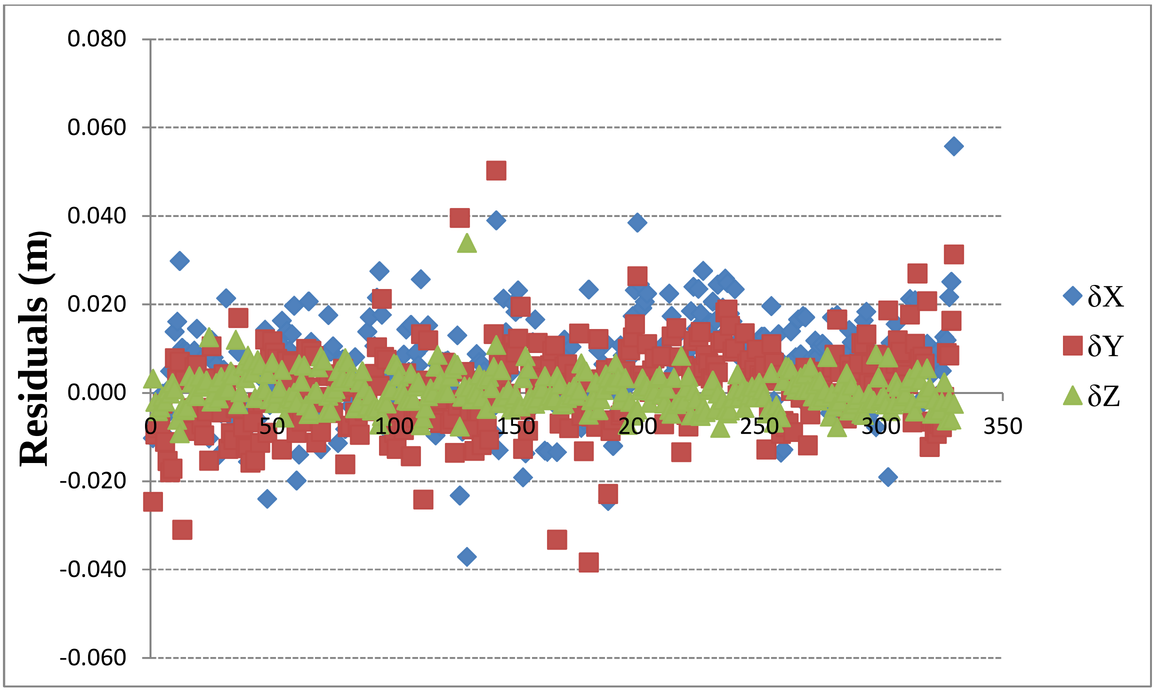

Figure 4. 7: Residual plots showing the overall scatter of coordinate differences between GAMIT/GLOBK DGPS and APPS PPP solutions

CHAPTER FIVE

5. CONCLUSION AND RECOMMENDATIONS

5.1 Conclusions

In this research it has been shown that for all stations the PPP solution is very close to DGPS solution. Using the known fact that DGPS is accurate method of position determination, it is concluded that in in most cases as far as this thesis is concerned PPP solution is also accurate. The residual values with reference to a differential solution are within -2 to 2cm and the overall range is from -4 to 5.6cm. This justifies that PPP post processing can be a viable alternative to long time DGPS observation. But as discussed in section 3.7, sometimes low quality data \may contaminate online PPP solution. For this particular research, the results of GPS site KWSI on 229th day of 2006 was outlier due to bad quality of the data on that particular day. MagicGNSS and APPS results gave inconsistent results when solving position for KWSI on 229th day of 2006.

This indicates that PPP solution should be used with care because such blunders which did not occur in DGPS network analysis may yield misleading results. This is due the facts that, PPP is faced by relatively weak resolution of phase ambiguities, and in addition it is still affected by undifferenced clock biases. Nevertheless, inexistence of correlations between stations may also be useful in that if one station misbehaves for example, its errors are not disseminated into other stations but only affects the results of that particular station and unless averaging is done, the effect is for the specific date of observation. The APPS solution for KWSI on day 229 could not contaminate the daily solution (226, 227 and 228) of the same site. PPP daily solution can also be one of the means to assess quality of observations for a single site made at different times.

It has further been shown in section 3.7 that for online services, more than one Options of online PPP may be helpful in identifying blunders due to bad data. In this research it has been verified that, for quality data the results are consistent in all the used online software packages.

In general, with these results, it has been shown that if care is taken to use good quality observations, PPP solution can be used in geodetic measurement. It can be used for geodetic control establishment, and thus a viable method. Its main advantage is cost effectiveness. It is thus, very useful especially where resources in terms of funds and personnel are scarce.

5.2 Recommendations

(a) PPP is relatively new technique as compared to DGPS. Therefore, not many software package developments for geodetic measurements include its possibility. In Bernese software the option is available, but Bernese has limitation in that it is commercial software. Therefore, this option is still a challenge to regular users of GPS positioning. It is recommended that PPP software packages should also be made publicly available. If this is done then more research can be done to diagnose all possible sources of errors, and discover techniques for their mitigation.

(b) The online option is available, but when processing data, the user has no full control over the software. Everything is done at his own risk in a black box. The only way for PPP online users to do independent checks is to use all the available online solutions. This means that to check the accuracy of the results, the GPS data must be submitted to more than one online processing centres.

(c) In this investigation only static observations were used. There also exists an online solution provided if the receiver were roving. Accuracy of the results in this kinematic mode can also be tested using the GAMIT/GLOBK RTK option or any other software capable of producing very accurate DGPS results. In this investigation, the PPP solution, have been remarkably very encouraging. On the other hand, this is probably due to long hours of observation. In this research only static observations of at least 24 hours of observations were used. Every RINEX file submitted was 24 hours of observation. Since PPP suffers long convergence time, an investigation must be made of short time observations.

(d) Even though one observation out of 331 observations used yielded inconsistent results, it cannot be neglected or deemed insignificant in the assessment. More research should therefore be done to investigate all possible biases in PPP solution. In more practical term, PPP should currently be used with extra care, to avoid such rare cases that may contaminate the results. For instance, if such blunder is introduced in one station, it may contaminate the network when used as reference station for DGPS. For control extension based on control GPS station established by PPP techniques, an independent check using a different station is therefore very important.

APPENDICES

I: GPS data preparation for processing

To convert the UNIX compressed Hatanaka format to RINEX files, two steps were followed, the first step was to use UNIX “uncompress” to change the files into binary Hatanaka format. The second step was to change the Hatanaka format to RINEX using crx2rnx command.

The “uncompress” and “crx2rnx” commands can be applied to files one by one or to all files.

To a single file: Uncompress (SITEDOYN.YYd.Z) and crx2rnx (SITEDOYN.YYd) respectively. The result is the RINEX format with o extension (SITEDOYN.YYo)

To convert all files at once, “UNCOMPRESS *.Z” was used to remove the UNIX compression .Z extension and thereafter the UNIX regular expression “ls | awk '{print "crx2rnx",$1}' | sh” was used to convert the hatanaka format to RINEX format, and then rm *d was used to remove all the hatanaka files.

II: TEQC results for data quality check of kwsi228.06o

version: teqc 2013Mar15

```
 SV+---------|--------|--------|--------|--------|--------|--------|--------+ SV
  6|ooo                                  Looooooooooooooooooooooooooo|  6
 22|oooo                                            Looooooooooooooo| 22
 21|o,oooo                               Looooooooooooooooooooooo| 21
 14|oooooooo                                             mooooooooooo| 14
  7|oooooooooo                                              1oooooooo|  7
 15|oooooooooo                                  Looooooooooooooooooo| 15
  1|oooooooooooo                                              Looooo|  1
 25|ooooooooooooooo                                         Looooooooooo| 25
  3|oooooooooooooooo                                              1oo|  3
 16|oooooooooooooooooooo                                          Loooooo| 16
 19| Looooooooooooooooooooo                                             | 19
 23|    Loooooooooooooooooooooooooooooo                                   | 23
 11|       Looooooooooooooooooo                                          | 11
 13|        Looooooooooooooooooooooooooooooo                                 | 13
 20|           1oooooooooooooooooooo                                      | 20
 27|             Loooooooooooooooooooooooooooo                           | 27
  8|               Loooooooooooooooomooomooomoooo                          |  8
 24|                 Loooooooooooooooooooooooooooo                       | 24
 28|                    LoooooooooooooLooooo                              | 28
  4|                    Loooooooooooooooooooooooooooo                     |  4
 17|                       LoooooooooooooooooLoo                          | 17
  2|                          Loooooooooooooooooooooooooo                |  2
 10|                             LoooIoooooooooooooooooooooooo            | 10
 29|                                  Loooooooooooooooooooo               | 29
 26|                                    Lmoooooooooooooooooooo             | 26
  5|                                     Loooooooooooooooooooooooooooo     |  5
  9|                                        moooooooooooooooooooo         |  9
 30|                                                 Looooooooooooooooooo | 30
 18|                                                  Looooooooooooooooooo | 18
Obs|abbaaa9aaaa999999999999aaaaaabbaaa9abbcaaaaaaa888889bba99988a99abbbbbcca|Obs
Clk|                                                                       |Clk
   +---------|--------|--------|--------|--------|--------|--------|--------+
00:00:00.000                                                    23:59:30.000
2006 Aug 16                                                      2006 Aug 16
```

****

QC of RINEX file(s) : kwsi2280.06o

****

4-character ID   : KWSI
Receiver type   : ASHTECH UZ-12 (# = ZR520015105) (fw = CJ100A16 ---X)
Antenna type   : ASH701945C_M   NONE (# = CR620015103)

Time of start of window : 2006 Aug 16 00:00:00.000
Time of end of window : 2006 Aug 16 23:59:30.000
Time line window length : 23.99 hour(s), ticked every 3.0 hour(s)
Observation interval   : 30.0000 seconds

Total satellites w/ obs : 29
NAVSTAR GPS SVs w/o OBS : 12 31 32
Rx tracking capability : 12 SVs
Poss. # of obs epochs   :   2880
Epochs w/ observations :   2880
Epochs repeated   :   0 (0.00%)
Complete observations   : 27226
 Deleted observations   :   1
Obs w/ SV duplication   :   0 (within non-repeated epochs)
Moving average MP1   : 0.547671 m
Moving average MP2   : 0.568547 m
Points in MP moving avg : 50
Mean S1 S2   : 7.42 (sd=0.72 n=27226) 6.66 (sd=0.75 n=27227)
No. of Rx clock offsets : 0
Total Rx clock drift   : 0.000000 ms
Rate of Rx clock drift : 0.000 ms/hr
Avg time between resets : Inf minute(s)
Freq no. and timecode   : 2 9719 ffffff
Report gap > than   : 10.00 minute(s)
      but < than   : 90.00 minute(s)
epochs w/ msec clk slip : 0
other msec mp events   : 6 (: 17)   {expect ~= 1:50}
IOD signifying a slip   : >400.0 cm/minute
IOD slips   :   1
IOD or MP slips   :   7
     first epoch   last epoch   hrs   dt #expt #have   %   mp1   mp2 o/slps
SUM 06 8 16 00:00 06 8 16 23:59 24.00 30   n/a 27226 n/a 0.55 0.57   3889

III: TEQC results for quality check of KWSI2290.06o

version: teqc 2013Mar15

```
 SV+---------|--------|--------|--------|--------|--------|--------|--------+ SV
  6|ooo                                    Loooooooooooooooooooooooooooo|  6
 22|oooo                                           Loooooooooooooo| 22
 21|ooooo                                      LooooLooooooooooooooomm| 21
 14|oooooooo                                           Loomoooooooooo| 14
  7|oooooooooo                                            Looooooooo|  7
 15|oooooooooo                                    Looooooooooooooooooo| 15
  1|ooooooooooooo                                           Looooo|  1
 25|oooooooooooooooo                                      Looooooooooo| 25
  3|ooooooooooooooooo                                         Looo|  3
 16|ooooooooooooooooooooo                                   Looooooooo| 16
 19|Looooooooooooooooooooo                                        | 19
 23|   Loooooooooooooooooooooooooo                                 | 23
 11|       Looooooooooooooooooo                                   | 11
 13|        Loooooooooooooooooooo--------Lo                       | 13
 20|           Looooooooooooooooooo                              | 20
 27|            Looooooooooooooooo--------Loooo                   | 27
  8|               Looooooooooooo--------Loooooooo                |  8
 24|                Looooooooooo--------Loooooooo                 | 24
 28|                  Looooooooo--------1o                      | 28
  4|                   Lomooooo--------Looooooooooo               |  4
 17|                      Lomooo--------Loooooo                  | 17
  2|                         Lo--------Loomoooooooooooooo          |  2
 10|                            L-------Looooooooooooooooooooo      | 10
  5|                           --------LmImoooooooooooooooooooooooooo    |  5
 29|                            --------Loooooooooooooooom         | 29
 26|                            --------Looooooooooooooooooo        | 26
  9|                                     LoooooooooooooooooL      |  9
 30|                                               Looooooooooooooooom | 30
 18|                                                Looooooooooooooooooo | 18
Obs|bbbaa99aaa8999999999999aaaaaab      ccaaaaaaa888889bb998989a99bbabbccba|Obs
Clk|                         ^^^^^^^^^                           |Clk
   +---------|--------|--------|--------|--------|--------|--------|--------+
00:00:00.000                                          23:59:30.000
2006 Aug 17                                            2006 Aug 17
```

****
QC of RINEX file(s) : kwsi2290.06o
****

4-character ID   : KWSI
Receiver type   : ASHTECH UZ-12 (# = ZR520015105) (fw = CJ100A16 ---X)
Antenna type   : ASH701945C_M   NONE (# = CR620015103)

Time of start of window : 2006 Aug 17 00:00:00.000
Time of end of window : 2006 Aug 17 23:59:30.000

Time line window length : 23.99 hour(s), ticked every 3.0 hour(s)
Observation interval : 30.0000 seconds
Total satellites w/ obs : 29
NAVSTAR GPS SVs w/o OBS : 12 31 32
Rx tracking capability : 12 SVs
Poss. # of obs epochs : 2880
Epochs w/ observations : 2560
Epochs repeated : 0 (0.00%)
Complete observations : 23927
Deleted observations : 4
Obs w/ SV duplication : 0 (within non-repeated epochs)
Moving average MP1 : 0.540015 m
Moving average MP2 : 0.566252 m
Points in MP moving avg : 50
Mean S1 S2 : 7.45 (sd=0.75 n=23927) 6.68 (sd=0.78 n=23930)
No. of Rx clock offsets : 0
Total Rx clock drift : 0.000000 ms
Rate of Rx clock drift : 0.000 ms/hr
Avg time between resets : Inf minute(s)
Freq no. and timecode : 2 9720 fff3ff
Report gap > than : 10.00 minute(s)
but < than : 90.00 minute(s)
epochs w/ msec clk slip : 0
other msec mp events : 10 (: 31) {expect ~= 1:50}
IOD signifying a slip : >400.0 cm/minute
IOD slips : 2
IOD or MP slips : 12
first epoch last epoch hrs dt #expt #have % mp1 mp2 o/slps
SUM 06 8 17 00:00 06 8 17 23:59 21.33 30 n/a 23927 n/a 0.54 0.57 1994

IV: APPS results summary kwsi2280.06o

APPS Summary file for site KWSI. Produced from RINEX file kwsi2280.06o on Wed Jul 24 08:56:00 UTC 2013
The reference frame is ITRF 2008 (with semi-major axis = 6378137 m; flattening factor = 1/298.257222101)
Output data rate is 300 seconds. Minimum elevation angle is 7.5 degrees.
Satellite antenna phase center offset and maps taken from IGS Standards igs08_1604.atx.
#
Receiver antenna phase center offset and maps taken from IGS Standards igs08_1604.atx.
Receiver antenna phase center offset relative to the antenna reference is 0 m
The antenna reference point offset from the monument reference, based on the RINEX file header, is 0.0925 m
#
Product used to process kwsi2280.06o: JPL Final
#
Static point positioning mode (a single set of site coordinates are estimated):
#
Total number of Phase measurements: 2685. RMS post-fit Phase residuals: 0.008 m. Number of excluded Phase measurements: 0
Total number of Pseudorange measurements: 2685. RMS post-fit PRange residuals: 0.616 m. Number of excluded PRange measurements: 0
#
Estimated Cartesian coordinates: X = 5138279.6776 m Y = 3761453.9063 m Z = -383792.3140 m
Sigmas of Cartesian coordinates: SigX = 0.0023 m SigY = 0.0020 m SigZ = 0.0007 m
Estimated Geodetic coordinates (WGS84/GRS80): Lat = -3.47220515 deg East_Lon = 36.20582053 deg Height = 1419.6248 m
Sigmas of Geodetic coordinates: SigLat = 0.0006 m SigLon = 0.0015 m SigHeight = 0.0027 m
#
Time variable estimated parameters:

#Secs_from_start	GPS_Time(yyyy:mm:dd:hh:mm:ss.ssss)	HZTrop(m)	WZTrop(m)	Sig(m)	TropGrad_N(m)	Sig(m)	TropGrad_E(m)	Sig(m)	Clock(m)	Sig(m)
0.0000	2006:08:16:00:00:0.0000	1.9485	0.1446	0.002	0.0000	0.0003	-0.0005	0.0002	-11.610	0.020
300.0000	2006:08:16:00:05:0.0000	1.9485	0.1445	0.002	0.0000	0.0003	-0.0005	0.0002	-11.360	0.020
600.0000	2006:08:16:00:10:0.0000	1.9485	0.1446	0.002	0.0000	0.0003	-0.0005	0.0002	-11.325	0.020
900.0000	2006:08:16:00:15:0.0000	1.9485	0.1449	0.002	0.0000	0.0003	-0.0004	0.0002	-11.152	0.020
1200.0000	2006:08:16:00:20:0.0000	1.9485	0.1453	0.002	0.0000	0.0002	-0.0004	0.0002	-11.720	0.020
1500.0000	2006:08:16:00:25:0.0000	1.9485	0.1456	0.002	0.0000	0.0002	-0.0004	0.0002	-12.171	0.020
1800.0000	2006:08:16:00:30:0.0000	1.9485	0.1459	0.002	0.0000	0.0002	-0.0004	0.0002	-12.047	0.020
2100.0000	2006:08:16:00:35:0.0000	1.9485	0.1462	0.001	0.0000	0.0002	-0.0004	0.0002	-12.370	0.020
2400.0000	2006:08:16:00:40:0.0000	1.9485	0.1462	0.001	0.0000	0.0002	-0.0003	0.0002	-12.142	0.020
2700.0000	2006:08:16:00:45:0.0000	1.9485	0.1461	0.001	0.0000	0.0002	-0.0003	0.0002	-12.745	0.020
3000.0000	2006:08:16:00:50:0.0000	1.9485	0.1461	0.001	0.0000	0.0002	-0.0003	0.0002	-12.295	0.020
3300.0000	2006:08:16:00:55:0.0000	1.9485	0.1461	0.001	0.0000	0.0002	-0.0003	0.0002	-13.131	0.020
3600.0000	2006:08:16:01:00:0.0000	1.9485	0.1460	0.001	0.0000	0.0002	-0.0003	0.0002	-13.296	0.020
3900.0000	2006:08:16:01:05:0.0000	1.9485	0.1459	0.001	0.0000	0.0002	-0.0003	0.0002	-13.502	0.020
4200.0000	2006:08:16:01:10:0.0000	1.9485	0.1455	0.001	0.0000	0.0002	-0.0003	0.0002	-13.414	0.020
4500.0000	2006:08:16:01:15:0.0000	1.9485	0.1452	0.001	0.0000	0.0002	-0.0003	0.0002	-13.062	0.020
4800.0000	2006:08:16:01:20:0.0000	1.9485	0.1451	0.001	0.0001	0.0002	-0.0004	0.0002	-12.614	0.020
5100.0000	2006:08:16:01:25:0.0000	1.9485	0.1452	0.001	0.0001	0.0002	-0.0004	0.0002	-13.952	0.020
5400.0000	2006:08:16:01:30:0.0000	1.9485	0.1452	0.001	0.0001	0.0002	-0.0003	0.0002	-13.670	0.020
5700.0000	2006:08:16:01:35:0.0000	1.9485	0.1455	0.001	0.0001	0.0002	-0.0003	0.0002	-13.493	0.020
6000.0000	2006:08:16:01:40:0.0000	1.9485	0.1455	0.001	0.0001	0.0002	-0.0004	0.0002	-13.126	0.020

V: APPS results summary KWSI2290.06O

APPS Summary file for site KWSI. Produced from RINEX file kwsi2290.06o on Wed Jul 24 08:57:38 UTC 2013
The reference frame is ITRF 2008 (with semi-major axis = 6378137 m; flattening factor = 1/298.257222101)
Output data rate is 300 seconds. Minimum elevation angle is 7.5 degrees.
Satellite antenna phase center offset and maps taken from IGS Standards igs08_1604.atx.
#
Receiver antenna phase center offset and maps taken from IGS Standards igs08_1604.atx.
Receiver antenna phase center offset relative to the antenna reference is 0 m
The antenna reference point offset from the monument reference, based on the RINEX file header, is 0.0925 m
#
Product used to process kwsi2290.06o: JPL Final
#
Static point positioning mode (a single set of site coordinates are estimated):
#
Total number of Phase measurements: 1882. RMS post-fit Phase residuals: 0.016 m. Number of excluded Phase measurements: 460
Total number of Pseudorange measurements: 961. RMS post-fit PRange residuals: 16.873 m. Number of excluded PRange measurements: 1381
#
Estimated Cartesian coordinates: X = 5173768.6201 m Y = 3713805.7073 m Z = -372991.3446 m
Sigmas of Cartesian coordinates: SigX = 0.1443 m SigY = 0.1080 m SigZ = 0.0562 m
Estimated Geodetic coordinates (WGS84/GRS80): Lat = -3.37431019 deg East_Lon = 35.67133035 deg Height = 1541.2208 m
Sigmas of Geodetic coordinates: SigLat = 0.0533 m SigLon = 0.0930 m SigHeight = 0.1554 m
#
Time variable estimated parameters:

#Secs_from_start	GPS_Time(yyyy:mm:dd:hh:mm:ss.ssss)	HZTrop(m)	WZTrop(m)	Sig(m)	TropGrad_N(m)	Sig(m)	TropGrad_E(m)	Sig(m)	Clock(m)	Sig(m)
0.0000	2006:08:17:00:00:0.0000	1.9485	-1.9383	0.041	0.3415	0.0040	0.1487	0.0072	-8199.583	0.397
300.0000	2006:08:17:00:05:0.0000	1.9485	-1.9383	0.041	0.3415	0.0040	0.1487	0.0072	-8465.256	0.398
600.0000	2006:08:17:00:10:0.0000	1.9485	-1.9383	0.041	0.3415	0.0040	0.1487	0.0072	-9359.033	0.399
900.0000	2006:08:17:00:15:0.0000	1.9485	-1.9383	0.041	0.3415	0.0040	0.1487	0.0072	-10232.237	0.399
1200.0000	2006:08:17:00:20:0.0000	1.9485	-1.9383	0.041	0.3415	0.0040	0.1487	0.0072	-11086.937	0.400
1500.0000	2006:08:17:00:25:0.0000	1.9485	-1.9383	0.041	0.3415	0.0040	0.1487	0.0072	-11922.362	0.400
1800.0000	2006:08:17:00:30:0.0000	1.9485	-1.9383	0.041	0.3415	0.0039	0.1487	0.0072	-12741.403	0.401
2100.0000	2006:08:17:00:35:0.0000	1.9485	-1.9383	0.041	0.3415	0.0039	0.1487	0.0072	-13544.971	0.401
2400.0000	2006:08:17:00:40:0.0000	1.9485	-1.9383	0.041	0.3415	0.0039	0.1487	0.0072	-14334.824	0.401
2700.0000	2006:08:17:00:45:0.0000	1.9485	-1.9383	0.041	0.3415	0.0039	0.1487	0.0072	-8826.507	351100000
3000.0000	2006:08:17:00:50:0.0000	1.9485	-1.9383	0.041	0.3415	0.0039	0.1487	0.0072	-7756.405	351100000
3300.0000	2006:08:17:00:55:0.0000	1.9485	-1.9383	0.041	0.3415	0.0039	0.1487	0.0072	-2324.871	331300000
3600.0000	2006:08:17:01:00:0.0000	1.9485	-1.9383	0.041	0.3415	0.0039	0.1487	0.0072	-57447.429	1.035
3900.0000	2006:08:17:01:05:0.0000	1.9485	-1.9384	0.041	0.3415	0.0039	0.1487	0.0072	-18131.542	1.017
4200.0000	2006:08:17:01:10:0.0000	1.9485	-1.9384	0.041	0.3415	0.0039	0.1487	0.0072	-8135.085	442300000
4500.0000	2006:08:17:01:15:0.0000	1.9485	-1.9384	0.041	0.3415	0.0039	0.1487	0.0072	-23087.929	40450000
4800.0000	2006:08:17:01:20:0.0000	1.9485	-1.9384	0.041	0.3415	0.0039	0.1487	0.0072	-10737.411	44230000
5100.0000	2006:08:17:01:25:0.0000	1.9485	-1.9384	0.041	0.3415	0.0039	0.1487	0.0072	18174.579	1.018
5400.0000	2006:08:17:01:30:0.0000	1.9485	-1.9384	0.041	0.3415	0.0039	0.1487	0.0072	-1449.833	493200000
5700.0000	2006:08:17:01:35:0.0000	1.9485	-1.9384	0.041	0.3415	0.0039	0.1487	0.0072	3808.131	1.015
6000.0000	2006:08:17:01:40:0.0000	1.9485	-1.9384	0.041	0.3415	0.0039	0.1487	0.0072	-5126.371	442300000
6300.0000	2006:08:17:01:45:0.0000	1.9485	-1.9384	0.041	0.3415	0.0039	0.1487	0.0072	-93.200	493200000.(
6600.0000	2006:08:17:01:50:0.0000	1.9485	-1.9384	0.041	0.3415	0.0039	0.1487	0.0072	5131.534	493200000
6900.0000	2006:08:17:01:55:0.0000	1.9485	-1.9384	0.041	0.3415	0.0039	0.1487	0.0072	4508.259	442300000
7200.0000	2006:08:17:02:00:0.0000	1.9485	-1.9384	0.041	0.3415	0.0039	0.1487	0.0072	3566.840	404500000
7500.0000	2006:08:17:02:05:0.0000	1.9485	-1.9384	0.041	0.3415	0.0039	0.1487	0.0072	-6561.550	404500000
7800.0000	2006:08:17:02:10:0.0000	1.9485	-1.9384	0.041	0.3415	0.0039	0.1487	0.0072	-17105.685	37500000
8100.0000	2006:08:17:02:15:0.0000	1.9485	-1.9384	0.041	0.3415	0.0039	0.1487	0.0072	-56737.719	1.015
8400.0000	2006:08:17:02:20:0.0000	1.9485	-1.9384	0.041	0.3415	0.0039	0.1487	0.0072	-6223.738	265200000
8700.0000	2006:08:17:02:25:0.0000	1.9485	-1.9385	0.041	0.3415	0.0039	0.1487	0.0072	-7292.407	265200000

VI: Position time series of campaign stations

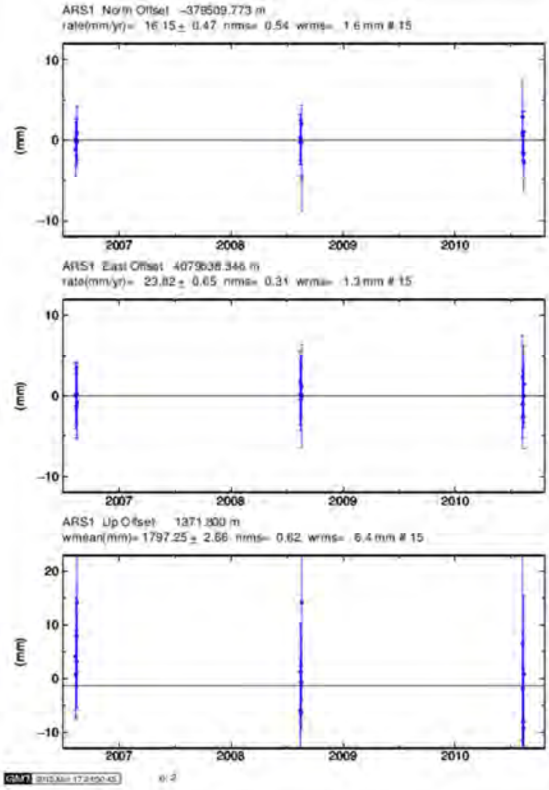

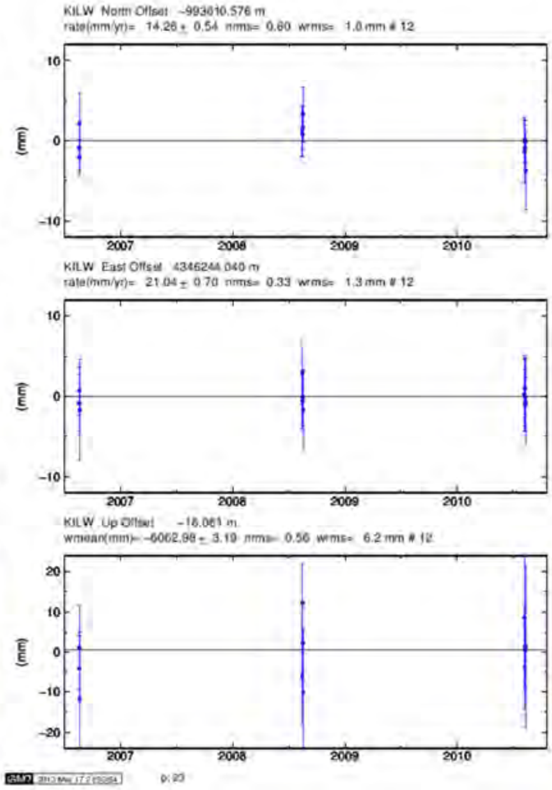

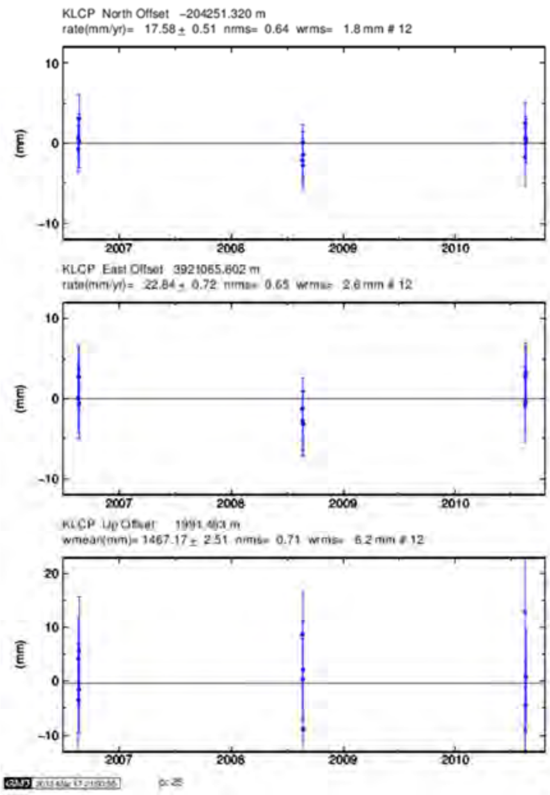

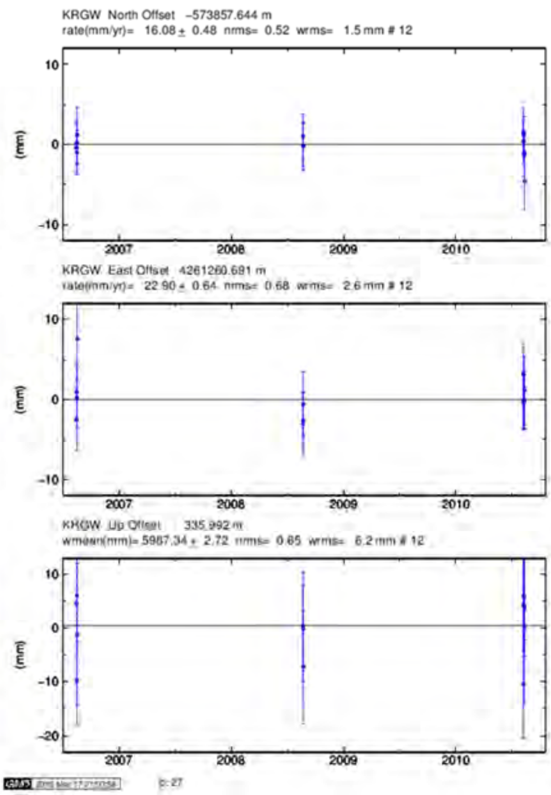

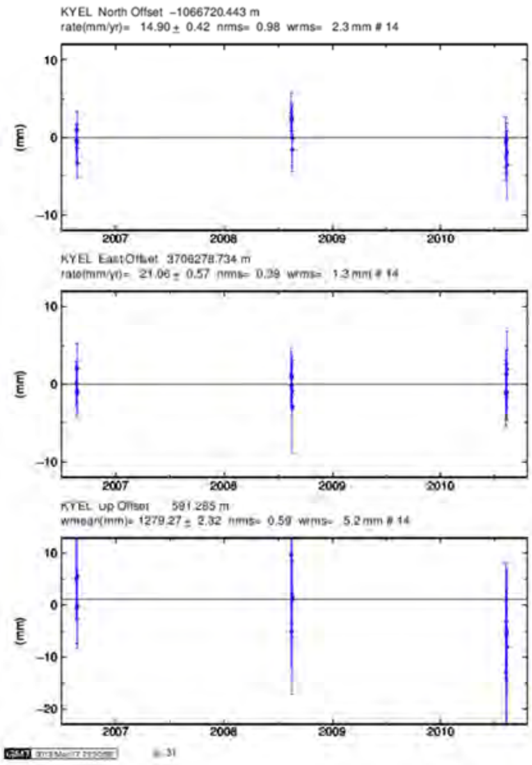
KYEL North Offset -1066720.443 m
rate(mm/yr)= 14.90 ± 0.42 nrms= 0.98 wrms= 2.3 mm # 14
KYEL East Offset 3706278.734 m
rate(mm/yr)= 21.06 ± 0.57 nrms= 0.39 wrms= 1.3 mm # 14
KYEL Up Offset 591.285 m
wmean(mm)= 1279.27 ± 2.32 nrms= 0.59 wrms= 5.2 mm # 14

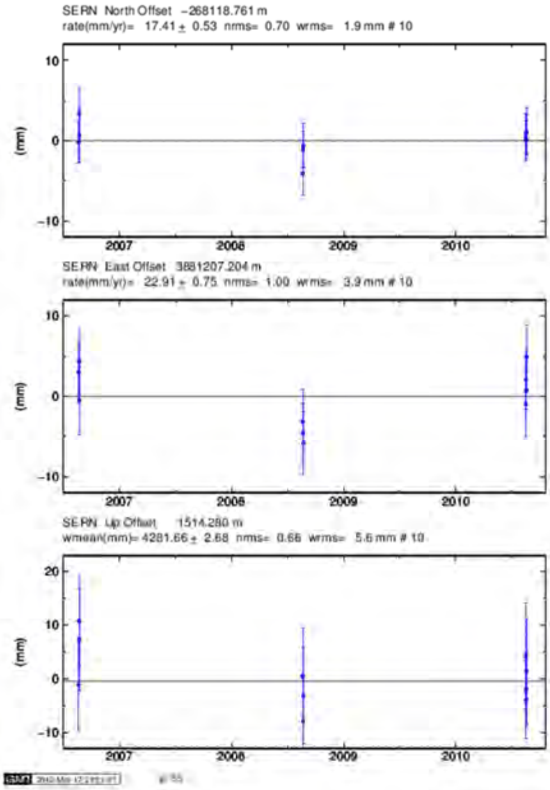
SERN North Offset -268118.761 m
rate(mm/yr)= 17.41 ± 0.53 nrms= 0.70 wrms= 1.9 mm # 10
SERN East Offset 3881207.204 m
rate(mm/yr)= 22.91 ± 0.75 nrms= 1.00 wrms= 3.9 mm # 10
SERN Up Offset 1514.280 m
wmean(mm)= 4281.66 ± 2.68 nrms= 0.66 wrms= 5.6 mm # 10

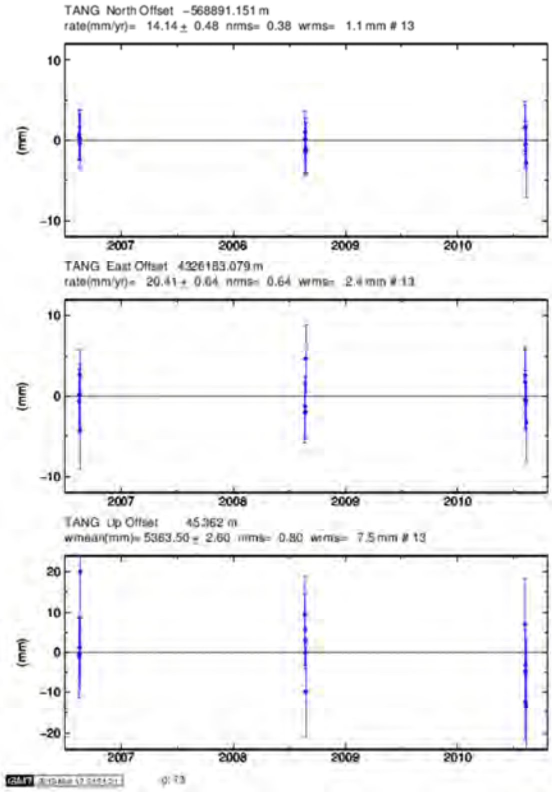
TANG North Offset -568891.151 m
rate(mm/yr)= 14.14 ± 0.48 nrms= 0.38 wrms= 1.1 mm # 13
TANG East Offset 4326183.079 m
rate(mm/yr)= 20.41 ± 0.64 nrms= 0.64 wrms= 2.4 mm # 13
TANG Up Offset 45.362 m
wmean(mm)= 5363.50 ± 2.60 nrms= 0.80 wrms= 7.5 mm # 13

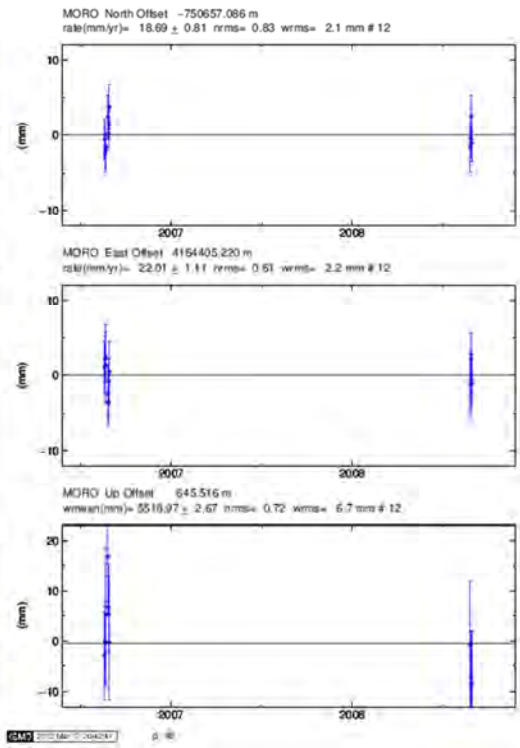
MORO North Offset -750657.086 m
rate(mm/yr)= 18.69 ± 0.81 nrms= 0.83 wrms= 2.1 mm # 12
MORO East Offset 4164405.220 m
rate(mm/yr)= 22.01 ± 1.11 nrms= 0.61 wrms= 2.2 mm # 12
MORO Up Offset 645.516 m
wmean(mm)= 5518.97 ± 2.67 nrms= 0.72 wrms= 6.7 mm # 12

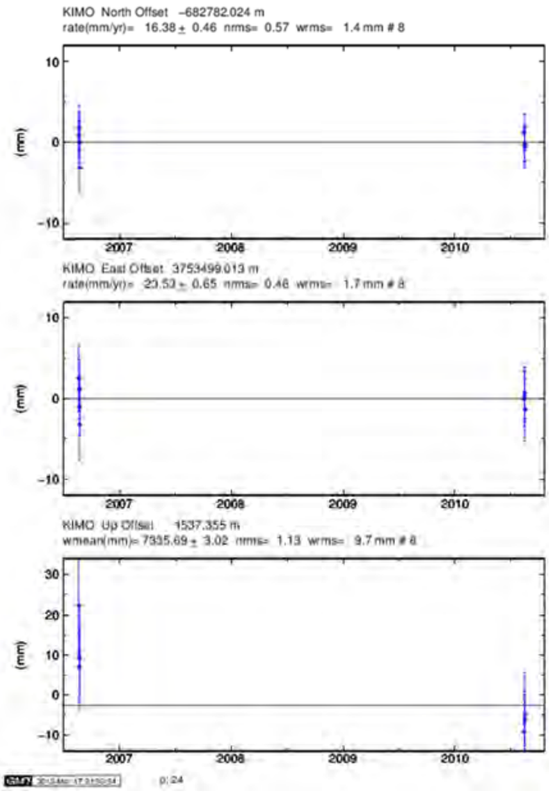
KIMO North Offset -682782.024 m
rate(mm/yr)= 16.38 ± 0.46 nrms= 0.57 wrms= 1.4 mm # 8
KIMO East Offset 3753499.013 m
rate(mm/yr)= 23.53 ± 0.65 nrms= 0.48 wrms= 1.7 mm # 8
KIMO Up Offset 1537.355 m
wmean(mm)= 7335.69 ± 3.02 nrms= 1.13 wrms= 9.7 mm # 8
(mm)
2007
2008
2009
2010
p. 24

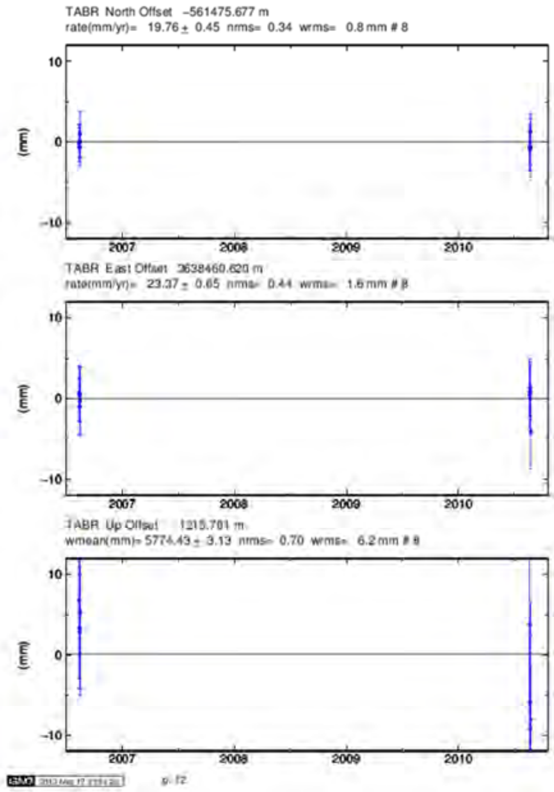
TABR North Offset -561475.677 m
rate(mm/yr)= 19.76 ± 0.45 nrms= 0.34 wrms= 0.8 mm # 8
TABR East Offset 3638460.620 m
rate(mm/yr)= 23.37 ± 0.65 nrms= 0.44 wrms= 1.6 mm # 8
TABR Up Offset 1215.781 m
wmean(mm)= 5774.43 ± 3.13 nrms= 0.70 wrms= 6.2 mm # 8
(mm)
2007
2008
2009
2010

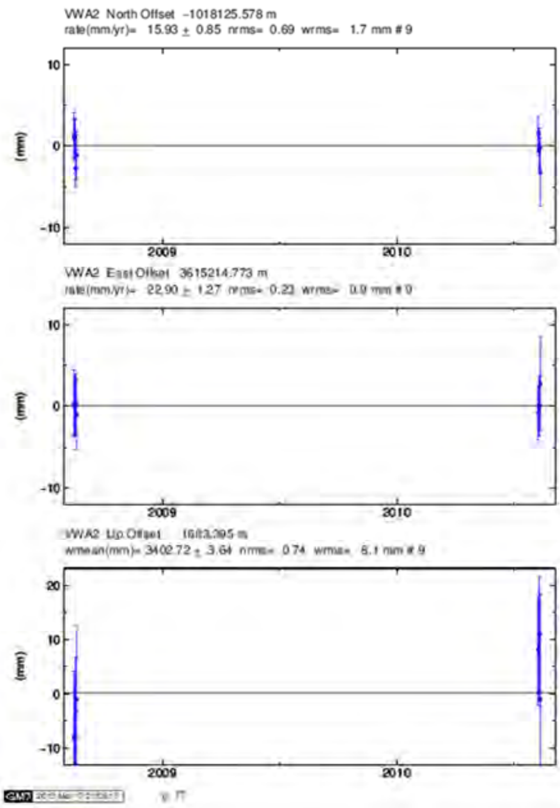
VWA2 North Offset -1018125.578 m
rate(mm/yr)= 15.93 ± 0.85 nrms= 0.69 wrms= 1.7 mm # 9
VWA2 East Offset 3615214.773 m
rate(mm/yr)= 22.90 ± 1.27 nrms= 0.23 wrms= 0.9 mm # 9
VWA2 Up Offset 1683.395 m
wmean(mm)= 3402.72 ± 3.64 nrms= 0.74 wrms= 6.1 mm # 9
(mm)
2009
2010

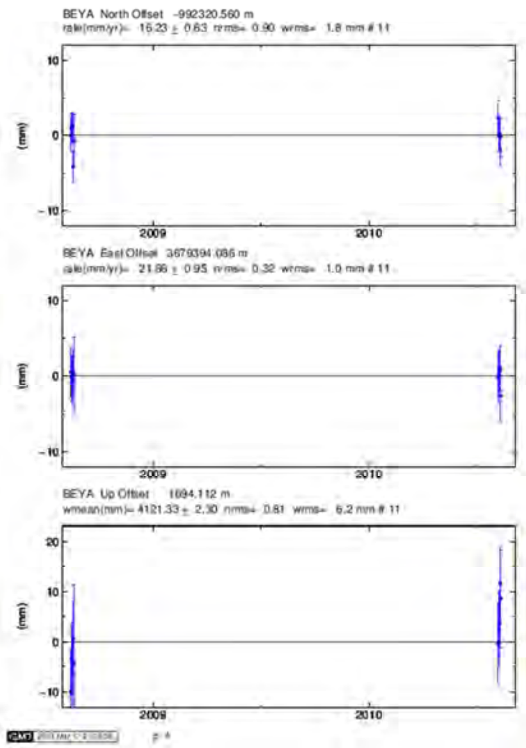
BEYA North Offset -992320.560 m
rate(mm/yr)= 16.23 ± 0.63 nrms= 0.90 wrms= 1.8 mm # 11
BEYA East Offset 3679394.086 m
rate(mm/yr)= 21.86 ± 0.95 nrms= 0.32 wrms= 1.0 mm # 11
BEYA Up Offset 1694.112 m
wmean(mm)= 4121.33 ± 2.30 nrms= 0.81 wrms= 6.2 mm # 11
(mm)
2009
2010

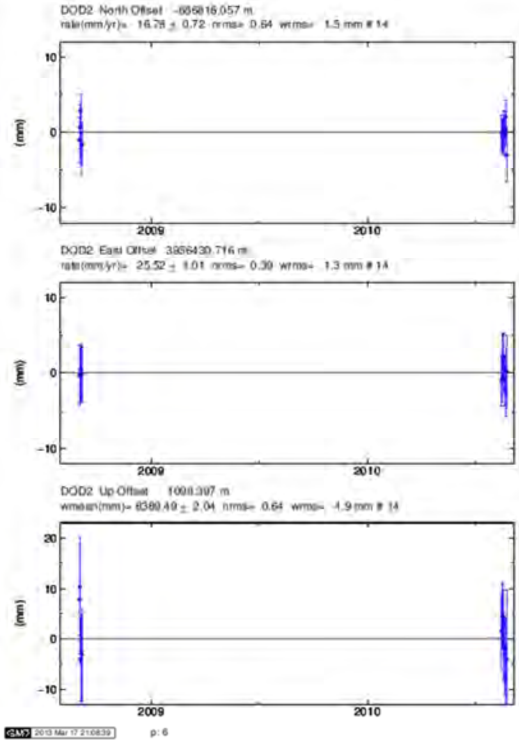
DOD2 North Offset
DOD2 East Offset
DOD2 Up Offset
(mm)
2009
2010

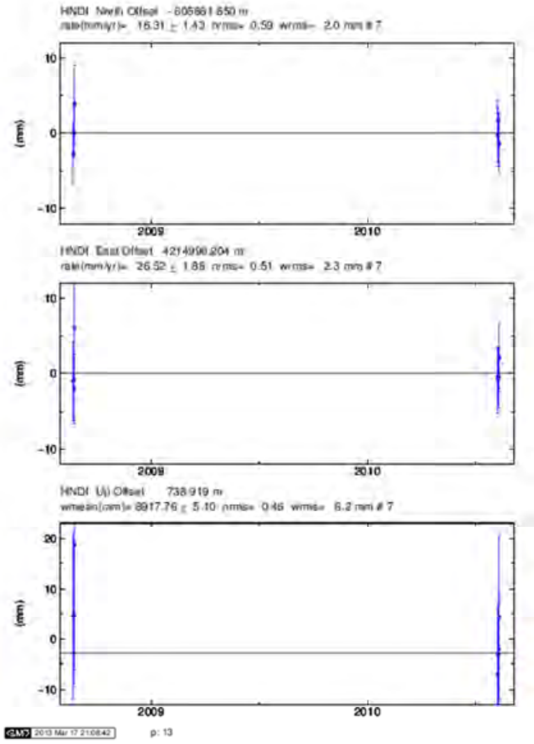
HNDI North Offset
HNDI East Offset
HNDI Up Offset
(mm)
2009
2010

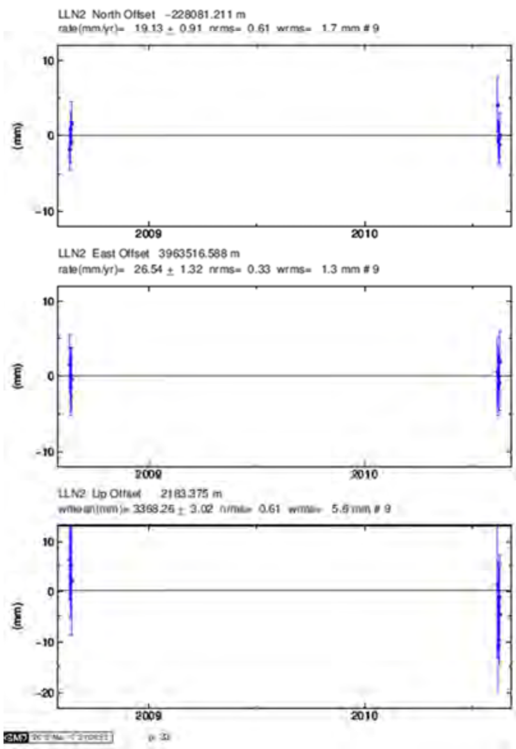
LLN2 North Offset -228081.211 m
rate(mm/yr)= 19.13 ± 0.91 nrms= 0.61 wrms= 1.7 mm # 9
LLN2 East Offset 3963516.588 m
rate(mm/yr)= 26.54 ± 1.32 nrms= 0.33 wrms= 1.3 mm # 9
LLN2 Up Offset 2183.375 m
(mm)
2009
2010

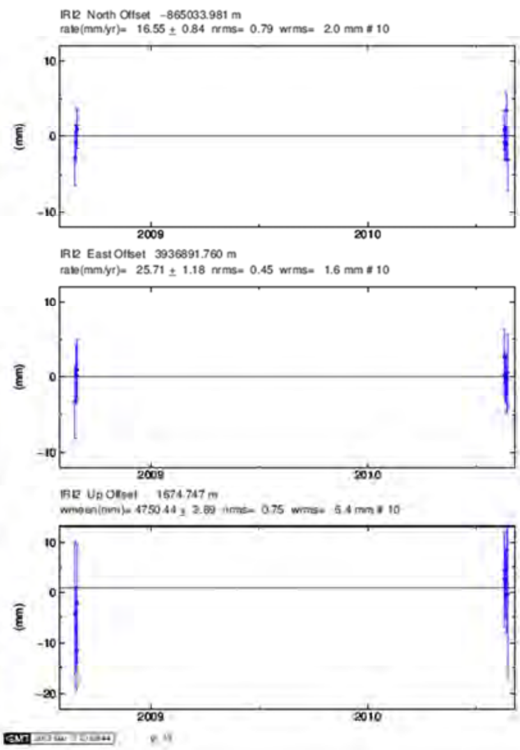
IRI2 North Offset -865033.981 m
rate(mm/yr)= 16.55 ± 0.84 nrms= 0.79 wrms= 2.0 mm # 10
IRI2 East Offset 3936891.760 m
rate(mm/yr)= 25.71 ± 1.18 nrms= 0.45 wrms= 1.6 mm # 10
IRI2 Up Offset 1674.747 m
(mm)
2009
2010

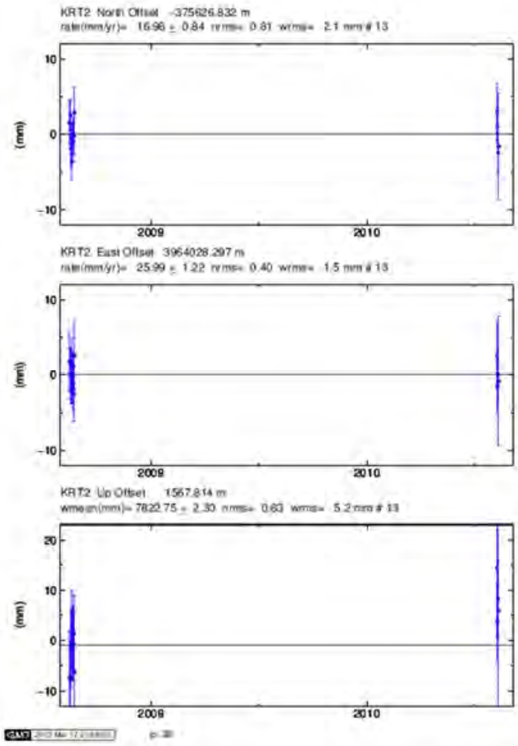
KRT2 North Offset -375626.832 m
rate(mm/yr)= 16.96 ± 0.84 nrms= 0.81 wrms= 2.1 mm # 13
KRT2 East Offset 3964028.297 m
rate(mm/yr)= 25.99 ± 1.22 nrms= 0.40 wrms= 1.5 mm # 13
KRT2 Up Offset 1567.814 m
wmean(mm)= 7822.75 ± 2.30 nrms= 0.63 wrms= 5.2 mm # 13
(mm)
2009
2010

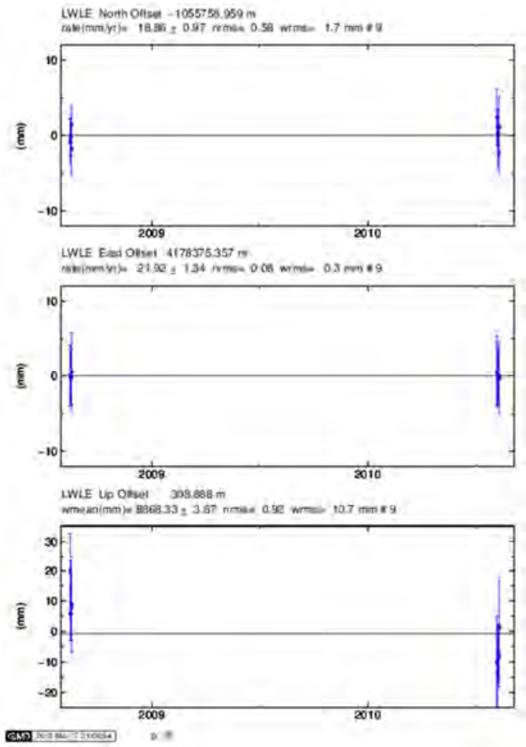
LWLE North Offset -1055758.959 m
rate(mm/yr)= 18.86 ± 0.97 nrms= 0.58 wrms= 1.7 mm # 9
LWLE East Offset 4178375.357 m
rate(mm/yr)= 21.92 ± 1.34 nrms= 0.08 wrms= 0.3 mm # 9
LWLE Up Offset 308.888 m
wmean(mm)= 8868.33 ± 3.87 nrms= 0.92 wrms= 10.7 mm # 9
(mm)
2009
2010

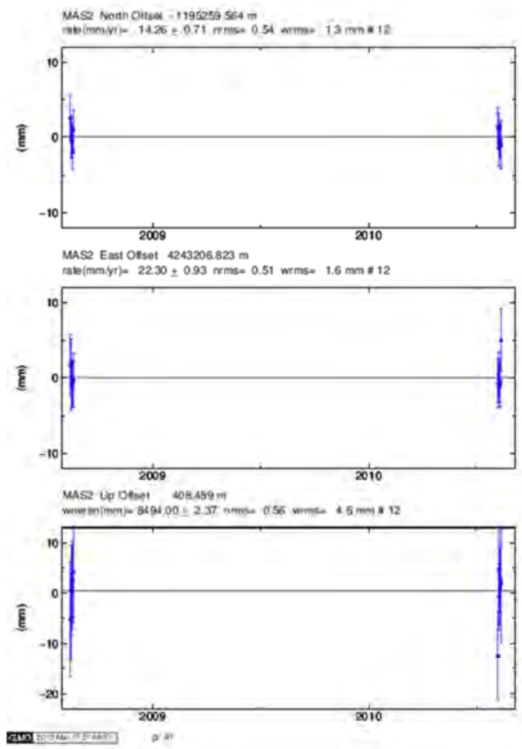
MAS2 North Offset -1195259.564 m
rate(mm/yr)= 14.26 ± 0.71 nrms= 0.54 wrms= 1.3 mm # 12
MAS2 East Offset 4243206.823 m
rate(mm/yr)= 22.30 ± 0.93 nrms= 0.51 wrms= 1.6 mm # 12
MAS2 Up Offset 408.459 m
wmean(mm)= 8494.00 ± 2.37 nrms= 0.56 wrms= 4.6 mm # 12
(mm)
2009
2010

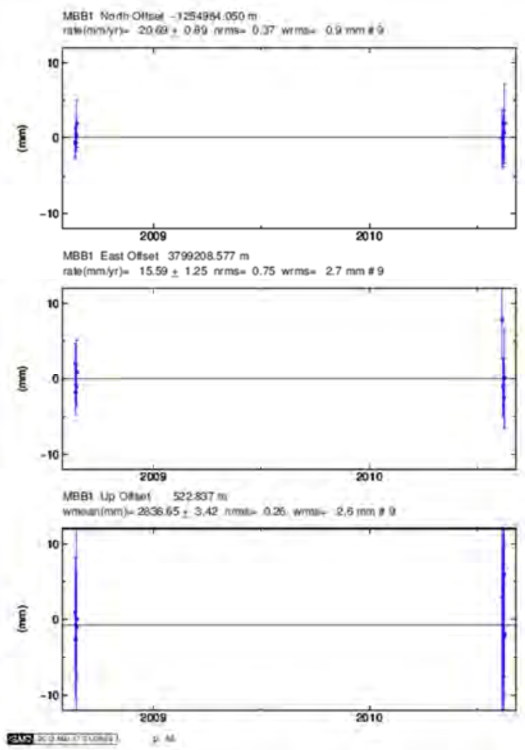
MBB1 North Offset -1254984.050 m
rate(mm/yr)= 20.69 ± 0.89 nrms= 0.37 wrms= 0.9 mm # 9
MBB1 East Offset 3799208.577 m
rate(mm/yr)= 15.59 ± 1.25 nrms= 0.75 wrms= 2.7 mm # 9
MBB1 Up Offset 522.837 m
wmean(mm)= 2836.65 ± 3.42 nrms= 0.26 wrms= 2.6 mm # 9
(mm)
2009
2010

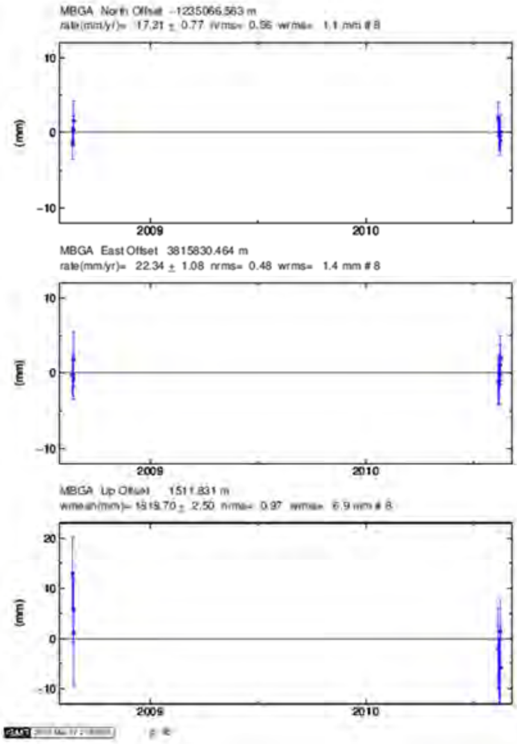
MBGA North Offset -1235066.563 m
rate(mm/yr)= 17.21 ± 0.77 nrms= 0.56 wrms= 1.1 mm # 8
MBGA East Offset 3815830.464 m
rate(mm/yr)= 22.34 ± 1.08 nrms= 0.48 wrms= 1.4 mm # 8
MBGA Up Offset 1511.831 m
wmean(mm)= 1819.70 ± 2.50 nrms= 0.97 wrms= 6.9 mm # 8
(mm)
2009
2010

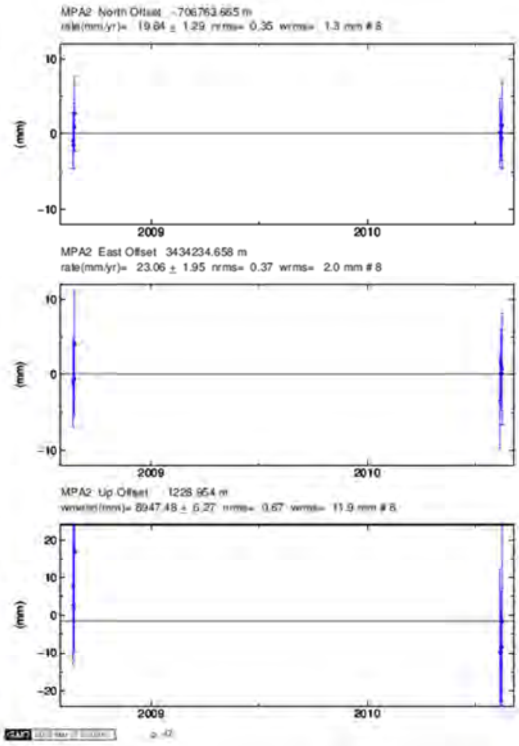
MPA2 North Offset -706763.665 m
rate(mm/yr)= 19.84 ± 1.29 nrms= 0.35 wrms= 1.3 mm # 8
MPA2 East Offset 3434234.658 m
rate(mm/yr)= 23.06 ± 1.95 nrms= 0.37 wrms= 2.0 mm # 8
MPA2 Up Offset 1228.954 m
wmean(mm)= 8947.48 ± 6.27 nrms= 0.67 wrms= 11.9 mm # 8
(mm)
2009
2010

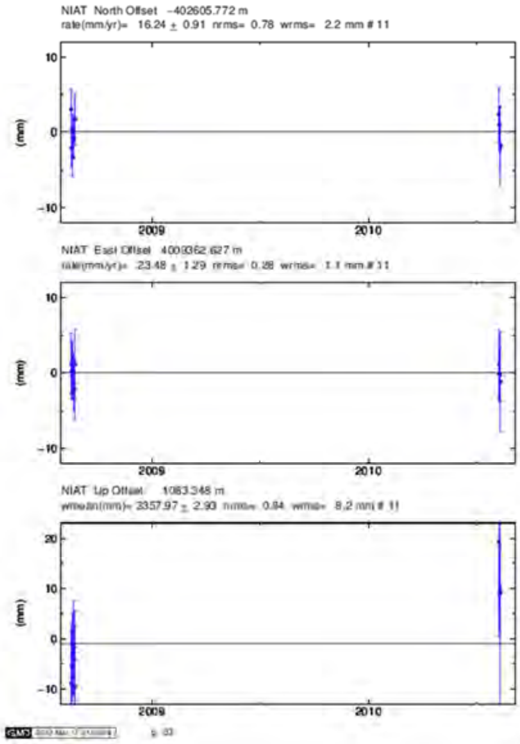
NIAT North Offset -402605.772 m
rate(mm/yr)= 16.24 ± 0.91 nrms= 0.78 wrms= 2.2 mm # 11
NIAT East Offset 4009362.627 m
rate(mm/yr)= 23.48 ± 1.29 nrms= 0.28 wrms= 1.1 mm # 11
NIAT Up Offset 1083.348 m
wmean(mm)= 2357.97 ± 2.93 nrms= 0.84 wrms= 8.2 mm # 11
(mm)
2009
2010

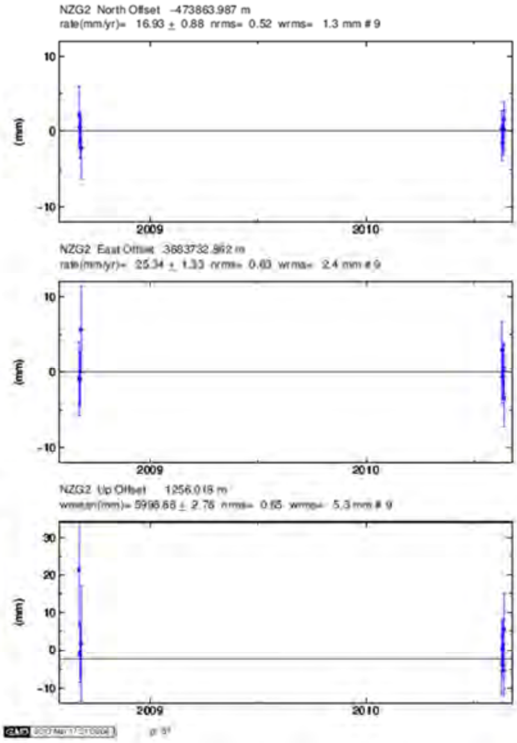
NZG2 North Offset -473863.987 m
rate(mm/yr)= 16.93 ± 0.88 nrms= 0.52 wrms= 1.3 mm # 9
NZG2 East Offset 3683732.862 m
rate(mm/yr)= 25.34 ± 1.33 nrms= 0.63 wrms= 2.4 mm # 9
NZG2 Up Offset 1256.018 m
wmean(mm)= 5998.88 ± 2.76 nrms= 0.65 wrms= 5.3 mm # 9
(mm)
2009
2010

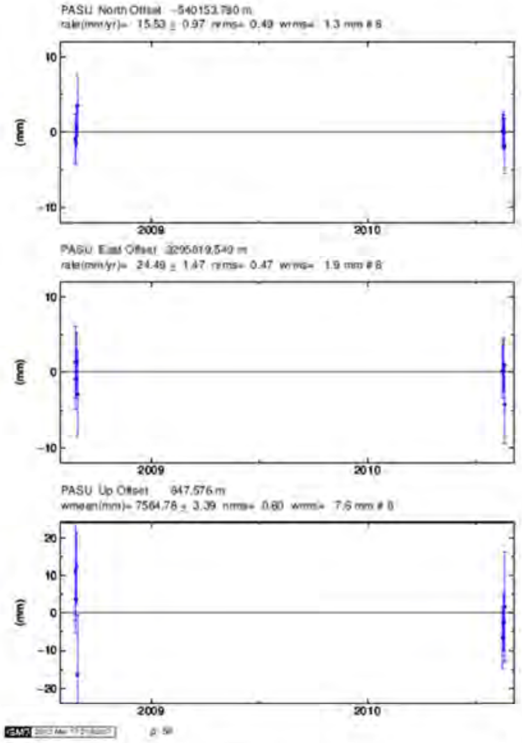
PASU North Offset -540153.790 m
rate(mm/yr)= 15.53 ± 0.97 nrms= 0.49 wrms= 1.3 mm # 8
PASU East Offset 3295819.540 m
rate(mm/yr)= 24.49 ± 1.47 nrms= 0.47 wrms= 1.9 mm # 8
PASU Up Offset 847.576 m
wmean(mm)= 7564.78 ± 3.39 nrms= 0.80 wrms= 7.6 mm # 8
(mm)
2009
2010
GMT

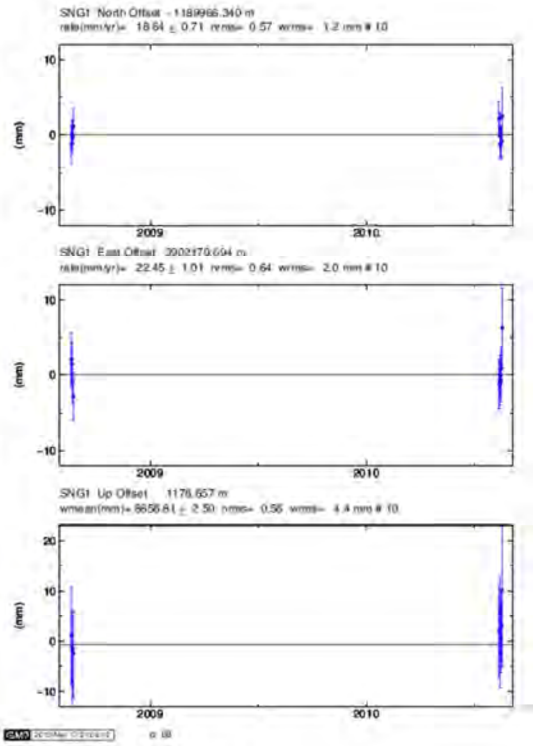
SNG1 North Offset -1189966.340 m
rate(mm/yr)= 18.64 ± 0.71 nrms= 0.57 wrms= 1.2 mm # 10
SNG1 East Offset 3902170.694 m
rate(mm/yr)= 22.45 ± 1.01 nrms= 0.64 wrms= 2.0 mm # 10
SNG1 Up Offset 1176.657 m
wmean(mm)= 8658.61 ± 2.50 nrms= 0.56 wrms= 4.4 mm # 10
(mm)
2009
2010
GMT

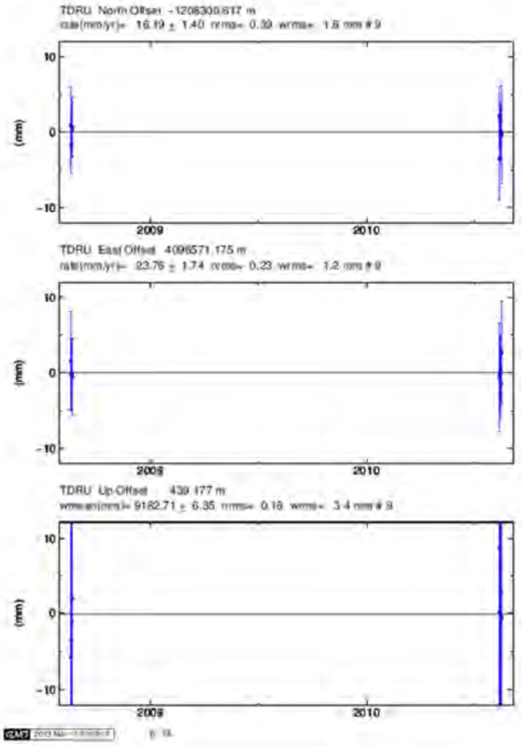
TDRU North Offset -1208300.617 m
rate(mm/yr)= 16.19 ± 1.40 nrms= 0.39 wrms= 1.6 mm # 9
TDRU East Offset 4096571.175 m
rate(mm/yr)= 23.76 ± 1.74 nrms= 0.23 wrms= 1.2 mm # 9
TDRU Up Offset 439.177 m
wmean(mm)= 9182.71 ± 6.35 nrms= 0.16 wrms= 3.4 mm # 9
(mm)
2009
2010
GMT

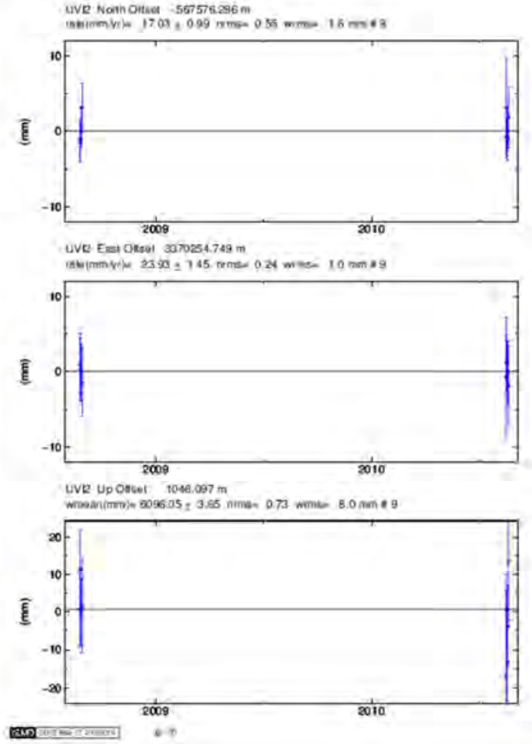
UVI2 North Offset -567576.296 m
rate(mm/yr)= 17.03 ± 0.99 nrms= 0.56 wrms= 1.6 mm # 9
UVI2 East Offset 3370254.749 m
rate(mm/yr)= 23.93 ± 1.45 nrms= 0.24 wrms= 1.0 mm # 9
UVI2 Up Offset 1046.097 m
wmean(mm)= 6096.05 ± 3.65 nrms= 0.73 wrms= 8.0 mm # 9
(mm)
2009
2010
GMT

VII: Data extraction from summary results

Coordinate extraction from GAMIT/GLOBK solution

X Y Z and corresponding sigmas were extracted using “grep”

```
grep 'Unc.' globk_comb.org.rpt >> GamitXYZ
```

Extraction of X Y Z and their respective sigmas was done using unix command taking the advantage of the data structure. For instance:

cat file_name |awk '{print $1 "\t" $2 "\t" $3 "\t" $4 "\t" $9 "\t" $10 "\t" $11 }' > output_file this was to avoid columns 5 -7 which contain adjuments of X Y Z and column 7 referencing the decimal year.

Coordinate extraction from APPS solution

Sample of the result for a single site for 24hours observation is given here under.

```
# APPS Summary file for site ARS1. Produced from RINEX file
ARS12250.06o on Wed Mar 6 15:13:52 UTC 2013
# The reference frame is ITRF 2008 (with semi-major axis = 6378137 m;
flattening factor = 1/298.257222101)
# Output data rate is 300 seconds. Minimum elevation angle is 7.5
degrees.
# Satellite antenna phase center offset and maps taken from IGS
Standards igs08_1604.atx.
#
# Receiver antenna phase center offset and maps taken from IGS
Standards igs08_1604.atx.
# Receiver antenna phase center offset relative to the antenna
reference is 0 m
# The antenna reference point offset from the monument reference,
based on the RINEX file header, is 0.0405 m
#
# Product used to process ARS12250.06o: JPL Final
#
# Static point positioning mode (a single set of site coordinates are
estimated):
#
# Total number of Phase measurements:         1389. RMS post-fit Phase
residuals:    0.014 m. Number of excluded Phase measurements:   0
```

```
# Total number of Pseudorange measurements:   1389. RMS post-fit
PRange residuals:   0.536 m. Number of excluded PRange measurements:
0
#
# Estimated Cartesian coordinates:     X = 5105080.3001 m     Y =
3807010.3956 m     Z =  -376832.8283 m
# Sigmas of Cartesian coordinates:  SigX =        0.0030 m SigY =
0.0028 m SigZ =        0.0009 m
# Estimated Geodetic coordinates (WGS84/GRS80):    Lat =   -3.40919405
deg     East_Lon =   36.71299038 deg     Height = 1371.8240 m
# Sigmas of Geodetic coordinates: SigLat =        0.0009 m
SigLon =        0.0022 m    SigHeight =    0.0035 m
#
# Time variable estimated parameters:
#Secs_from_start  GPS_Time(yyyy:mm:dd:hh:mm:ss.ssss)  HZTrop(m)
WZTrop(m)  Sig(m)    TropGrad_N(m)  Sig(m)   TropGrad_E(m)   Sig(m)
Clock(m)   Sig(m)
        0.0000          2006:08:13:11:00:0.0000       1.9610    0.1071
0.002    -0.0007         0.0003  -0.0014          0.0003 40053.323
0.028
      300.0000          2006:08:13:11:05:0.0000       1.9610    0.1073
0.002    -0.0007         0.0003  -0.0013          0.0003 20538.781
0.028
      600.0000          2006:08:13:11:10:0.0000       1.9610    0.1076
0.002    -0.0007         0.0002  -0.0013          0.0003  1631.036
0.028
```

……
.

The summary X Y Z and their respective sigmas is preceded by # symbol. This structure helped in data extraction using the unix regular expressions. First the symbol # was replaced by respective station name in each file using 'find replace' function before combining the results in a single file for each year

Then the unix regular expression was used to extract data from many results files at a time for each year's data set. For instance grep 'X' *.sum >> XYZ_APPS2006 # this printed out XYZ and SigX SigY SigY on consecutive lines but still with unwanted # at the beginning of each line.

However the format of the resulting file support another regular expression using “awk” to extract required data.

Example of awk expression used to extract X,Y, Z from 2006 APPS solution

cat XYZ_APPS2006 |awk '{if($7!="=" && $11 !="=" && $15 !="=") print $1 " " $7 " " $11 " " $15}' > tzxyz_2006 #this printed out X Y Z.

cat XYZ_APPS2006|awk '{if($8!="m" && $12 !="m" && $16!="m")print $1 " " $8 " " $12 " " $16}' > Tzsigmas_2006 #this printed out SigX SigY SigZ

VIII: R-Program used to compute residuals mean and Standard Deviations.

Sample of R- program used to compute residuals mean and standard deviation for the 2006 data set

```
Delta6 <- function(G06,A06)
{
apps6 <- read.table(A06)
gdata6 <- read.table(G06)
ap6 <- as.data.frame(apps6)
g6 <- as.data.frame(gdata6)
lbl6 <- g6[,1]
dX06 <- g6[,2]-ap6[,2]
dY06 <- g6[,3]-ap6[,3]
dZ06 <- g6[,4]-ap6[,4]
dSigX06 <- g6[,5]-ap6[,5]
dSigY06 <- g6[,6]-ap6[,6]
dSigZ06 <- g6[,7]-ap6[,7]
T06 <- cbind(dX06,dY06,dZ06,dSigX06,dSigY06,dSigZ06)
return(T06)
}
sink ("06_dXYZ")
Delta6("gamitdata_2006","appsdata_2006")
```

The output from R contains a row labels as ordinal values. These were excluded using unix commands and replaced by their station names

```
eg. cat 06_dXYZ | awk '{print $2 "\t" $3 "\t" $4 "\t" $5 "\t" $6 "\t"
$7}'
 cat 06_dXYZ | awk '{print $2 "\t" $3 "\t" $4 "\t" $5 "\t" $6 "\t"
$7}' > 06XYZ
cat 08_dXYZ | awk '{print $2 "\t" $3 "\t" $4 "\t" $5 "\t" $6 "\t" $7}'
> 08XYZ
cat 10_dXYZ | awk '{print $2 "\t" $3 "\t" $4 "\t" $5 "\t" $6 "\t" $7}'
> 10XYZ
```

Mean and Standard deviation were computed using R function apply( )

```
 mm <-read.table("06XYZ")
> mean06 <- apply(mm,2,mean)
> sd06 <- apply(mm,2,sd)
> msd06 <- rbind(mean06,sd06)
> write.table(msd06,file="meansdev06_R")
```

REFERENCES

Ahn, Y.W. (2009), "Positioning Enhancement Based on a New Weighting Scheme to Solve an Ill-Conditioned Case." Geodetic Research Laboratory, Department of Geodesy and Geomatics Engineering, University of New Brunswick, Fredericton, New Brunswick, Canada.

Ahn, Y. (2012), "Lecture notes on GPS Error Sources and Mitigation"

Ahn, Y.W., Kim, D., Dare, P. and Langley, R.B. (2005), "Long Baseline GPS RTK Performance in a Marine Environment using NWP Ray-Tracing Technique under Varying Tropospheric Conditions." Geodetic Research Laboratory, Department of Geodesy and Geomatics Engineering, University of New Brunswick, Fredericton, New Brunswick, Canada,)

Böder, V., Menge, F., Seeber, G., Wübbena, G. and Schmitz, M.(2001), "How to deal withStation Dependent Errors – New developments of the absolute field calibration of PCV and Phase-Multipath with a Precise Robot.", Paper presented at: 14th International Technical Meeting of the Satellite Division of the Institute of Navigation, ION GPS-2001, Salt Lake City, Utah, USA.

Chen, D. (1993), "Fast Ambiguity Search Filter (FASF): A Nova1 Concept for GPS Ambiguity Resolution," Proceedings of the 6th International Technical Meeting of the Satellite Division of The Institute of Navigation (ION GPS 1993), Salt Lake City, UT, September 1993, pp. 781-787.

Chen, D. and Lachapelle, G. (1995), "A Comparison of the FASF and Least-Squares Search Algorithms for ON-THE-FLY Ambiguity Resolution", Navigation, Journal of The Institute of Navigation, Vol. 42, No. 2, Summer 1995, pp. 371-390.

Choy, S., Zhang, K. and Silcock, D. (2008), "An Evaluation of Various Ionospheric Error Mitigation Methods used in Single Frequency PPP.", Journal of Global Positioning Systems Vol. 7, No. 1: 62-71

Counselman, C.C. and Gourevitch, S. A. (1981), "Miniature Interferometer Terminals for Earth Surveying: Ambiguity and Multipath with Global Positioning System", Geoscience and Remote Sensing, IEEE Transactions on, page(s): 244 - 252 Volume: GE-19, Issue: 4, Oct. 1981.

Dach, R., Hugentobler, U., Fridez, P., Meindl, M. (2007), "User manual of the Bernese GPS Software Version 5.0." Astronomical Institute, University of Bern.

De Agostino, M. Piras, M. and Porporato, C. (2008), "The new L2C GPS code: Signal andPositioning Quality Analysis." Proceedings of the 21st International Technical meeting of the Satellite Division of the Institute of Navigation (ION GNSS 2008), Savanna GA, September, pp.1649-1657.

Elósegui, P., Davis, J.L., Jaldehag, R.T.K., Johansson, J.M., Niell, A.E. and Shapiro, I.I. (1995) "Geodesy using the Global Positioning System: the effects of Signal Scattering on estimates of Site Position." Journal of Geophysical Research, 100: doi 10.1029/95JB00868, issn: 0148 – 0227.

El-Rabbany, A. (2002), "Introduction to GPS the Global Positioning System" Artech House, Boston . London G109.5E6. LCDR.

Estey, L. and Wier, S. (2013), "Teqc Tutorial: Basics of Teqc Use and Teqc Products." (http://facility.unavco.org/software/teqc/)

Frei, E. and Beutler, G. (1990), "Rapid static positioning based on the fast ambiguity resolution approach "FARA": theory and first results." Manuscripta Geodaetica, Vol. 15, No.4, pp. 325-356.

Geng, J., Shi, C.,Ge, M. Dodson, ·A.H.,Lou, Y.Zhao, Q., and Liu, J. (2011), "Improving the estimation of fractional-cycle biases for ambiguity resolution in precise point positioning," Springer-Verlag.

Grewal, M.S., Weill, L. R., and Andrews, A.P. (2007), "Global Positioning Systems, Inertial Navigation and Integration" A John Wiley & Sons, Inc., Hoboken, New Jersey.

Hatch, R. R. (2006), "A New Three-Frequency, Geometry-Free, Technique for Ambiguity Resolution," Proceedings of the 19th International Technical Meeting of the Satellite Division of The Institute of Navigation (ION GNSS 2006), Fort Worth, TX, pp. 309-316.

Hedfors, J. (2005) "TQCPLOT" Uppsala University.

Herring, T (2012), "GAMIT: Daily GPS Processing, Lecture 2", Massachusetts Institute of Technology, USA.

Herring, T. A., King, R. W. and McClusky, S. C. (2010), "Introduction to GAMIT/GLOBK, Reliese 10.4.", Department of Earth, Atmospheric, and Planetary Sciences**,** Massachusetts Institute of Technology. USA.

Hopfield, H.S. (1969), "Two quadratic tropospheric refractivity profile for correcting satellite data",Journal of Geophisicl Research, 74 (18) pp. 4487-4499.

Hoffmann-Wellenhof, B., Lichtenegger, H. and Wasle, E. (2008), "GNSS – Global Navigation Satellite Systems GPS, GLONASS, Galileo, and more" Springer Wien, New York.

Joosten, P. and Tiberius, C. (2002), "LAMBDA: FAQs.", GPS solutions (in press). DOI 10.1007/s10291 -002 – 0004 – 8

Kaplan E.D., Hegarty, C. J. (2006), "Understanding GPS Principles and Applications." Second Edition, ARTECH HOUSE, INC. Boston, London, 2006.

Kim, D. and Langley R.B., (1999),"An Optimized Least-Squares Technique for Improving Ambiguity Resolution and Computational Efficiency.", Geodetic Research Laboratory, Department of Geodesy and Geomatics Engineering University of New Brunswick, Fredericton, N.B., Canada.

Landau, H. and Euler, H.J.(1992), "On-the-Fly Ambiguity Resolution for Precise Differential Positioning," Proceedings of the 5th International Technical Meeting of the Satellite Division of The Institute of Navigation (ION GPS 1992), Albuquerque, NM, September 1992, pp. 607-613.

Larson, K.M., and Agnew, D.C. (1991), "Application of the Global Positioning System to Crustal deformation measurement 1. Precision and Accuracy." Journal of Geophysics. Res. 96, 16547-16565.

Leandro, R. F. Thirumuthi, T., Sukeová, L., Langley, R.B. and Santos, M.C. (2008), "Analysis of GPS L2C Signal Quality and its Impact on PPP Performance." Proceedings of the 2008 National Technical Meeting of The Institute of Navigation, San Diego, CA, January 2008, pp. 1020-1031. P.

Leandro, R., Santos, M. and Langley, R. B. (2006), "UNB Neutral Atmosphere Models: Development and Performance," Geodetic Research Laboratory, Department of Geodesy and Geomatics Engineering, University of New Brunswick, Fredericton, Canada. Source:

Leveson, I. (2006), "Benefits of the new GPS signal The L2C study", InsideGNSS July/August 2006, www.insidegnss.com

Li, W., Yuan, Y., Ou, J., Li, H., and Li, Z. (2012), "A New Global Zenith Tropospheric delay Model IGGtrop for GNSS Applications" Chinese Science Bulletin, Vol. 57.

Li, X., Zhang, X. and Ge, M. (2010). "Regional reference network augmented Precise Point Positioning for instantaneous ambiguity resolution" Springer-Verlag.

Loyer, S., Perosanz, F., Mercier, F., Capdeville, H. and Marty, J.C. (2012), "Zero-difference GPS ambiguity resolution at CNES–CLS IGS Analysis Center." Springer-Verlag.

Mader, G.L. (1990). "Ambiguity function techniques for GPS phase initialization and kinematic solutions." Proceedings of the Second International Symposium on Precise Positioning with the Global Positioning System, Ottawa, Canada, September 3–7:1233–1247.

Melbourne, W.G. (1985), "The case for ranging in GPS based geodetic systems." Proceedings of first international symposium on precise positioning with Global Positioning Systems, Rockville, 15-19 April, pp. 373-386.

Meurer, M., Erker, S., Thölert, S. Montenbruck, O., Hauschild, A. and Langley, R.B. (2009), "GPS L5 first Light, A preliminary Analysis of SV49's Demonstration Signal." GPS world, 20 (6), 49, – 58.

Musa, T.A., Lim, S. and Rizos, C. (2005), "Low Latitude Troposphere: A Preliminary Study Using GPS CORS Data in South East Asia." School of Surveying and Spatial Information Systems, The University of New South Wales, Sydney, NSW 2052, Australia

Nel Samama. (2008), "Global Positioning, Technologies and Performance" John Wiley & Sons, Inc., Hoboken, New Jersey,

Ovstedal, O., Kjorsvik, N.S., and Gjevestad J. G. O. (2006), "surveying using GPS Precise Point Positioning." www.insidegnss.com.

PAIS, F. G. (2011), "The Description of the Main Techniques of Resolving the Phase Ambiguities, the Advantages, Disadvantages and their Characteristics" National Centre of Geodesy, Cartography, Photogrammetry and Remote Sensing, RevCAD – Journal of Geodesy and Cadastre.

Pany, T. (2003), "Tropospheric GPS Slant Delays at Very Low Elevations." Proceeding of International Workshop on GPS Meteorology Tsukuba (2003).

Prasad, R. and Ruggieri, M. (2005), "Applied satellite navigation using GPS, GALILEO, and augmentation systems," Artech house, Boston, London.

Remondi, B.W. (1984), "Using the Global Positioning System (GPS) phase observable for relative geodesy: modeling, processing, and results." University of Texas at Austin, Center for Space Research.

Remondi, B. (1984), "Using the Global Positioning System phase observable for relative geodesy: Modelling, processing and results." Ph.D. Dissertation, University of Texas, Austin. 360 pp. National Geodetic Information Center, NOAA, Rockville, MD 20852.

Remondi B.W. (1990a), "Pseudo-kinematic GPS results using the Ambiguity Function Method." National Information Center, Rockville, Maryland, NOAA Technical Memorandum NOS NGS-52.

Saastamoinen, J. (1973), "Contributions to the theory of atmospheric refraction", Bulletin Géodésique 107(1): 13-34.

Seeber, G. (2003), "Satellite Geodesy, 2nd completely revised and extended edition" Walter de Gruyter,Berlin , New York.

Teunissen, P.J.G (1994a). "A New Method for Fast Carrier Phase Ambiguity Estimation." Proceeding IEEE Position, Location and Navigation Symposium PLANS'94. Las Vegas, Nevada, USA. April, pp.562-573.

Vaníček, G., Beutler, A., Kleusberg, R.B., Langley, R., Santerre, D.E. and Wells, (1985),"DIPOP - Differential Positioning Program Package for the Global Positioning System." (Geodesy and Geomatics Engineering Technical Reports; 115).

Wübbena, G. (1985), "Model and program developments for cm-positioning with GPS." Proceed. FIG Joint Meeting Inertial, Doppler and GPS measurements for National and Engineering Surveys, 443-565, München.

Wübbena, G. Schmitz, M. and Bagge, A. (2009). "Some thoughts on satellite induced phase shifts a.k.a. "the L2C quarter cycle problem" and the impact on RINEX and RTCM," Geo++ white paper, Gabsen.

Yu, G. and Liu, J. (2003) "Dual-space Ambiguity Resolution Approach Theory and Application" Journal of Global Positioning Systems (2003) Vol. 2, No. 1: 18-26.

DECLARATION

I **Leonard Vincent Bamuhiga,** declare that, this thesis on "**Comparison of PPP and Double Differencing Solutions (case study using campaign GPS stations in Tanzania)"** is my own writing and has never been presented and will not be presented in any other institution for any degree award.

SUBMITTED BY:

Leonard Vincent Bamuhiga	Signature	14/08/2013 Date

CONFIRMATION:

Dr. Tulu Besha

For Dr. Adissu Humegnaw Advisor	Signature	14/08/2013 Date
Dr. Tulu Besha Bedada Co-Advisor	Signature	14/08/2013 Date